

Aus der Klinik und Poliklinik für Dermatologie und Allergologie  
der Ludwig-Maximilians Universität  
München

Direktor: Professor Dr. med. Dr. h.c. Gerd Plewig

**Stress and Growth Related Keratinocyte Pathways:  
Investigation of the Novel Immediate Early Gene  
IEX-1 in Primary Human Keratinocytes  
and the HaCaT Human Keratinocyte Cell Line**

Dissertation  
zum Erwerb des Doktorgrades der Medizin  
an der Medizinischen Fakultät der  
Ludwig-Maximilians Universität zu München

vorgelegt von  
David Alexander Schilling  
aus München

2003

Mit Genehmigung der Medizinischen Fakultät  
der Ludwig-Maximilians Universität zu München

1. Berichterstatter:	Prof. Dr. med. Dr. h.c. G. Plewig
2. Berichterstatter:	Prof. Dr. med. G. Enders
Mitberichterstatter:	Prof. Dr. med. M. Schleicher Prof. Dr. med. W. Hörz
Mitbetreuung durch den promovierten Mitarbeiter:	Dr. med. D. Peus
Dekan:	Prof. Dr. med. Dr. h.c. Klaus Peter
Tag der mündlichen Prüfung:	09.01.2003

In Liebe und Dankbarkeit  
meinen Eltern  
gewidmet

Der experimentelle Teil der vorliegenden Arbeit wurde im Zeitraum September 1998 bis Oktober 2000 im Rahmen eines wissenschaftlichen Austauschprogramms der Klinik und Poliklinik für Dermatologie und Allergologie der Ludwig-Maximilians Universität München und des Department of Dermatology Research der Mayo Clinic Rochester, USA an folgenden Laboratorien durchgeführt:

Laboratory for Molecular Biology and Dermatology Research  
Laboratory for Biochemistry and Nephrology Research

Mayo Clinic Rochester, Minnesota/USA

Teilergebnisse und Vorarbeiten der vorliegenden Arbeit wurden veröffentlicht und auf internationalen Kongressen vorgestellt:

„IEX-1, an Immediate Early Gene, Increases the Rate of Apoptosis in Keratinocytes“  
D Schilling, MR Pittelkow and R Kumar  
(2001) Oncogene 20: 7992-7997

„IEX-1 Induces Cell Proliferation or Apoptosis: Growth and Stress Related Events in Keratinocytes“ D Schilling, K Feldmann, R Kumar, K Squillace and MR Pittelkow  
61<sup>st</sup> Annual Meeting of the Society for Investigative Dermatology, Chicago May 2000

„IEX-1 Expression and Protein Localization in Normal and Pathologic Skin“ KA Feldmann, D Schilling, JP Grande, R Kumar, A Sekulic and MR Pittelkow  
61<sup>st</sup> Annual Meeting of the Society for Investigative Dermatology, Chicago May 2000

„Thallium Inhibits Proliferation, Modulates Signal Transduction, and Alters Terminal Differentiation in Cultured Keratinocytes“ C Krautmacher, D Peus, K Squillace, D Schilling, JL Arbiser and MR Pittelkow  
60<sup>th</sup> Annual Meeting of the Society for Investigative Dermatology, Chicago May 1999

## Table of Contents

Table of Contents.....	i
Abbreviations.....	iii
I. Zusammenfassung.....	iv
II. Abstract.....	vi
1. Introduction.....	1
1.1 Epidermis: Structure and Differentiation.....	2
1.2 The Human Epidermal Growth Factor Receptor (EGFR).....	4
1.3 Apoptosis and its Role in the Epidermis.....	5
1.4 The Immediate-Early-X-Ray-Gene-1 ( <i>IEX-1</i> ).....	7
1.5 Objectives of the Study.....	9
2. Materials and Methods.....	11
2.1 Materials.....	11
2.1.1 Chemicals.....	11
2.1.2 Tissue Culture Materials and Working Solutions.....	11
2.1.3 DNA Vectors.....	14
2.1.4 Antibodies, Ligands and Inhibitors.....	14
2.1.5 Solutions for Immunostaining.....	15
2.1.6 RNA Solutions.....	15
2.1.7 Radioactive Materials.....	16
2.1.8 Molecular Size Markers.....	17
2.1.9 Technical Devices.....	17
2.2 Cell Culture and Cell Lines.....	18
2.2.1 Preparation of Foreskin Specimens.....	18
2.2.2 Passing the Cell Cultures.....	18
2.2.3 Culture of HaCaT Cells.....	18
2.2.4 Transfected HaCaT Cells.....	19
2.3 Plasmid and Fragment Preparation.....	19
2.3.1 Transformation, Selection and Amplification of Bacteria.....	19
2.3.2 Plasmid/Fragment Preparation.....	20
2.3.3 Transfection.....	20
2.3.4 Plasmid Constructs.....	20
2.5 Northern (RNA) Analysis.....	21
2.5.1 Oligo-dT Cellulose Preparation.....	21
2.5.2 mRNA Isolation.....	21
2.5.3 Gel Electrophoresis and Transfer.....	22
2.5.4 Preparation of cDNA Probes.....	22
2.5.5 Hybridization, Exposure and Stripping.....	23
2.5.6 Analyzing the Blots.....	23
2.6 <i>IEX-1</i> – Protein Localization.....	23
2.6.1 <i>IEX-1</i> Immunostaining.....	23

2.6.2 Localization of GFP-tagged <i>IEX-1</i> .....	25
2.7 [ <sup>3</sup> H]-Thymidine Incorporation Assay .....	26
2.8 Apoptosis Assays .....	26
2.8.1 Caspase 3 Activity Assay .....	26
2.8.2 Nucleosome ELISA .....	27
2.9 Luciferase Assay.....	27
2.10 Cell Treatment .....	28
2.10.1 Gamma-Irradiation .....	28
2.10.2 UV-B Irradiation.....	28
2.10.3 Chemical Treatment.....	29
2.11 Experimental Setups and Statistics .....	29
3. Results.....	30
3.1 Effects of Apoptotic or Mitogenic Stimuli on <i>IEX-1</i> .....	30
3.1.1 <i>IEX-1</i> Expression after $\gamma$ -Radiation.....	30
3.1.2 <i>IEX-1</i> Expression after UV-B Radiation .....	30
3.1.3 <i>IEX-1</i> Expression after H <sub>2</sub> O <sub>2</sub> -Treatment .....	31
3.1.4 Stimulation with EGF .....	31
3.1.5 Summary on Stress-Inducing and Mitogenic Treatment .....	34
3.2 Effects of Apoptotic Stimuli on <i>IEX-1</i> Expression in HaCaT Cells.....	34
3.2.1 UV-B Radiation.....	34
3.2.2 Camptothecin Incubation.....	35
3.3 <i>IEX-1</i> Promoter Activity.....	36
3.4 Localization of <i>IEX-1</i> Protein in HaCaT Cells .....	37
3.4.1 <i>IEX-1</i> Localization in HaCaT Cells by GFP-Tagging .....	37
3.4.2 <i>IEX-1</i> Immunostaining in HaCaT Cells.....	38
3.5 <i>IEX-1</i> Overexpression - Influence on Cell Responses.....	40
3.5.1 <i>IEX-1</i> Overexpression: mRNA Levels in Transfected HaCaT Cells.....	40
3.5.2 [ <sup>3</sup> H]-Thymidine Incorporation Growth Assays: ZEO versus IEX Cells ....	40
3.5.3 Induction of Apoptosis in <i>IEX-1</i> Overexpressing Cell Lines .....	42
3.5.4 Serum Deprivation.....	47
3.6 Localization of <i>IEX-1</i> in Skin Tissue .....	49
4. Discussion.....	50
4.1 Discussion of Methods .....	50
4.2 Discussion of Results.....	53
4.3 Conclusions .....	64
4.4 Future Perspectives in <i>IEX-1</i> Research.....	65
5. Summary.....	67
6. References.....	68
Figures and Tables .....	78
Acknowledgements.....	79
Lebenslauf.....	80

---

## Abbreviations

BPE	Bovine Pituitary Extract
BSA	Bovine Serum Albumine
CDK	Cyclin Dependent Kinase
DEPC	Diethylpyrocarbonate
EGF	Epidermal Growth Factor
EGFR	Epidermal Growth Factor Receptor
FASL	FAS Ligand
FITC	Fluorescein-Isothiocyanate
GAPDH	Glyceraldehyde-3-Phosphate-Dehydrogenase
GFP	Green Fluorescent Protein
HaCaT	Human adult low Calcium high Temperature
HK	Human Keratinocytes
IEX	HaCaT cell line overexpressing the IEX-1 gene
IEX-1	Immediate Early X-Ray Gene 1
IEX-1L	Long variant of IEX-1
LSM	Laser Scanning Microscope
M <sub>R</sub>	Molecular Mass
PBS	Phosphate Buffered Saline
PCD	Programmed Cell Death
PKC	Phosphokinase C
ROS	Reactive Oxygen Species
SDS	Sodium-Dodecylsulfate
SSC	Sodium Chloride/Sodium Citrate
TBS	Tris Buffered Saline
TE	Tris/EDTA
TIS	Transcription Initiation Site
TPA	12-0-Tetradecanoyl-13-Acetate
Tris	Tris(hydroxymethyl)aminomethane
UVR	Ultraviolet Radiation
ZEO	HaCaT transfected with sham Zeocin expression vector

## I. Zusammenfassung

Zelluläre Mechanismen als Antwort auf Zellstress oder Zellschäden spielen eine wesentliche Rolle in der physiologischen Verteidigungsstrategie gegen hyperproliferative Krankheiten, genotoxische Schäden, Mutationen oder maligne Entartung. Die Expression von *Immediate Early* Genen, die nachfolgende zelluläre Ereignisse initiieren und koordinieren, ist ein wichtiger erster Schritt der zellulären Stressantwort.

*IEX-1* ist ein vor kurzem entdecktes *Immediate Early* Gen, von dem gezeigt werden konnte, dass es durch die Einwirkung von Gammastrahlen, Phorbolestern und Ultraviolettstrahlung induziert wird.

Ziel dieser Arbeit war es, die Funktion von *IEX-1* in der Stressantwort von Keratinozyten genauer zu charakterisieren. Nicht nur die zelluläre Antwort auf Stress, sondern auch die mitogene Stimulation und die Rolle von *IEX-1* in Bezug auf Apoptosereaktionswege sollten untersucht werden. Weiteres Interesse galt der Analyse der *IEX-1*-Proteinlokalisierung während dieser Ereignisse.

Mit Hilfe des Northern Blot Verfahrens konnte gezeigt werden, dass *IEX-1* nach Gamma-Bestrahlung von primären menschlichen Keratinozyten innerhalb von Minuten induziert und dann sehr rasch wieder herunter geregelt wird, ähnlich wie schon zuvor mit einer Keratinozyten-Tumorzelllinie gezeigt wurde. Außerdem bewirkte UV-Strahlung und Behandlung mit reaktiven Sauerstoffradikalen eine rasche, aber vorübergehende Induktion von *IEX-1*. Zusätzlich rief die Inkubation der Keratinozyten mit *epidermal growth factor* (EGF) erhöhte *steady state* Spiegel von *IEX-1* mRNA hervor.

Ähnliche Beobachtungen konnten an der HaCaT-Zelllinie, einer nicht-tumorigenen Keratinozytenlinie gemacht werden.

Die Regulation der *IEX-1*-Genexpression durch den *epidermal growth factor*-Rezeptor (EGFR) wurde mittels eines *IEX-1*-Promotor – Luciferase Assays untersucht. Dabei wurde der EGF-Rezeptor mit dem hochspezifischen EGFR-Tyrosinkinaseinhibitor PD153035 blockiert. Der Rezeptorblockade folgte ein starker Rückgang der *IEX-1*-Promotoraktivität.



Die Auswirkungen der Überexpression von *IEX-1* in HaCaT-Zellen wurde untersucht. Wachstumsstudien mit [3H]-Thymidin-Inkorporationsassays ergaben, dass *IEX*-Überexpression das Wachstum beschleunigt. Um die Auswirkungen von *IEX-1* auf die Apoptose zu untersuchen, wurden *IEX-1* überexprimierende HaCaT-Zellen mit ultravioletter Bestrahlung, dem DNA-toxischen Agens Captothecin oder Serumentzug behandelt. Die Apoptoserate wurde mittels Caspase-3-Enzymaktivität und Oligonucleosomenbildung im Zellplasma quantifiziert. Die entsprechenden Assays konnten erstmalig für adhärente Keratinozytenkulturen etabliert werden. Unter normalen Wachstumsbedingungen ohne Stress konnte kein Unterschied in der basalen Apoptoserate zwischen *IEX-1*-überexprimierenden Zellen und Kontrollzellen beobachtet werden. Wurden die Zellen jedoch Stress ausgesetzt, dann trat in den *IEX-1*-überexprimierenden Zellkulturen in erhöhtem Maße Apoptose auf.

Das *IEX-1*-Protein konnte mit immunhistochemischen sowie molekularbiologischen Methoden vorwiegend im Zellkern lokalisiert werden, wo es sich in unterschiedlicher Verteilung zeigte. Stressinduzierende Behandlung der Zellen konnte keine Translokation des Proteines oder eine Veränderung im Verteilungsmuster bewirken. Untersuchung an menschlicher Epidermis mittels immunhistochemischer Färbung zeigte, dass *IEX-1* hauptsächlich in den basalen und suprabasalen Schichten der Epidermis exprimiert wird.

Mit diesen Ergebnissen konnte erstmals gezeigt werden, dass *IEX-1* eine wichtige Rolle sowohl in der Kontrolle der Apoptose als Folge von Zellstress, als auch in der Vermittlung von Zellreplikation unter optimalen Wachstumsbedingungen zukommt. Die Wirkung von *IEX-1* scheint dabei eng an den Differenzierungsstatus der Keratinozyten gebunden zu sein. Als Produkt eines *Immediate early* Gens spielt *IEX-1* eine Rolle in der Vermittlung von Keratinozytenwachstum und Keratinozytenüberleben, ähnlich wie die wichtigen Zellzyklusproteine *p53*, *p21<sup>Waf1</sup>*, *c-myc* und andere verwandte Proteine. Damit zeichnet es sich als ein weiterer elementarer Baustein im Mosaik der Reaktionswege zur Regulierung von Zellwachstum und Bekämpfung von maligner Entartung ab.

## II. Abstract

Cellular stress and damage response mechanisms play a crucial role in physiological defense against hyperproliferative diseases, genotoxic injury, mutations and malignancy. An important first step in the cellular stress response is upregulation of immediate early genes that initiate and coordinate subsequent cellular events.

*IEX-1* is a novel immediate early gene that has been shown to be induced by gamma irradiation, phorbol ester treatment and ultraviolet irradiation.

Goal of this thesis was to more specifically characterize the role of *IEX-1* in keratinocytes. Special emphasis was directed to elucidating the cellular response to stress and mitogenic stimulation and the role of *IEX-1* in mediating apoptosis as well as localizing the protein within the cell during these events.

By northern blot analysis, it could be shown that gamma irradiation of primary human keratinocytes results in a time dependent, rapid induction of *IEX-1* expression followed by prompt downregulation, similar to previous findings in a squamous cell carcinoma cell line. In addition, UV-irradiation or treatment with the reactive oxygen species hydrogen peroxide also induced *IEX-1* expression rapidly and transiently. Further incubation with the mitogenic factor for keratinocyte Epidermal Growth Factor (EGF) resulted in increased steady state levels of *IEX-1* mRNA.

Compared to normal keratinocytes, similar observations were made in the non-tumorigenic keratinocyte cell line HaCaT.

Regulation of *IEX-1* gene expression by the EGF-Receptor (EGFR) was investigated using an *IEX-1*-promoter-luciferase-reporter-gene assay and blockage of EGFR by the highly specific EGFR-tyrosine kinase inhibitor PD153035. Blockage of the receptor was followed by a marked decrease in *IEX-1* promoter activity.

Effects of *IEX-1* overexpression in HaCaT cells were investigated. *IEX-1* overexpression enhanced proliferation, as confirmed by [3H]-thymidine incorporation assay. To examine the effects of *IEX-1* on apoptosis induced by various agents, *IEX-1* over-expressing HaCaT were challenged with ultraviolet radiation, the DNA damaging agent camptothecin or serum-deprivation. Cell survival, caspase 3-activity and nucleosome formation were measured to assess apoptosis. There was no difference

observed in baseline apoptotic activity of cells cultured under non-stressed conditions, when comparing the *IEX-1* overexpressing and the control cell line. However, upon stress-induction, the *IEX-1* overexpressing cells showed markedly higher levels of apoptosis.

Data characterizing the intracellular localization of *IEX-1* were obtained by immunohistochemical staining as well as by molecular biological methods. *IEX-1* was predominantly located within the cell nucleus, forming several intranuclear patches. Treatment with various stress-inducing agents did not significantly alter the localization or cause translocation of the *IEX-1* protein.

Distribution of *IEX-1* within the skin and epidermis was assessed by immunocytochemistry of human skin specimens and revealed predominant localization of *IEX-1* within the nucleus and cytoplasm of the basal epidermal and suprabasal layers.

These findings implicate *IEX-1* in the control of apoptosis upon cell stress as well as promotion of cell replication during favorable growth conditions. The function of *IEX-1* seems to be closely linked to the differentiation status of the keratinocyte. As an immediate early gene product, *IEX-1* is a novel regulator of keratinocyte growth and survival, similar to other critical cell cycle control proteins, such as *p53*, *p21<sup>Waf1</sup>*, *c-myc* and related proteins. This suggests that *IEX-1* is another crucial element in the pattern of regulatory pathways of cell growth and defense against malignant transformation.



## 1. Introduction

Molecular mechanisms mediating the cell response to damaging stress have recently gained scientific interest. These cellular responses play crucial roles in preventing tumorigenesis or dysregulated and excessive cell growth. Many of the mechanisms and agents that lead to cancer growth, such as exposure to sunlight or toxic chemical agents, and their impact on the damage of the cellular genome are beginning to be identified [1,2]. However, little is known about the specific intracellular molecular mechanisms that suppress or promote tumorigenesis. A more complete understanding of the control, function and mode of action of these molecular stress responses will be important in future therapeutic approaches against cancer and other hyperproliferative diseases [3].

Critical physiological defense mechanisms protecting against malignant mutation after exposure of cells to DNA damaging events include cell cycle growth arrest and DNA repair or cell death, including apoptosis, the latter being a form of programmed cell suicide. Either of these cellular decisions is a suitable mechanism to prevent a mutated cell from entering a hyperproliferative state and endangering the whole organism [4,5]. Some of these defense mechanisms are initiated and controlled as part of the immediate early cell stress response that occurs within minutes to one hour of the event. The early phase of the stress response is associated with activation of intracellular kinase pathways that lead to rapid and transient induction of so-called immediate early genes and transcription factors that, in turn, regulate progression through the cell cycle or growth arrest, DNA and cell repair, or apoptosis [6-8] (Figure 1).

*IEX-1* is a novel member of the immediate early response gene family. It is rapidly induced by known carcinogens, such as  $\gamma$ - and UV-B radiation, and the tumor promoting agent 12-O-tetradecanoyl-13-acetate (TPA) [9]. *IEX-1* seems to enhance proliferation, and its expression might be regulated by cellular differentiation [10,11]. However, the function and regulatory pathways in *IEX-1* expression and activity remain undefined. The investigations in this thesis further characterize the role of *IEX-1* in terms of cell growth, differentiation and apoptosis, using a keratinocyte culture model.

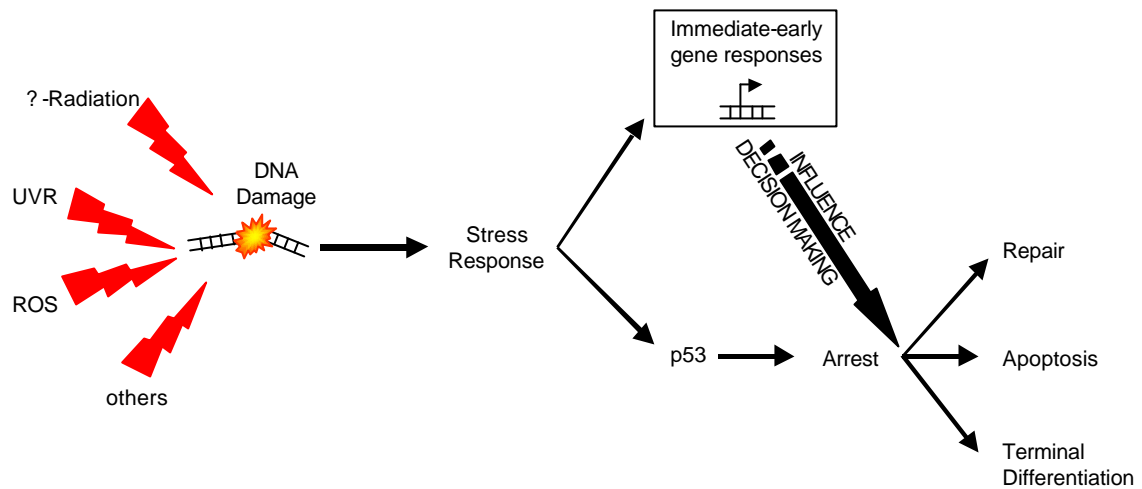


**Figure 1. Cellular Stress Responses.** Cells are stressed by different stimuli that can lead to DNA damage. DNA damage results in activation of different enzymatic pathways that eventually lead to changes in cell cycle progression. The cell may enter a growth arrest phase, proceed to irreversible terminal differentiation, repair the cell damage or, in case of irreparable damage, undergo programmed cell death. p53 is an important cell cycle regulatory gene that plays a key role in mediating either repair, apoptosis or terminal differentiation. Immediate early genes influence the future destiny of the cell.

### 1.1 Epidermis: Structure and Differentiation

The epidermis is a highly differentiated and specialized tissue with morphologically distinctive strata of keratinocytes that form discrete, functionally different layers [12,13]. In the basal layer, undifferentiated stem cells are found. With their controlled mitotic activity, stem cells are responsible for the continuous self-renewing growth characteristics of the epidermis [14,15]. During this process, daughter cells migrate, after few cycles of amplification, in about four weeks from the basal layer to the surface where they then cornify and nonviable cells finally are desquamated [14,16]. The metamorphosis from the postmitotic, barely differentiated keratinocyte to the fully cornified, enucleated corneocyte is called terminal differentiation and has been considered by some investigators being a form of programmed cell death [17-19]. Early in the course of terminal differentiation, the cell irreversibly loses its ability to progress through the cell cycle and replicate [20]. It is likely that loss of ability to divide and induced expression of the differentiated phenotype are closely linked events [20,21]. The phenotypical changes are marked by changes in cell size and shape, and are accompanied by dehydration [22]. On their way to the surface the keratinocytes express a variety of enzymes, cytoskeletal and membrane proteins that are typical for the different layers in the epidermis. They can be regarded as

differentiation markers: Involucrin and transglutaminase are early differentiation markers in the stratum spinosum, while loricrin, filaggrin and differentiated keratins are widely expressed throughout the stratum granulosum [13,22,23] (Figure 2).

The molecular mechanisms regulating initiation and commitment to terminal differentiation still are poorly understood. There is evidence that not only interaction of para- and autocrine soluble growth factors with their receptors, but also communication between the extracellular matrix and membrane-bound integrin as well as shape and tension of the replicating keratinocyte influence subsequent cellular development [24,25]. Signaling cascades induced by these mediators eventually lead to the regulation and expression of immediate early genes that encode for transcription factors. These transcription factors, in turn, control genes that eventually lead to changes in cell cycle progression and induction of terminal differentiation or apoptosis [22,26,27].

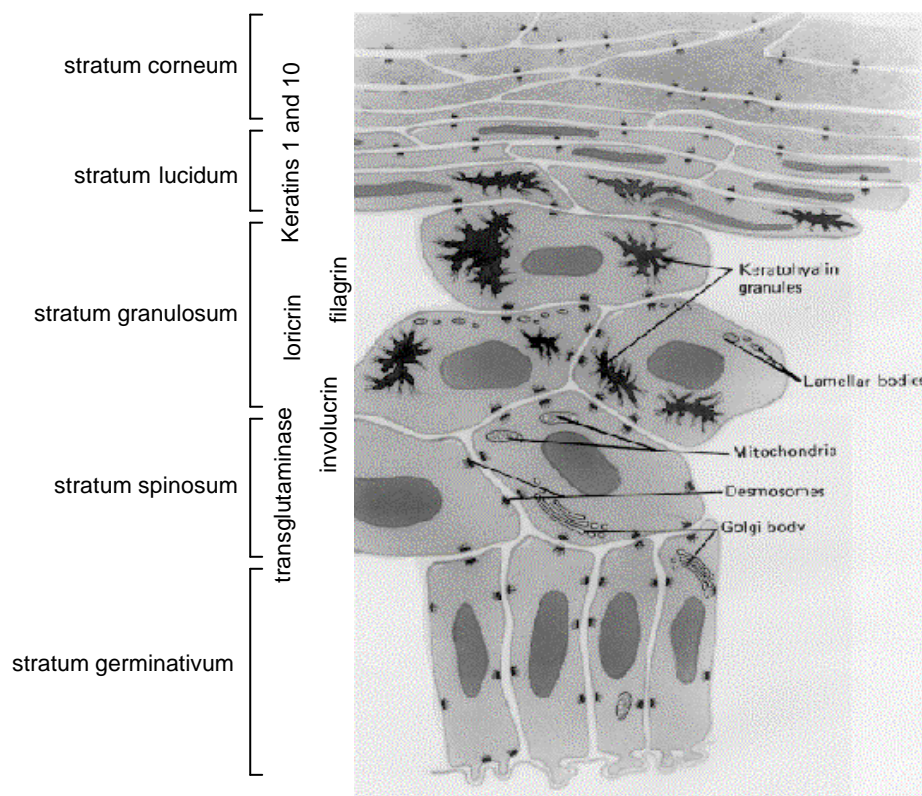


**Figure 2. Structure of Epidermis** (modified from Montagna and Mischke [13]) The epidermis consists of different layers that are characterized by morphology and expression of distinct differentiation markers.

## 1.2 The Human Epidermal Growth Factor Receptor (EGFR)

EGFR is widely expressed on nucleated cells, except for melanocytes and select cell lineages within the hematopoietic system [28]. In normal human skin, EGFR shows a typical distribution pattern with greatest abundance in the basal, proliferative layers and lower abundance in the upper, differentiated layers [29]. Altered EGFR expression is associated with a variety of pathological conditions. For example, EGFR is expressed throughout all epidermal layers of various hyperproliferative skin diseases, such as psoriasis [30,31]. Many epithelial cancers show overexpression, amplification or mutation of EGFR, with exaggerated EGFR expression, being associated with a poorer clinical prognosis [32,33].

The epidermal growth factor receptor is a transmembrane glycoprotein tyrosine kinase that consists of an extracellular ligand binding domain, a transmembrane domain and an intracellular protein kinase domain [28]. Association of Epidermal Growth Factor (EGF), a representative ligand for EGFR, to the binding domain of EGFR mediates homo-dimerization of the receptor, resulting in activation of the cytoplasmic receptor phosphotyrosine kinase [34]. This activated receptor complex is able to phosphorylate intracellular substrates, such as Ras, which, in turn, act as second messengers and initiate downstream phosphorylation of intracellular signal transducers that mediate cell cycle progression, DNA synthesis and mitosis [35,36]. The receptor is inactivated by internalization of the receptor-ligand-complex, fusion with lysosomes, and subsequent recycling to the membrane [37,38].

EGFR is not only activated by specific ligand-receptor interaction but also by rather non-specific chemical or physical stimuli (stress signals), such as UVR and radicals. There is also evidence that the EGFR phosphorylation domain can be activated by different internal reaction pathways [26,39]. This indicates that EGFR mediated signaling is not a linear transduction pathway, but is integrated as part of a complex communication network that enables cellular adaptation of growth and proliferation to internal and external stimuli [26].

EGFR signaling can be inhibited by blocking autophosphorylation of the autocatalytic EGFR domain [39]. The agent PD153035 is a potent and highly specific inhibitor of the EGF receptor tyrosine kinase and does not influence the expression of EGFR mRNA levels [40,41]. Besides having therapeutic potential in the treatment of EGF-dependent tumors, where EGFR blockade can decrease tumor cell proliferation and



induce apoptosis, PD153035 is a useful tool for in vitro investigation of EGFR dependent pathways [42].

### 1.3 Apoptosis and its Role in the Epidermis

Apoptosis is a special cellular mechanism for Programmed Cell Death (PCD) and is a critical growth regulatory mechanism in multicellular organisms. Apoptosis eliminates aged, damaged or mutated cells and maintains tissue integrity. Apoptosis therefore serves as a critical function for the organism in cancer defense, control of the immune response and in organ development [43,44].

Apoptosis is a highly coordinated, energy dependent and genetically determined event that is characterized by expression of distinct morphological features, activation of specific proteolytic enzymes, e.g. caspases, cell shrinkage, membrane changes, and non-random degradation of DNA into oligonucleosomes [45,46]. Apoptosis has been termed physiologic cell death, in contrast to necrosis, that displays typical features of pathologic cell death (Table 1).

Whether a cell undergoes necrosis or apoptosis depends on various factors, including the strength and properties of the insult or stress-induced stimulus, and the differentiation state of the cell [47,48].

<b>Necrosis</b>	<b>Apoptosis</b>
<b>Morphology</b>	
<ul style="list-style-type: none"> <li>• Loss of membrane integrity</li> <li>• Swelling of cytoplasm and organelles</li> <li>• Complete cell lysis</li> </ul>	<ul style="list-style-type: none"> <li>• Membrane blebbing, maintained integrity</li> <li>• Shrinkage of cytoplasm, condensation of cytoplasm</li> <li>• Fragmentation of cell into membrane bound vesicles</li> </ul>
<b>Biochemistry</b>	
<ul style="list-style-type: none"> <li>• Passive process, no energy-requirement</li> <li>• Early loss of ion homeostasis</li> <li>• Random digestion of DNA</li> </ul>	<ul style="list-style-type: none"> <li>• Energy-dependent process</li> <li>• Tightly regulated enzyme cascades</li> <li>• Non-random DNA-fragmentation</li> </ul>
<b>Physiology</b>	
<ul style="list-style-type: none"> <li>• Groups of cells affected at same time</li> <li>• Evoked by non-physiologic insult</li> <li>• Inflammatory response</li> </ul>	<ul style="list-style-type: none"> <li>• Individual cells affected</li> <li>• Induced by physiologic stimuli</li> <li>• No inflammatory response</li> </ul>

**Table 1. Features of Necrosis and Apoptosis.** (modified from Eisel D, “Apoptosis and Cell Proliferation” [49])

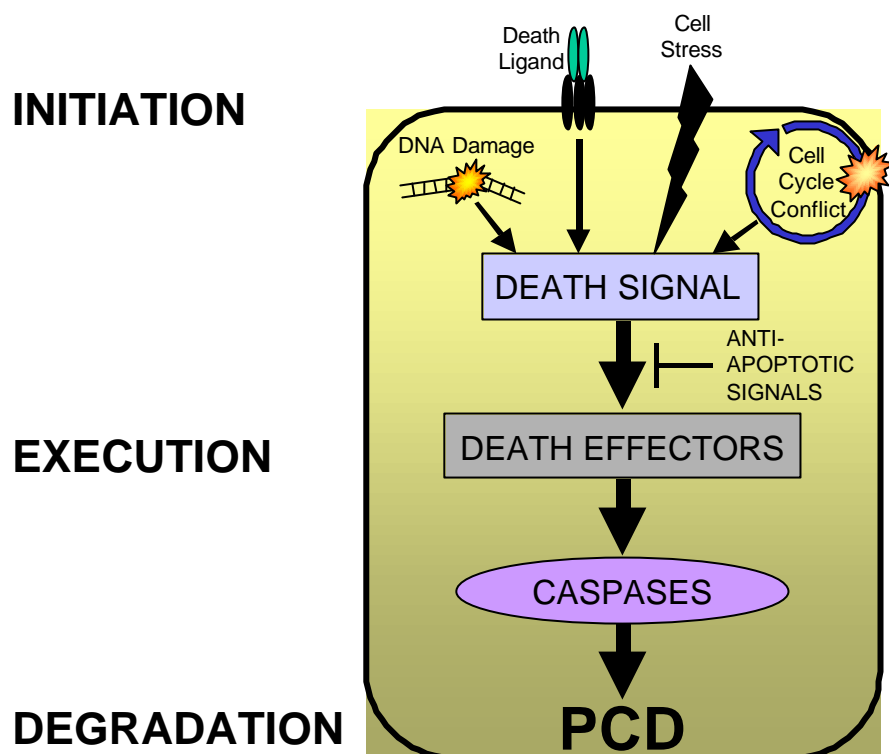


**Figure 3. Stages in Apoptosis.**

The process of apoptosis can be divided into three separate stages: the *initiation phase*, when the cell is exposed to an apoptotic stimulus, the *execution phase*, when activities of pro-apoptotic and anti-apoptotic pathways converge and determine the eventual fate of the cell, and finally the *degradation phase*, which is the critical, irreversible point, when enzyme cascades are activated and the cell triggers its suicide program [50]. Apoptosis is initiated by a variety of different stimuli that eventually converge into a common death program. Activation of membrane bound death receptors [51], oxidative stress [52], DNA damage [53] and growth-factor depletion [54] have been shown to force cells into apoptosis. Conflicting intracellular signals during passage through the cell cycle (cell cycle conflict) can lead to cellular activation of the suicide program [55]. All these triggers cause recruitment of different pro-apoptotic and anti-apoptotic pathways, resulting in a stronger or weaker death signal. In the execution phase, the eventual fate of the cell is being defined, in such that the cell could be committed to die, with activation of the central executioner apparatus of the cell. The degradation phase is initiated by activating proteolytic

enzyme cascades, known as caspases, that lead to inactivation of protective, anti-apoptotic proteins and activation of a pro-apoptotic complex of proteins, and result in disassembly of the cell [4,56,57] (Figure 3).

Several studies have implicated that terminal differentiation of keratinocytes in the epidermis may represent a form of programmed cell death. Despite of morphologic and biochemical parallels between apoptosis and epidermal terminal differentiation, it is not clear whether normal keratinocyte terminal differentiation is a form of apoptosis. There is strong evidence *in vivo*, as well as *in vitro*, that terminal differentiation and apoptosis are distinct cellular events, regulated by different stimuli [58].

The relevance of apoptosis in epidermal pathology has been shown for a number of skin diseases. For example, various forms of alopecia or lichen planus have been reported to be associated with extensive apoptosis, whereas psoriasis and some carcinomas of the skin show inhibition of apoptosis [59]. The occurrence of so-called sunburn cells in the epidermis after UV irradiation also reflect the morphological properties of maintenance of tissue integrity by apoptosis [60] and exhibits molecular features of apoptosis [61]. Similarly, keratinocytes *in vitro* also have been shown to undergo apoptosis after ultraviolet irradiation [62].

#### **1.4 The Immediate-Early-X-Ray-Gene-1 (*IEX-1*)**

Several research groups have independently discovered and investigated *IEX-1*. For this reason, different names have been ascribed to the same gene. *IEX-1*, *DIF-2* and *p22/PRG1* are designations for the same gene, as analysis of the GeneBank data reveals [63]. In this work *IEX-1*, the name assigned in the first publication, will be used.

*IEX-1* was first discovered in a squamous cell carcinoma cell line which had been exposed to X-ray irradiation. The gene meets all criteria of a radiation induced immediate early gene: Rapid induction within 15 minutes after 10 Gy gamma-irradiation, independent of *de novo* protein synthesis, rapid degradation of mRNA, and possible mediation by a PKC-dependent pathway. Because of its characteristics, the newly described gene was named Immediate Early X-Ray Gene-1 (*IEX-1*) [9].

The 1.2 kb gene transcript of *IEX-1* is translated into a 156 amino acid protein with a molecular mass ( $M_R$ ) of 20,000 and a predicted isoelectric point between 8.85 and 9.0.

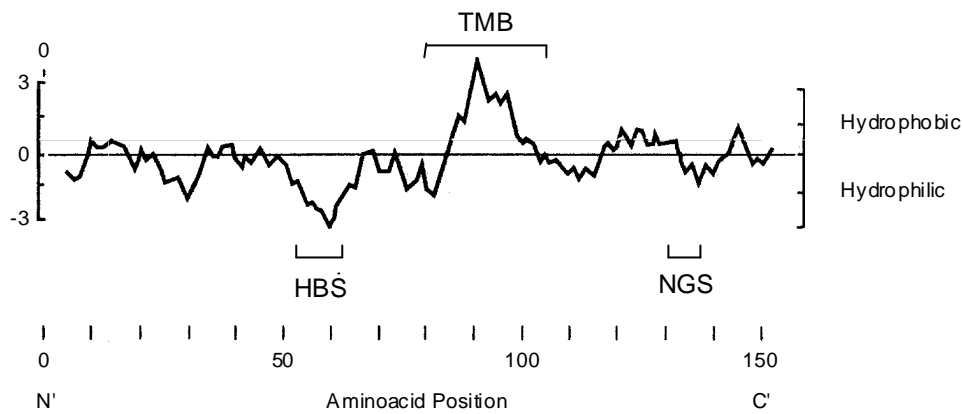


**Figure 4. Protein Structure of *IEX-1*.** (Modified from Kondratyev et al. [9])  
 TMB: Transmembrane Domain; HBS: Histone Binding Site; NGS: N-Glycosylation Site

Computer analysis revealed a putative transmembrane domain and a histone binding sequence. In the presence of microsomal membranes, the protein occurs in a glycosylated form, with a  $M_R$  of 26,000 [9,11] (Figure 4).

By *in situ* hybridization, the gene was located on chromosome 6, p21.3. Known genes in this region exhibit no structural and functional similarities [64]. No other human homologues have been detected, but there is strong homology to *gly96* and *PRG1*, mouse and rat genes, respectively, yet also with unknown function, that previously have been reported to be growth factor inducible immediate early genes [64-66].

The *IEX-1* gene consists of two exons and a single 112bp intron sequence, similar to the published mouse and rat genes [64]. The existence of a long form of *IEX-1*, called *IEX-1L*, had also been reported. The *IEX-1L* transcript was thought to be the result of alternative splicing, preserving the intron sequence. This insertion results in a polypeptide that is 37 amino acids longer than *IEX-1* [67]. However, existence of *IEX-1L* has recently been disputed and attributed to an artificial, mutated variant that is not expressed *in vivo* [68].

The 5' flanking region of the *IEX-1* gene shows high conservation between the mouse, rat and human homologues. There are common binding sites for the transcription factors *NFκB* and *SP1* within a minimal promoter element. The gene possesses only one specific transcription initiation site (TIS) [64]. Furthermore, there is a functional binding site for *p53* in the promoter region of the human gene [69].

*IEX-1* is strongly upregulated following treatment of cells with stress-inducing stimuli, such as  $\gamma$ -radiation, TPA or the death factor ligand FASL [9,67].

*IEX-1* mRNA is highly expressed in several cell types. Monocytes strongly express *IEX-1*, and the transcript is significantly downregulated upon cell differentiation to macrophages [11]. Treatment of human keratinocytes with 1,25-Vitamin D<sub>3</sub> at concentrations that induce growth arrest and differentiation markers in keratinocytes resulted in the initial downregulation of *IEX-1* expression, followed by marked upregulation several days later. Similar changes in *IEX-1* expression were observed in keratinocytes upon reaching confluency in cell culture: *IEX-1* mRNA expression initially decreased and then increased with post-confluent culture [10,70].

*In vivo* *IEX-1* mRNA and protein are abundant in epithelial tissues with a high cell turn over rate, such as GI-tract and vascular endothelium, and are less abundant in tissues with low cell turnover, such as brain [10,71].

<b>Treatment</b>	<b><i>IEX-1</i> mRNA</b>	<b>Cell Type</b>	<b>Reference</b>
X-Ray	↑	SCC-35	Kondratyev et al., 1996
TPA	↑	SCC-35; HK	Kondratyev et al., 1996
UV-B	↑	HK	Kumar et al., 1998
Differentiation	↓	Monocytes	Pietzsch et al., 1998
1,25-D <sub>3</sub>	↓ → ↑	HK	Kobayashi et al., 1998
Confluency	↓ → ↑	HK	Kobayashi et al., 1998
FASL	↑	Jurkat	Wu et al., 1998

**Table 2. Overview of *IEX-1* Features.**

### 1.5 Objectives of the Study

The previous findings on *IEX-1* lead to the conjecture that *IEX-1* is involved in the cellular stress response and also may mediate proliferation. Further, *IEX-1* might play a role in cell differentiation.

The goal of this thesis was to investigate the function of the novel early response gene *IEX-1* in human keratinocytes and the keratinocyte-derived human cell line HaCaT as model-systems for epithelial cell growth and differentiation. Particular emphasis was put on the investigation of the role of *IEX-1* in mediating proliferation, cellular differentiation and apoptosis in keratinocytes.

*IEX-1* expression in response to stress-inducing stimuli in human keratinocytes and HaCaT were investigated by Northern blot. *IEX-1* promoter studies using a reporter gene-assay were performed to elucidate possible pathways involved in *IEX-1* regulation.

The effects of *IEX-1* on proliferation, programmed cell death and differentiation were examined by gene overexpression experiments in HaCaT cells, with the intent to define possible roles of *IEX-1* in the cellular stress response and growth controlling signaling pathways.

Proliferation was assessed with [3H]-thymidine incorporation assays. Apoptosis was induced by UV-B radiation, chemotoxic exposure and serum withdrawal, and cell responses were evaluated with two different apoptosis assays.

Intracellular localization of *IEX-1* protein was investigated by immunostaining and laser-confocal microscopy of Green Fluorescent Protein (GFP)-tagged *IEX-1* protein in transfected HaCaT cells.

Epidermal distribution of *IEX-1* was determined to yield further indications of possible functions of the gene in tissue homeostasis.

## 2. Materials and Methods

### 2.1 Materials

#### 2.1.1 Chemicals

All chemicals used were obtained from SIGMA (St. Louis, MO) unless stated otherwise.

Reagents were weighed on a Sartorius 1202 NP balance. A Mettler AE160 balance was used for weights below 1 mg.

Buffers and solutions were prepared with sterile water de-ionized in a Millipore Milli Q Water System.

Reagents were pH-adjusted at room temperature with a Corning pH-Meter 140.

#### 2.1.2 Tissue Culture Materials and Working Solutions

For this thesis primary human keratinocytes and keratinocyte derived cell lines were used. The spontaneously immortalized keratinocyte cell line HaCaT was a generous gift from Dr. Fusenig (Heidelberg, Germany).

The transfected HaCaT cell lines IEX and ZEO, as well as the HaCaT cell line transfected with the luciferase promoter construct, were established as described in the methods section.

Human neonatal foreskin specimens for the preparation of keratinocyte cultures were obtained from Rochester Methodist Hospital.

All growth media for keratinocytes as well as for HaCaT cells were supplemented with penicillin (50 U/ml) and streptomycin (50 µg/ml) as precautionary measure to prevent bacterial contamination of the cell cultures.

All cell lines were incubated at 37°C in a humidified atmosphere containing 5% CO<sub>2</sub> and 95% air.

### 2.1.2.1 Growth Media for Keratinocytes

For keratinocyte culture, depending on the desired conditions, three different growth media were used. All three were based on the MCDB153 basal medium.

MCDB153 basal medium Contains: Arginine•HCl ( $1 \times 10^{-3}$  moles/l), Histidine•HCl•H<sub>2</sub>O ( $8 \times 10^{-3}$  moles/l), Isoleucine ( $1.5 \times 10^{-3}$  moles/l), Leucine ( $5 \times 10^{-2}$  moles/l), Lysine•HCl ( $1 \times 10^{-2}$  moles/l), Methionine ( $3 \times 10^{-3}$  moles/l), Phenylalanine ( $3 \times 10^{-3}$  moles/l), Threonine ( $1 \times 10^{-2}$  moles/l), Tryptophan ( $1.5 \times 10^{-3}$  moles/l), Tyrosine ( $1.5 \times 10^{-3}$  moles/l), Valine ( $3 \times 10^{-2}$  moles/l), Choline chloride ( $1 \times 10^{-2}$  moles/l), Serine ( $6 \times 10^{-2}$  moles/l), Biotin ( $6 \times 10^{-6}$  moles/l), Ca pantothenate ( $1 \times 10^{-4}$  moles/l), Niacinamide ( $3 \times 10^{-5}$  moles/l), Pyridoxine HCl ( $3 \times 10^{-5}$  moles/l), Thiamine HCl ( $1 \times 10^{-4}$  moles/l), KCl ( $1.5 \times 10^{-1}$  moles/l), Folic acid ( $9 \times 10^{-5}$  moles/l), Na<sub>2</sub>HPO<sub>4</sub>•7H<sub>2</sub>O ( $1 \times 10^{-1}$  moles/l), CaCl<sub>2</sub>•2H<sub>2</sub>O ( $2 \times 10^{-1}$  moles/l), MgCl<sub>2</sub>•6H<sub>2</sub>O ( $6 \times 10^{-1}$  moles/l), FeSO<sub>4</sub>•7H<sub>2</sub>O ( $5 \times 10^{-3}$  moles/l), Phenol Red ( $3.3 \times 10^{-3}$  moles/l) Riboflavin ( $1 \times 10^{-4}$  moles/l), Asparagine ( $1 \times 10^{-2}$  moles/l), Proline ( $3 \times 10^{-2}$  moles/l), Putrescine ( $1 \times 10^{-4}$  moles/l), Vitamin B<sub>12</sub> ( $3 \times 10^{-5}$  moles/l), Alanin ( $1 \times 10^{-2}$  moles/l), Aspartic Acid ( $3 \times 10^{-3}$  moles/l), Glutamic Acid ( $1 \times 10^{-2}$  moles/l), Glycine ( $1 \times 10^{-2}$  moles/l), Adenine ( $1.8 \times 10^{-2}$  moles/l), myo-Inositol ( $1 \times 10^{-2}$  moles/l), Lipoic Acid ( $1 \times 10^{-4}$  moles/l), Thymidine ( $3 \times 10^{-4}$  moles/l),



$\text{CuSO}_4 \cdot 5\text{H}_2\text{O}$  ( $1 \times 10^{-6}$  moles/l),  $\text{CuSO}_4 \cdot 5\text{H}_2\text{O}$  ( $1 \times 10^{-7}$  moles/l),  $\text{H}_2\text{SeO}_3$  ( $3 \times 10^{-6}$  moles/l),  $\text{MnSO}_4 \cdot 5\text{H}_2\text{O}$  ( $1 \times 10^{-7}$  moles/l),  $\text{Na}_2\text{SiO}_3 \cdot 9\text{H}_2\text{O}$  ( $5 \times 10^{-5}$  moles/l),  $(\text{NH}_4)_6\text{MO}_7\text{O}_{24} \cdot 4\text{H}_2\text{O}$  ( $1 \times 10^{-7}$  mol/l),  $\text{NH}_4\text{VO}_3$  ( $5 \times 10^{-7}$  moles/l),  $\text{NiCl}_2 \cdot 6\text{H}_2\text{O}$  ( $5 \times 10^{-8}$  moles/l),  $\text{SnCl}_2 \cdot 2\text{H}_2\text{O}$  ( $5 \times 10^{-8}$  moles/l),  $\text{ZnSO}_4 \cdot 7\text{H}_2\text{O}$  ( $5 \times 10^{-5}$  moles/l)

Also added per four liters of medium:

Glucose 4.324 g, NaCl 30.398 g, HEPES 26.4 g, NaAcetate 2 g $\cdot$ 3H<sub>2</sub>O, L-Glutamine 3.5 g, NaPyruvate 0.22 g, Cysteine 0.168 g, NaHCO<sub>3</sub> 4.704 g after adjusting the pH to 7.4

Standard Medium (GF-)	MCDB153 supplemented with: 0.1mmol/l Calcium Chloride, 0.1mmol/l Ethanolamine, 0.1 mmol/l Phosphoethanolamine, $5 \times 10^{-7}$ mol/l Hydrocortisone
Defined Medium	Standard Medium supplemented with growth factors: 10 ng/ml EGF, 0.5 mg/l Insulin
Complete Medium (GF+)	Defined Medium supplemented with 140 mg/l bovine pituitary extract (BPE)
Bovine Pituitary Extract	150 grams of bovine pituitaries (both sexes, Pel Freeze, Rogers, AR) were homogenized in 250 ml cold 0.15 M NaCl, stirred for 90 minutes at 4°C and then centrifuged (9800 rpm). Supernatant was stored at -70°C.

### 2.1.2.2 Growth Media for HaCaT Cells

HaCaT cells and all HaCaT derived cell lines were grown in Dulbecco's Modified Eagle Medium (DMEM, Mediatech Cellgro, Va, AK) supplemented with 10% Fetal Bovine Serum (FBS) (Gibco BRL, NY). For the stably transfected cell lines the specific selection antibiotic was added.

### 2.1.2.3 Working Solutions and Buffers

Solution A	10 mM Glucose, 3 mM KCl, 130 mM NaCl, 0,1419 g/l Na <sub>2</sub> HPO <sub>4</sub> , 0,0033 mM Phenol Red, 30 mM HEPES adjusted to pH 7,4 with 1 mM NaOH
Phosphate Buffered Saline (PBS)	80 mM Na <sub>2</sub> HPO <sub>4</sub> , 100mM NaCl, 20mM NaH <sub>2</sub> PO <sub>4</sub> .2H <sub>2</sub> O diluted to 1000 ml with distilled water – adjusted to pH 7.4 with 1 mM NaOH
Tris Buffered Saline (TBS)	100 mM Tris pH7.4, 138 mM NaCl, 27 mM KCl

### 2.1.3 DNA Vectors

pcDNA3.1/zeo(-)	Invitrogen, Carlsbad, CA
pGL3, pRL-TK	Promega, Madison, WI
EGFP/C1, EGFP/N1	Clontech Laboratories, Palo Alto, CA

### 2.1.4 Antibodies, Ligands and Inhibitors

Camptothecin	SIGMA, St. Louis, MO
EGF	Collaborative Research, Madison, WI (cat# 4001)

PD153035	Parke-Davis Pharmaceutical Research, MI, USA
Goat Anti-Rabbit IgG	Molecular Probes, Eugene, OR biotinylated (cat# B-2770) FITC (cat# F-2765)
<i>IEX-1</i> Ab	synthetic peptide, sequence: AGRPSASRGHRKRSRRALYPR (polyclonal Ab against portion of <i>IEX-1</i> , raised in rabbits, established in the laboratory of Biochemistry and Nephrology, Dr. R. Kumar as reported before [10,70].)

### 2.1.5 Solutions for Immunostaining

Fixation Solution	Methanol/Acetone (1:1)
Blocking Buffer	5% goat serum, 1% glycerol, 0.1% Bovine Serum Albumine (BSA), 0.1% fish skin gelatine, 0.04% Sodium Azide
ABC-Reagent	Vectastain ABC-Go kit (basic), Vector Laboratories, Burlingame, CA

### 2.1.6 RNA Solutions

Lysis Buffer	500ml: 5 ml 1M Tris-HCl, 10 ml 5M NaCl, 5 ml 0.2M EDTA, 429.5 ml H <sub>2</sub> O, 0.5 ml Diethylpyrocarbonate (DEPC), 50 ml 10% SDS
High Salt Buffer	500 ml: 5 ml 1M Tris-HCl, 50 ml 5.0M NaCl, 2.5 ml 0.2M EDTA, 432 ml H <sub>2</sub> O,

	0.5 ml DEPC, 10 ml 10% Sodium Dodecylsulfate (SDS)
Low Salt Buffer	500 ml: 5 ml 1M Tris-HCl, 10 ml 5M NaCl, 2.5 ml 0.2M EDTA, 472 ml H <sub>2</sub> O, 0.5 ml DEPC, 10 ml 10% SDS
No Salt Buffer	500 ml: 0.5 ml 1M Tris-HCl, 0.5 ml 0.2M EDTA, 97 ml H <sub>2</sub> O, 0.1 ml DEPC, 2 ml 10% SDS
Tris/EDTA-Buffer (TE-Buffer)	500 ml: 0.6055 g 1,0 M Tris Base, 0.186 g 0,2 M EDTA 2H <sub>2</sub> O, concentrated HCl to pH8
Hybridization Buffer	Amersham Life Sciences (hybridization buffer tablets)
Stripping Solution	2 ml 0.1% Sodium Chloride/Sodium Citrate (SSC), 20 ml 10% SDS, 378 ml H <sub>2</sub> O
Tracking Dye	50% glycerol, 1mM EDTA, 0.4% bromophenol blue, 0.4% xylene cyanol

### 2.1.7 Radioactive Materials

[ <sup>3</sup> H]-thymidine	NEN Research products, Delaware, USA (cat# NET-027Z)
[ $\alpha$ - <sup>32</sup> P]-dCTP	Amersham Life Sciences, Arlington Heights, IL, USA (cat# AA0005)

### 2.1.8 Molecular Size Markers

All molecular size markers were obtained from Gibco BRL, Life Technologies, MA

DNA Ladder	cat# 15612-013
RNA Ladder	cat# 15620-016
Protein Standard	cat# 161-0303

### 2.1.9 Technical Devices

Centrifuges	Beckman J-6M Beckman TJ-6 Beckman J2-21M Eppendorf Centrifuge 5417R
Computers/Software	Apple Power Macintosh, IBM, AcerNote Light programs: Microsoft Word 8, Microsoft Excel 5, Canvas 6, Adobe Photoshop 4, EndNote, Scion Image
Flourescence Plate Reader	Cytoflour II Platereader, PerCeptive Biosystems
Freezers and Refrigerators	Kenmore and Forma Scientific
Hybridization Oven	Hybaid micro-4, Labnet
Incubators	Forma Scientific
Microscopes	Phasecontrast: NIKON TMS, Edina, MN Confocal Laserscanning: LSM 310, Zeiss Jena, Germany
Photometer	IL1400A, International Light
$\gamma$ -Radiation Chamber	J.L. Shepard, San Fernando, CA
Spectrophotometer	Beckman DU-64, Arlington Heights, IL
Speed Vacuum	Savant Integrated Speedvac System ISS100
Stratalinker	UV Stratalinker 1800, Stratagene
Scintillation Counter	Beckman LS 3801
Tissue Culture Hood	Forma Scientific
UV-Lamp	FS20 UV-Lamp, Westinghouse

## **2.2 Cell Culture and Cell Lines**

### **2.2.1 Preparation of Foreskin Specimens**

Human keratinocytes were isolated from neonatal foreskin specimens using the methods previously described [72]. Skin specimens were obtained from Rochester Methodist Hospital 1-2 hours after routine circumcision of newborn infants.

In brief, after removing subcutaneous tissue with surgical scissors, the epidermis was separated from dermal tissue by overnight incubation in 0.17% trypsin/EDTA and subsequent mechanical splitting by repeated aspiration with a 5 ml pipet. After suspension in Solution A, cells were pelleted by centrifugation, dissolved in Defined Medium and passed into T75 culture dish flasks containing 10 ml of Complete Medium.

### **2.2.2 Passing the Cell Cultures**

These primary cultures were maintained in a replicative state by feeding cells Complete Medium every other day. Seven to nine days later, at about 90% confluency, primary cultures were split and plated into secondary culture: cells were trypsinized for 25 minutes. After trypsin inactivation by addition of 2% FBS in Solution A, a cell count was performed with a hemacytometer and cells were centrifuged at 1000 rpm for 10 minutes at 4°C. Supernatant was aspirated, the pellet suspended in Defined Medium and transferred into new T75 tissue culture dishes at a density between  $1-10 \times 10^3$  cells/cm<sup>2</sup>. For each experiment, cells of these secondary cultures were passaged, using the above described method, and plated into the tissue culture dishes needed and grown to desired cell density.

### **2.2.3 Culture of HaCaT Cells**

HaCaT cells were grown in DMEM medium, supplemented with 10% Fetal Bovine Serum. For some experimental conditions cells were switched to media without FBS (so called “-Serum”). Cell cultures were split and passaged as described for keratinocytes.

### 2.2.4 Transfected HaCaT Cells

The stably transfected cell lines were established by transfection of the plasmids into the parent HaCaT, using Lipofectamin (Gibco-BRL, Gaithesburg, MD) and subsequent selection by culturing cells in basic HaCaT growth medium, containing the plasmid-specific selection antibiotic at the required concentration as mentioned below.

To investigate effects of *IEX-1* overexpression, a cell line was established, transfected with an expression vector containing the full length cDNA *IEX-1* sequence downstream of a CMV promoter (*IEX-1*/pcDNA3.1/zeo(-)). Another cell line containing the empty expression vector (pcDNA3.1/zeo(-)) served as control through all experiments. Both cell lines were selected in DMEM medium containing 400 µg/ml Zeocin and cultured in medium supplemented with 200 µg/ml Zeocin.

For experiments concerning the *IEX-1* promoter region, the gene sequence ranging from -1419 basepairs upstream to the beginning of the *IEX-1* exon sequence was inserted into the pGL3 vector. This *IEX-1*-luciferase gene construct (-1419P<sub>*IEX-1*</sub>/pGL3) was transfected into HaCaTs and selected by culture in Geneticin (200 µg/ml).

## 2.3 Plasmid and Fragment Preparation

### 2.3.1 Transformation, Selection and Amplification of Bacteria

For multiplication of plasmids DH5 $\alpha$  Competent Cells (Gibco BRL Life Technologies Inc., Gaithesburg, MD) were transformed with plasmids by using the heat shock method.

100 µl bacterial stock was incubated on ice for 30 minutes with 10 ng plasmid-DNA. After heat shocking in a 42°C waterbath and subsequent chilling on ice for 2 minutes, bacteria were incubated for one hour with 900 µl LB medium in an incubator shaker to allow translation of resistancy genes. Bacteria were plated on LB-agarose containing the selecting antibiotic and incubated overnight at 37°C.

The next day a single colony was transferred with a sterile wireloop from the plate into 100 ml of LB-medium containing the selecting antibiotic and incubated for another 16 hours in an incubator shaker.

### 2.3.2 Plasmid/Fragment Preparation

Bacteria were harvested by centrifugation and supernatant was decanted.

Plasmid preparation was performed using the Quiagen Plasmid Maxi Kit (Quiagen Inc., Chatsworth, CA) according to the manufacturer's protocol. Extracted plasmid DNA was dissolved in 10mM Tris Cl (pH8.5). Subsequently, DNA concentration was determined, by measuring the optical density at 260 nm in a spectrophotometer. To control the plasmid yield qualitatively and to separate the fragments from vector-DNA, a DNA restriction digestion assay was performed: DNA fragments were visualized on a UV transilluminator, and the correct size was verified by comparison to a a molecular size marker (DNA ladder, DNA/HindIII: Gibco BRL Life Technologies Inc., Gaithesburg, MD). Fragments for Northern Blotting were cut out and purified with the QIAEX II Gel extraction kit (Quiagen Inc., Chatsworth, IN).

### 2.3.3 Transfection

FuGene6 (Boehringer Mannheim, Indianapolis, IN) was used for transient transfection of HaCaT and human keratinocytes. Cells were grown to about 60% confluence, growth medium was exchanged and the DNA-FuGene6 mixture was added, in the ratio DNA/FuGene of 5/8. The DNA amount per 24 well was 1.25 µg and 2.5 µg per 6 well, dissolved in 60 µl or 125 µl Solution A, respectively.

16 hours after transfection, cells were treated and incubated for the required periods. Incubation periods did not exceed 40 hours past transfection.

### 2.3.4 Plasmid Constructs

#### 2.3.4.1 IEX-1 Promoter-Luciferase Constructs

The putative full length *IEX-1* promoter sequence, up to 1419bp upstream of the *IEX-1* gene, was inserted into the multiple cloning site of the *pGL3* vector upstream of the luciferase gene.

For transient transfections with the *pGL3* vector, cells were cotransfected with the *pRL-TK* plasmid as a transfection efficiency control. The amount of *pRL-TK* DNA was 1/10 of *pGL3* DNA.



#### **2.3.4.2 IEX-1-GFP Constructs**

The full length *IEX-1* sequence was subcloned upstream of the GFP-Gene in the EGFP/C1 vector to link the GFP C-terminally to *IEX-1*. For the N1-link, the IEX-sequence was inserted downstream of the GFP sequence in the EGFP/N1 vector (both vectors: Clontech Laboratories Inc., Palo Alto, CA). The empty EGFP/C1 vector served as a control.

### **2.5 Northern (RNA) Analysis**

All equipment, e.g. Eppendorf tubes, columns, glass pipettes having contact with RNA samples was previously treated with 0.1% diethylpyrocarbonate (DEPC) and autoclaving to eliminate RNA cleaving enzymes.

#### **2.5.1 Oligo-dT Cellulose Preparation**

For the mRNA extraction 0.06 g oligo-dT cellulose per T175 tissue culture dish were used. The oligo-dT cellulose was submitted to several washing steps, first in 0.1 M NaOH, then sterile, deionized water, followed by incubation in water containing 0.1% DEPC for several hours. Subsequently, DEPC was removed by washing the cellulose three times in high salt buffer. Cellulose was finally diluted in 2 ml high salt buffer per 0.06 g.

#### **2.5.2 mRNA Isolation**

After treatment of the cell cultures, poly A<sup>+</sup>RNA was isolated as described [72]. In brief, after washing, cells were lysed with lysis buffer, DNA was sheared by passing the lysate several times through a 21G needle. After bringing the salt concentration up to 0.5M NaCl, the cell lysates were incubated for at least two hours with the previously prepared oligo-dT cellulose on a rocker, before running over a BioRad mRNA extraction column. mRNA was eluted by several washing procedures with decreasing salt concentrations. mRNA was then precipitated at -20°C in 95% ethanol. mRNA was redissolved in TE buffer after pelleting by centrifugation.

mRNA yield was determined by measuring the optical density at 260 nm with a spectrophotometer according to the following formula:

$$(OD_{260}) * 40 * D * V = m$$

OD <sub>260</sub>	optical density at 260 nm
40	RNA coefficient [ $\mu$ g/ml]
D	dilution factor
V	probe volume [ml]
m	amount of RNA [ $\mu$ g]

### 2.5.3 Gel Electrophoresis and Transfer

5  $\mu$ g mRNA of each sample was dried in a speed vacuum centrifuge, diluted in 20  $\mu$ l TE buffer and 2  $\mu$ l tracking dye. For identification of RNA bands, a RNA ladder (0.24-9.5kb RNA Ladder, Gibco BRL Life Technologies, Gaithersburg, MD) mixed with ethidium bromide, was run in parallel on one lane of each gel. Samples were loaded on a 1.2% formaldehyde/agarose gel. Poly A<sup>+</sup>RNA was denatured and separated by electrophoresis, and subsequently transferred to a Nytrane nylon membrane by capillary transfer using the Turboblottter Blotter Pack in the Turboblottter Transfer System (all Schleicher&Schuell, Keene, NH) according to the manufacturer's protocol. After electrophoresis, before transfer, the gel was photographed under UV-B radiation to visualize the ethidium bromide labelled RNA ladder. The mRNA was crosslinked with the membrane by irradiation with 1500 J UV-B light in a UV Stratalinker.

### 2.5.4 Preparation of cDNA Probes

Transfection of bacteria, plasmid amplification and plasmid extraction was performed as described in chapters 2.3.1. and 2.3.2. Isolated plasmids were digested with the specific restriction enzymes. Samples were diluted in Tris/EDTA Buffer (TE-Buffer) and run on a 1% agarose gel containing 0.5  $\mu$ g/ml ethidium bromide. Fragment bands on the gel were visualized by UV-B irradiation, cut out and purified with the QUIAEX II Gel extraction kit (Quiagen, Chatsworth, IN).

The fragments were radioactively labeled with the Gibco BRL Random Priming Labeling Kit (Gaithersburg, MD). 50-100 ng of the probe was denatured by placing the Eppendorf tubes into boiling in water. The probe was immediately placed on ice. 2  $\mu$ l of dATP, dTTP, dGTP, 5  $\mu$ l of radiolabeled [ $\alpha$ -P<sup>32</sup>]dCTP, the random primer and the

Klenow Fragment of DNA Polymerase were added to the probe. Radiolabeled probes were purified by filtration through NICK columns (Pharmacia Biotech) containing Sephadex G-50 DNA Grade.

Radioactivity was determined in a scintillation counter.  $7.5 \times 10^6$  cpm of labeled probe was added per 15 ml hybridizing solution.

### **2.5.5 Hybridization, Exposure and Stripping**

Membranes were prehybridized for one hour at 43°C in 15 ml hybridization buffer and 15 ml deionized formamide, then hybridized with the randomly primed DNA probes for 4 hours at 43°C. After various washing steps with SSC and SDS, the blots were wrapped in plastic foil and exposed at -70°C to a Kodak BioMaxMR film.

For repeated probing with different DNA probes, the membrane was stripped by boiling for 10 minutes and incubation in stripping solution (0.1% SSC, 0.1% SDS) at 70°C for 15 minutes.

### **2.5.6 Analyzing the Blots**

To control for equal loading of mRNA, membranes were hybridized to a glyceraldehyde-3-phosphate-dehydrogenase (GAPDH) probe.

Exposed films were scanned and then subjected to densitometric analysis using Scion Image software. Area and intensity of film blackening of each lane was measured and normalized to the GAPDH signal of the same lane.

## **2.6 *IEX-1* – Protein Localization**

### **2.6.1 *IEX-1* Immunostaining**

#### ***2.6.1.1 Antibody Production and Pre-Immune Studies***

Staining of HaCaT cells and human skin tissue samples was performed with an affinity purified rabbit-anti-*IEX-1* peptide antibody directed to a portion of the *IEX-1* protein. The antibody was established in the Laboratory for Nephrology Research, Mayo Clinic Rochester and was a generous gift by Dr. R. Kumar. Antibody

specificity was verified by immunostaining studies using preabsorbed *IEX-1* antibody, as described [10,71]. In brief, preabsorbed antisera was prepared by adding 0.5 ml of a 1 mg/ml solution of the relevant BSA-conjugated *IEX-1* polypeptide in PBS to 1 ml post-immune rabbit serum to provide an excess of antigen. The mixtures were incubated overnight at 4°C. Supernatant was pipetted into a clean tube, centrifuged at 12,000 g, again 0.5 ml of the antigen solution was added and the mixture was incubated overnight at 4°C. Following centrifugation at 12,000 g supernatant was pipetted into clean tubes, recentrifuged for 15 min. The final supernatant sera was pipetted and stored at -70°C until use for staining experiments.

### **2.6.1.2 Immunohistochemistry of cultured cells**

Cells were grown on microscopic coverslips in 24 well tissue culture dishes. After removal of medium, cover slips were washed with PBS and cells were fixed in cold methanol/acetone (1:1) for 10 minutes.

When applying a biotinylated secondary antibody, endogenous peroxidase activity was blocked by incubation in 0.3% H<sub>2</sub>O<sub>2</sub>. Slips were air-dried and incubated with blocking buffer for 1 hour at room temperature. Slides were then incubated with the primary affinity purified *IEX-1* antibody diluted in blocking buffer (1:2,000) for 1 hour. Slides were washed 3 times with PBS and then incubated with a biotinylated secondary antibody for 45 minutes (concentration 10 µg/ml). Subsequently, slides were rinsed thoroughly with PBS. Slides were incubated for 30 minutes with ABC-Reagent (avidin-biotinylated horseradish peroxidase macromolecular complex), subsequently washed with PBS, treated with 3-amino-9-ethylcarbazole and counterstained with hematoxylin. Slides were mounted on a microscopic glass slide using aqueous mounting media, and viewed under a light microscope.

When applying a FITC-labeled antibody, slips were air-dried after fixation and incubated with blocking buffer for 1 hour at room temperature. Slides were then incubated with the primary affinity purified *IEX-1* antibody diluted in blocking buffer (1:2,000) for 1 hour. Slides were washed 3 times with PBS and then incubated with a FITC labeled secondary antibody for 45 minutes (concentration 10 µg/ml). Subsequently, slides were rinsed thoroughly with PBS. Slides were mounted on a microscopic glass slide using aqueous mounting media and viewed under a phase

contrast confocal laser scanning microscope (excitation wavelength: 495 nm, emission: 520 nm).

### **2.6.1.3 Immunohistochemistry of tissue sections**

Normal human paraffin-embedded tissues from biopsy specimens were obtained from Department of Pathology, Rochester Methodist hospital. Specimens were cut in 5  $\mu$ m-thick sections and placed on silianized slides. The staining procedure was carried out in the Department of Pathology, Mayo Clinic, Rochester using methods previously described [73]. In brief, following deparaffinization in xylene, slides were bathed in a series of ethanol solutions and then rinsed with tap water. After immersing sections in blocking buffer for 1 hour at 37°C, slides were incubated with the primary, affinity-purified *IEX-1* antibody (dilution 1:2000) for 1 hour at the same temperature. After thorough rinsing with TBS, sections were covered with FITC-labeled goat anti-rabbit antibody diluted in goat serum (10  $\mu$ g/ml) and incubated for one hour at 37°C. Again slides were rinsed in TBS and finally in deionized water. Coverslips were attached with Vectashield mounting media and sealed with nail polish.

Slides were viewed under a Zeiss LSM 510 confocal laser microscope, using an excitation wavelength of 495 nm for FITC, and a dual channel overlay with transmittent light in the red, GFP in the green channel. Channels were digitally overlaid.

### **2.6.2 Localization of GFP-tagged *IEX-1***

HaCaT cells or human keratinocytes were grown on autoclaved microscope cover slips in 24 tissue culture wells.

Cells were transfected with the IEX-GFP-Vector as described above. After treatment and incubation for various time periods, cells were washed with cold PBS and then fixed in -20°C methanol for 15 minutes. Cover slips were mounted with VectaShield (Vector Laboratories Inc., Burlingame, CA) mounting media on glass slides and sealed with rubber cement.

Slides were viewed under a Zeiss LSM 510 confocal laser microscope, using an excitation wavelength of 488 nm for GFP, and a dual channel overlay with transmittent light in the red, GFP in the green channel. Channels were digitally

overlayed to allow exact intracellular localization of the green fluorescence and the nuclei. Images were stored digitally.

## **2.7 [<sup>3</sup>H]-Thymidine Incorporation Assay**

[<sup>3</sup>H]-thymidine incorporation assays were performed in 24 well tissue culture plates. Wells were pulsed with 2 μCi per ml growth medium by applying radioactively methylated thymidine (NEN Life Sciences Inc., Boston, MA) suspended in Solution A. After two hours cultures were washed with 10% trichloroacetic acid and water. Cultures were incubated with 0.2M NaOH containing herring sperm DNA (40 μg/ml) for several hours to lyse cells and precipitate DNA. Radioactivity was measured in a scintillation counter. Triplets were used for each group and their activities were averaged.

## **2.8 Apoptosis Assays**

### **2.8.1 Caspase 3 Activity Assay**

Caspase 3 activity was assessed with the AC-DEVD-AMC caspase 3 fluorogenic substrate (PharMingen, San Diego, CA). Cells were grown in T60 tissue culture dishes to 90% confluency and then subjected to the specific apoptotic treatment. Detached cells were gathered by centrifugation of the growth medium. Samples were lysed in cold lysis buffer (10mM Tris HCl (pH 7.5), 10mM NaH<sub>2</sub>PO<sub>4</sub>/NaPO<sub>4</sub> (pH 7.5), 130mM NaCl, 1% Triton-X-100, 10mM NaPP<sub>1</sub>), scraped and transferred to the tube containing the pelleted detached cells. Cell debris were separated from lysate by centrifugation. Protein concentrations of samples were determined using the BIO-RAD D<sub>c</sub> protein assay kit (BIO-RAD, Hercules, CA).

Caspase 3 activity was determined by incubation of 5 μg AC-DEVD-AMC substrate with 50 μl lysate for one hour at 37°C and subsequent determination of fluorogenic activity in a Cytofluor plate reader (excitation: 380 nm, emission: 460 nm). Quadruplets were assayed per sample. The following controls were assayed in parallel: Lysate without substrate, pure lysis buffer with substrate and lysate, substrate plus AC-DEVD-CHO Caspase 3 inhibitor (PharMingen, San Diego, CA).

### 2.8.2 Nucleosome ELISA

A nucleosome enzyme-immunoassay was used to determine the number of apoptotic cells. The assay is based on a quantitative sandwich-enzyme-immunoassay using mouse monoclonal antibodies directed against histones. The Cell Death Detection ELISA<sup>PLUS</sup> Assay (Boehringer Mannheim, Indianapolis, IN) was performed according to the manufacturer's directions: Cells were grown to 90% confluency in 96 wells. Growth media was removed by inverting the culture plate. After adding 200  $\mu$ l lysis buffer to each well, cells were lysed for 30 minutes at room temperature on a plate shaker. Lysates then were pipetted into eppendorf tubes and centrifuged at 200 g for 10 minutes. 20  $\mu$ l of each sample were transferred to the streptavidin coated multi titer plate (MTP) for analysis (buffers and MTP included in the kit). Samples were analyzed immediately after transfer, quadruplets for each sample were assayed. Pure isolated DNA-nucleosome complex served as a positive control.

### 2.9 Luciferase Assay

To assess *IEX-1* promoter activity the DNA sequence ranging from the transcription initiation site (TIS) to basepair 1419 upstream of the *IEX-1* gene (*-1419pIEX-1*) was fused into the firefly luciferase reporter gene plasmid (*pGL3-basic*) at the *KpnI* and *NheI* restriction enzyme sites (the *P<sub>IEX-1</sub>/pGL3* construct was a generous gift by Dr. R. Kumar, Laboratory for Nephrology Research, Mayo Clinic Rochester).

HaCaT cells were cultured and treated in 6 well plates and transfected as described above. To adjust for differences in transfection efficiency, cells were cotransfected with the Renilla luciferase construct, *pRL-TK*, that constitutively expresses Renilla Luciferase at baseline levels.

The Promega Dual-Luciferase Reporter Assay System (Promega, Madison, WI) was used to determine luciferase activity. Cells were lysed using the Passive Lysis Buffer included in the kit. To enhance lysis and gain higher luciferase activity, samples were subjected to a freeze-thaw cycle at  $-20^{\circ}\text{C}$  and were subsequently refrozen at  $-70^{\circ}\text{C}$  until further use, as mentioned in the manufacturer's instructions.

The assay was carried out in a luminometer with the program mode set to a 2-second pre-measurement delay, followed by a 10-second measurement period for each assay.

The reaction was initiated by adding 20  $\mu$ l lysate to the luciferase assay reagent containing luciferin. Luminescence activity was measured for 10 seconds, then the reaction was quenched and the Renilla luciferase reaction was started by adding the Stop&Glo reagent containing Coelenterazine, the fluorogenic substrate for the Renilla luciferase (all reagents included in the kit). Again activity was measured for 10 seconds. Firefly luciferase activity was normalized over Renilla luciferase activity, values were averaged for each group (triplets) and expressed as a percentage value of the untreated control group.

A set of experiments was carried out using a HaCaT cell line stably transfected with the firefly luciferase construct *P<sub>IEX-1</sub>/pGL3*. Cells were cultured and treated in 6 well plates, lysed and assayed as described above, in this case without assaying for Renilla luciferase activity. Again values were averaged for each group (triplets) and expressed as a percentage value of untreated control.

### 2.10 Cell Treatment

#### 2.10.1 Gamma-Irradiation

For  $\gamma$ -irradiation a Caesium ( $^{137}\text{Cs}$ )  $\gamma$ -irradiator at a dose rate of 11.4 Gy/min was used. Exact radiation dose was achieved by a sliding lead-shield connected to a timer, separating the treatment chamber from the chamber containing  $^{137}\text{Cs}$ . Cells were grown in T175 tissue culture flasks to 90% confluency before treatment and kept in the incubator until harvest for final processing after treatment.

#### 2.10.2 UV-B Irradiation

For UV-B treatment, a FS20 UV lamp (Westinghouse, Twinsburg, OH) with a main emittance in the UV-B range, and a peak at 313 nm was used. Iso-dose lines were determined with a light meter and drawn on the platform where the lamp was secured to assure equal radiation doses for each sample. The distance from the light source filter to the sample was 10 cm, resulting in a radiation energy dose of 0.22 J/m<sup>2</sup>/sec (13.3 J/m<sup>2</sup>/min). The lamp was allowed to pre-warm for 15 minutes before treatment. Prior to irradiation, medium was collected from the cell culture dish and stored in a 37°C waterbath. Then the dish was washed once with prewarmed PBS to remove



detached cells and remaining ingredients of the medium that could interfere with the spectrum used for the irradiation (especially phenol red); 200  $\mu$ l, 1 ml, 2 ml PBS were added to 24 wells, T60 and T100 dishes, respectively to avoid dessication of the cell culture during irradiation. PBS was aspirated after the irradiation, the previously collected media was readded, and dishes were placed in the tissue culture incubator until harvest for the final processing.

### **2.10.3 Chemical Treatment**

Camptothecin was prepared as a 1mM stock solution in DMSO and stored at 4°C.

Shortly before treatment, stocks were diluted to the desired concentration in pre-warmed growth media. Medium was aspirated off the dishes and the medium containing the agent was added. Again, dishes were then incubated for various time periods before further processing.

EGF was prepared as a 10 $\mu$ g stock in Solution A and stored at -20°C. For treatment final solutions were mixed in prewarmed standard medium (GF-) and added to the culture dishes after aspiration of old medium. Dishes were then incubated for various time periods before final processing.

### **2.11 Experimental Setups and Statistics**

Northern blots were performed independently at least twice in similar settings, in some cases varying in the time course of the experiment. Blots were analyzed with computerized densitometry and adjusted to GAPDH. Results of the densitometric analysis for each condition were referred to the value of the control and expressed in relative increase, unless noted otherwise.

Biochemical and immunohistochemical assays were established and then performed three times independently in equal setting and time course. Results were averaged and the standard error of the mean was calculated using the Microsoft Excel Statistic Tool package. Unless noted otherwise, graphs show the average of three experiments (n=3), bars show Standard Error of the Mean (SEM).

## 3. Results

### 3.1 Effects of Apoptotic or Mitogenic Stimuli on *IEX-1* Expression in Keratinocytes

*IEX-1* expression has been shown to be upregulated in various cell types following treatment with stress-inducing stimuli. The goal of the following experiments was to investigate whether keratinocytes would also respond by rapid induction of *IEX-1* mRNA expression after exposure to treatments known to induce cell stress.

In all of the following experiments steady state (baseline) *IEX-1* mRNA expression in untreated cells remained at the same level over the time course of the experiment (data not shown).

#### 3.1.1 *IEX-1* Expression after $\gamma$ -Radiation

Keratinocytes were grown to about 90% confluency and then irradiated with 10 Gy  $\gamma$ -radiation in a radiation chamber. mRNA was extracted after different periods of time and Northern Blotting for *IEX-1* and GAPDH was performed.

In untreated subconfluent culture *IEX-1* mRNA expression is low. Within 15 minutes after radiation, *IEX-1* mRNA levels increased significantly. At two hours sustained expression of *IEX-1* mRNA was found. By 4 hours, *IEX-1* expression had decreased to basal levels similar to the untreated control group (Figure 5).

#### 3.1.2 *IEX-1* Expression after UV-B Radiation

*In vivo* the skin is exposed to sunlight and ultraviolet radiation. The minimal erythemally effective dose (MED) in sunlight is generally believed to be about 20 mJ/cm<sup>2</sup> [74]. To examine the effects of UV-B radiation on epidermal cells, subconfluent keratinocyte cell cultures were exposed to UV-B radiation. Preliminary dosing experiments were performed. Radiation energy doses below 20 mJ/cm<sup>2</sup> did not result in a marked *IEX-1* response, energy doses exceeding 60 mJ/cm<sup>2</sup> were followed by a high increase in necrotic and detached cells. For this reason keratinocytes were irradiated with 40 mJ/cm<sup>2</sup>, then mRNA was extracted and Northern Blotting for *IEX-1* and GAPDH was performed.

Within 30 minutes of exposure, a marked increase in *IEX-1* expression was observed, reaching a maximum after 2 hours. At four and eight hours after UV-B irradiation, *IEX-1* mRNA expression decreased and approached baseline levels (Figure 6).

### 3.1.3 *IEX-1* Expression after H<sub>2</sub>O<sub>2</sub>-Treatment

To investigate whether oxidative stress mediates *IEX-1* expression in keratinocytes, subconfluent keratinocyte cultures were incubated with growth media containing 200µM H<sub>2</sub>O<sub>2</sub> for different time periods, mRNA was extracted and subjected to Northern Blotting analysis.

Within one hour, a marked increase in *IEX-1* mRNA expression was observed, reaching a maximum after two hours and declining to almost baseline levels within four hours following incubation in H<sub>2</sub>O<sub>2</sub> containing media (Figure 7).

### 3.1.4 Stimulation with EGF

To determine effects of mitogenic stimuli on *IEX-1* expression, growth factor-deprived cell cultures were incubated with the Epidermal Growth Factor (EGF) for designated times. In previous experiments, a dose-dependent induction was found for *IEX-1* mRNA upon EGF treatment of keratinocytes with concentrations ranging from 0.1 to 10 ng/ml (data not shown).

Keratinocyte cultures in log phase growth in medium containing growth factors (Complete Medium, GF+) exhibited relatively low *IEX-1* mRNA expression. Deprivation of growth factors (Defined Medium, GF-) for 48 hours resulted in further decrease in *IEX-1* expression. Restimulation with EGF evoked strong *IEX-1* mRNA upregulation within one hour. Subsequently over the eight hour period *IEX-1* mRNA expression levels slowly declined but remained higher than basal expression levels under control culture conditions (Figure 8).

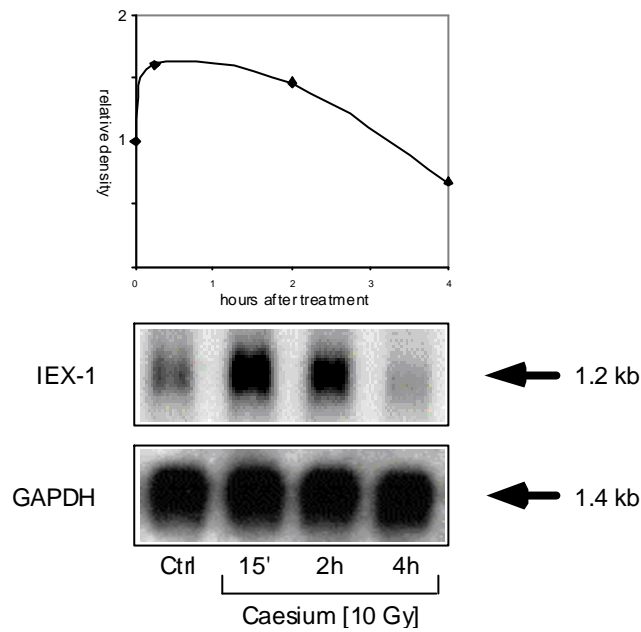


**Figure 5. *IEX-1* mRNA Expression after g-Radiation of Human Keratinocytes.** Human keratinocytes were grown to 90% confluency and irradiated with 10Gy. mRNA was extracted at designated time points and Northern blotting for *IEX-1* and GAPDH was performed. The blot demonstrates rapid *IEX-1* mRNA increase and followed by return to baseline levels within the subsequent four hours.

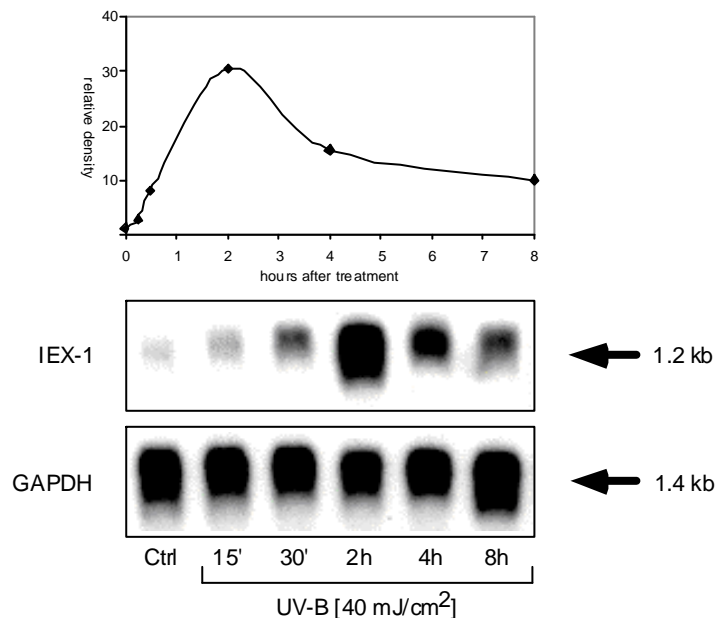


**Figure 6. *IEX-1* Expression after UV-B Irradiation of Human Keratinocytes<sup>1</sup>.** Human keratinocytes were grown to 90% confluency and irradiated with 40 mJ/cm<sup>2</sup> UV-B. mRNA was extracted at designated time points and Northern blotting for *IEX-1* and GAPDH was performed. The graph shows *IEX-1* expression normalized to GAPDH and relative to untreated control over time.

<sup>1</sup> Special thanks to Dr. med. K. Feldmann for performing the Northern Blot displayed.

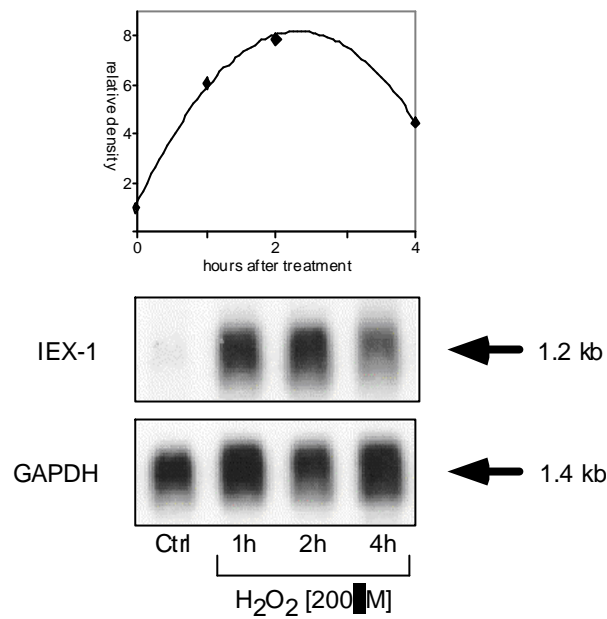


**Figure 7. *IEX-1* Expression after  $\text{H}_2\text{O}_2$  Exposure<sup>1</sup>.** Human keratinocytes were grown to 90% confluency and incubated with 200  $\mu\text{M}$   $\text{H}_2\text{O}_2$  for distinct periods of time. mRNA was extracted and Northern blotting for *IEX-1* and GAPDH was performed. The graph shows *IEX-1* expression normalized to GAPDH and relative to untreated control over time.

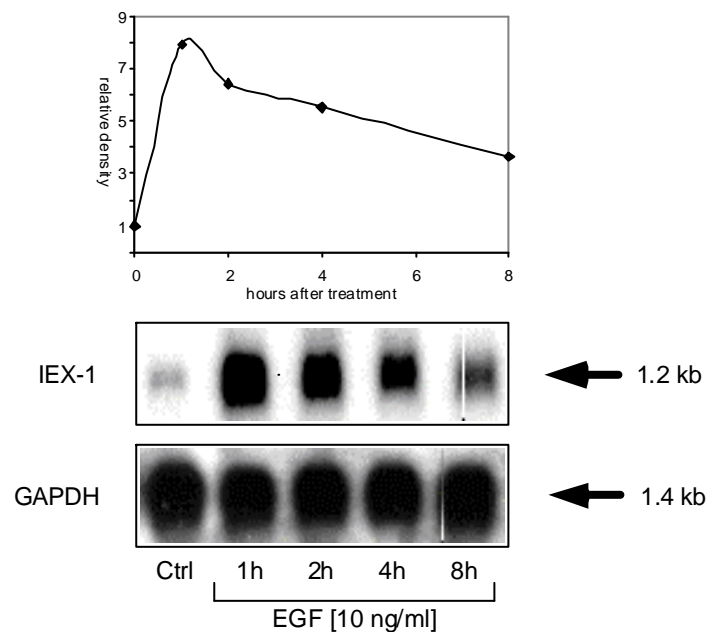


**Figure 8. *IEX-1* Upregulation after EGF-Stimulation of Human Keratinocytes.** Human keratinocytes were grown to 90% confluency, switched to Standard Medium (GF-) for 48 hours, and incubated with EGF for designated times. mRNA was extracted and Northern blotting for *IEX-1* and GAPDH was performed. The graph shows *IEX-1* expression normalized to GAPDH and relative to untreated control over time.

<sup>1</sup> Special thanks to T. Kobayashi, M.D. for performing the Northern Blot displayed.

### 3.1.5 Summary on Stress-Inducing and Mitogenic Treatment

The results of these series of experiments demonstrate that both stress-inducing stimuli, such as gamma-radiation, UV-B radiation and H<sub>2</sub>O<sub>2</sub>, as well as growth factor-mediated stimulation of keratinocytes induce *IEX-1* mRNA expression. The kinetics of induction and decline in expression of *IEX-1* distinctly vary among these stimuli.

### 3.2 Effects of Apoptotic Stimuli on *IEX-1* Expression in HaCaT Cells

Goal of the following experiments was to investigate the effects of apoptotic stimuli on the *IEX-1* mRNA expression levels in the spontaneously immortalized HaCaT cell line. Parental HaCaT cells were grown to 90% confluency and then treated either with UV-B radiation or by incubation with the DNA polymerase I inhibitor, camptothecin, as described in the Materials and Methods section. After incubation for various time periods, the cells were immediately lysed and mRNA extracted. Northern Blotting was performed and membranes were probed with radiolabeled GAPDH and *IEX-1* cDNA. A densitometric analysis of the blots was performed and intensity of signal is shown graphically as a function of time.

In unstressed, subconfluent cell cultures, the *IEX-1* expression in HaCaT cells is very low, as can be seen in lane 1 of Figure 9 and Figure 10 (untreated controls). Over the observed period of time for the following experiments, steady state *IEX-1* mRNA expression in untreated cells remained at baseline levels (data not shown).

#### 3.2.1 UV-B Radiation

Subconfluent cell cultures were irradiated with 40 mJ/cm<sup>2</sup> UV-B. At designated time points after treatment, mRNA was extracted and Northern blotting for *IEX-1* mRNA was performed. By 8 hours after treatment, large quantities of cells were detached, such that only small amounts of mRNA could be extracted.

Within 15 minutes after irradiation, no increase in *IEX-1* mRNA abundance could be noted. By 30 minutes, post-radiation a 244% increase was seen and levels steadily rose to 1053% at 12 hours after UV-treatment. After 12 hours, *IEX-1* mRNA expression started decreasing again (Figure 9).

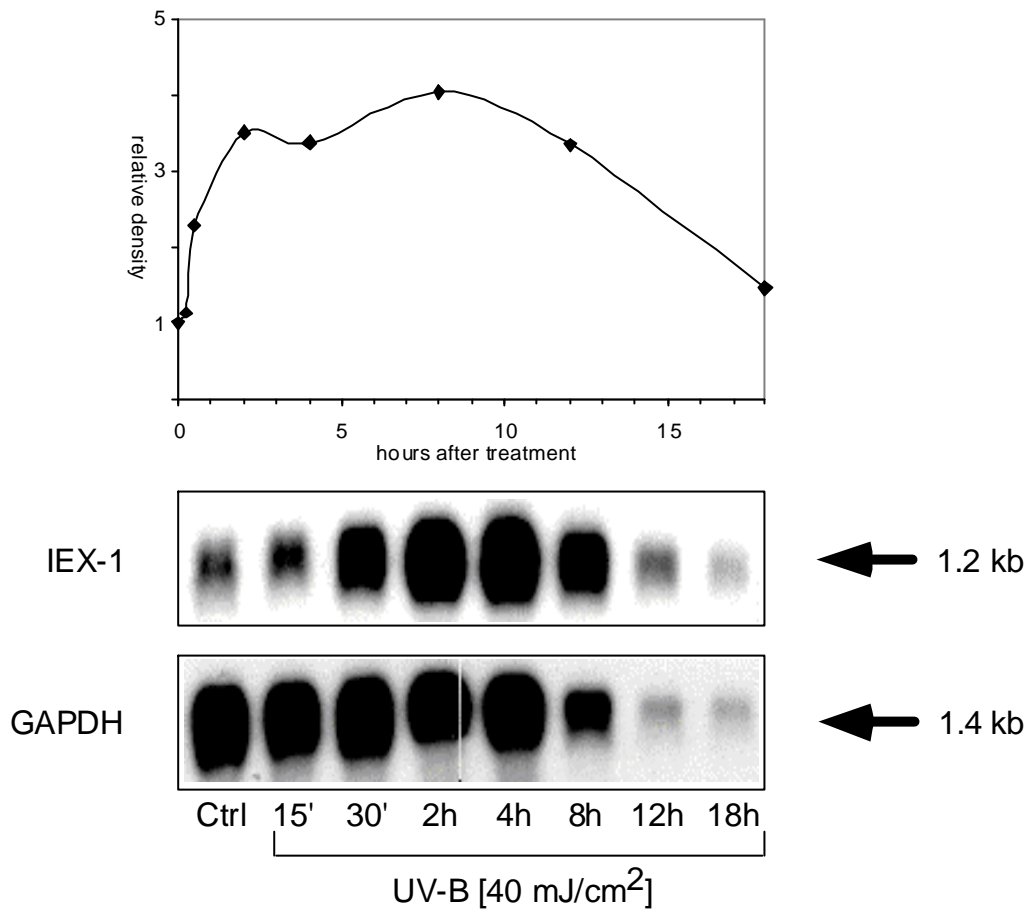


**Figure 9. *IEX-1* Upregulation after UV-B Radiation of HaCaT Cells.**<sup>1</sup> HaCaT cells were grown to 90% confluency and irradiated with 40 mJ/cm UV-B. mRNA was extracted after designated times and Northern blotting for *IEX-1* and GAPDH was performed. The graph shows *IEX-1* expression normalized to GAPDH relative to untreated control over time.

### 3.2.2 Camptothecin Incubation

Within 30 minutes of treatment, a marked increase in *IEX-1* mRNA expression could be observed. A slower elevation over the next 3.5 hours of treatment was also apparent, peaking at 4 hours, with an increase 1.5 times that detected at 30 minutes. Subsequently, decrease in *IEX-1* mRNA levels occurred. By eight hours the mRNA level of *IEX-1* had declined to 85% of the peak level at 4 hours. (Figure 10)

<sup>1</sup> Special thanks to Dr. med. K. Feldmann for performing the Northern Blot displayed.

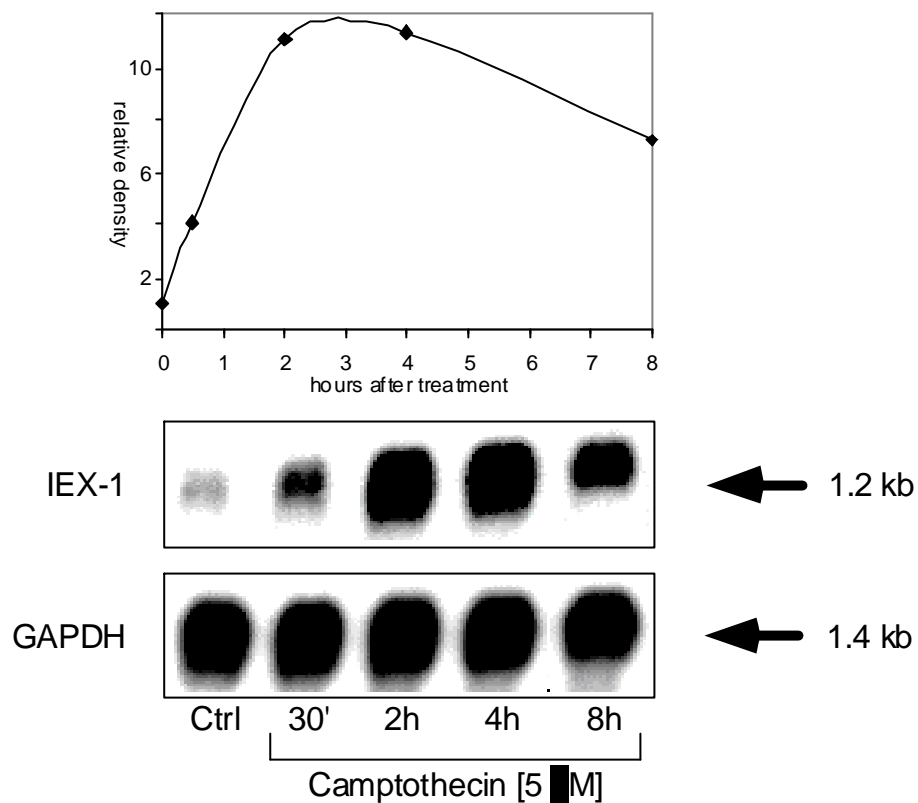


**Figure 10. *IEX-1* mRNA Upregulation Induced by Camptothecin Treatment of HaCaT Cells.** HaCaT cells were grown to 90% confluency and treated with 5  $\mu$ M Camptothecin. mRNA was extracted after specific times and Northern blotting for *IEX-1* and GAPDH was performed. The graph shows *IEX-1* expression normalized to GAPDH relative to untreated control.

### 3.3 *IEX-1* Promoter Activity

To investigate the effects of treatments on the *IEX-1* promoter activity, the 1419 bp gene sequence upstream of the *IEX-1* gene was subcloned into a luciferase expression vector as described in the Materials and Methods section ( $P_{IEX-1}/pGL3$ ). In cells transfected with this reporter construct, activation of the *IEX-1* promoter results in expression and subsequent translation of the luciferase protein. Luciferase converts luciferin, a gene product of the firefly, into a fluorochrome. Its fluorescent activity can be assayed in a luminometer.

HaCaT cells were permanently transfected with the pGL3 luciferase promoter bearing the full length *IEX-1* promoter sequence. Cells were cultured to 75% density, then either serum deprived for 48 hours or treated with the EGFR-blocking agent PD153035 for the same period. PD153035 treatment reduced promoter activity to



approximately 50%, whereas serum-deprivation decreased activity to 20% of untreated control cells in serum-containing medium (Figure 11).

Similar results were achieved in experiments using transiently transfected HaCaT cells with the  $P_{IEX-1}/pGL3$  vector, cotransfected with the Renilla  $pGL-3$  vector to control for transfection efficiency (data not shown).

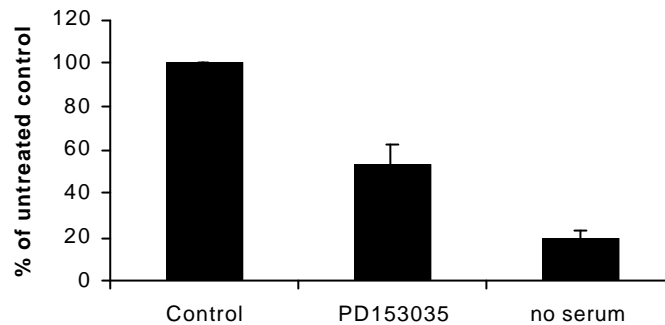


**Figure 11. *IEX-1* Promoter Activity after Blockade of EGFR or Serum-deprivation.** A HaCaT cell line was established to express luciferase under the control of the *IEX-1* promoter. Cells were grown to 90% confluency and either treated with PD153035 for 24 hours or serum-deprived for 48 hours. Cells were lysed and luciferase assay was performed. The results show fluorescence intensity relative to untreated control. Control cells were lysed at the time of initial treatment, to prevent further cell growth and increase in luciferase activity.

### 3.4 Localization of *IEX-1* Protein in HaCaT Cells

To investigate the localization of the *IEX-1* protein within the cell and to examine intracellular protein movement *in vitro*, microscopic localization experiments were performed. Two different approaches were chosen:

1. Immunostaining by indirect immunocytochemistry with antibodies against the *IEX-1* protein.
2. Protein tagging using HaCaT cells and *IEX-1* protein tagged with Green Fluorescent Protein (GFP).

#### 3.4.1 *IEX-1* Localization in HaCaT Cells by GFP-Tagging

The *IEX-1* gene sequence was subcloned into the GFP/c1 or the GFP/n1 vector such that, after translation of the plasmid mRNA, the GFP protein is linked either C-terminally or N-terminally to the *IEX-1* protein. Cells were transfected with each

vector separately, as described in Materials and Methods and then viewed by microscopy.

The transfection efficiency in HaCaT cells was low. Only about 10% of the cultured cells typically showed green fluorescence. Transfection of the blank GFP vector resulted in a homogeneous, pan-cellular distribution pattern of green fluorescence visualized under the laser scanning microscopy (data not shown). Only cells transfected with the expression vector for Green Fluorescent Protein linked C-terminally to the *IEX-1* protein (GFP/C1) demonstrated sufficient fluorescence to evaluate subcellular distribution of *IEX-1*. Cultures transfected with N-terminal linked GFP (GFP/N1) barely expressed GFP (data not shown).

Within the transfected cells that expressed the fusion protein, the fluorescence was clearly localized to the nucleus. Distinctive nuclear distribution patterns were observed, ranging from homogenous staining of the nucleus, to a spoke wheel pattern or punctuate intranuclear dot-pattern. No localization to other sub-structures or organelles could be found. Also treatment with various substances which have been identified to alter *IEX-1* mRNA expression, did not change the subcellular or intranuclear distribution of the fusion protein. These treatments included Camptothecin (5  $\mu$ M), UV-B (40 mJ/cm<sup>2</sup>) or 1,25-(OH)<sub>2</sub>-vitamin D<sub>3</sub> (data not shown). Varying treatment periods from 30 minutes up to 24 hours were examined, but no differences in *IEX-1* distribution or expression could be seen. (Figure 12)

These observations suggest that the *IEX-1* fusion protein is likely quite stable and not readily mobile within or between subcellular compartments.

#### **3.4.2 *IEX-1* Immunostaining in HaCaT Cells**

To localize *IEX-1* protein in human keratinocytes and HaCaT, cultured cells were immunostained with a rabbit polyclonal antibody directed against a portion of *IEX-1*. Cells were grown in chamber slides and the staining procedure was carried out as described in Materials and Methods.

Microscopic examination revealed distinct nuclear staining of keratinocytes and HaCaT cells, under subconfluent growth conditions. The nuclei showed discrete intranuclear, condensed speckled staining. The number of spots varied from one to six with diameters ranging from 1/20 to 1/5 of the nuclear diameter (Figure 13).

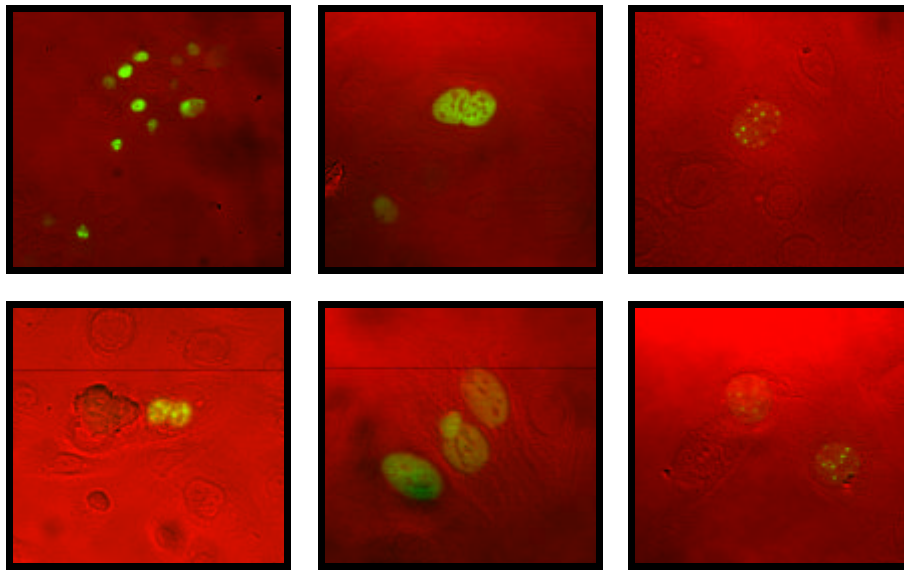


**Figure 12. Localization of GFP-tagged *IEX-1*.** HaCaT cells transfected with the GFP vector subcloned into the *IEX-1* sequence, were viewed by Laser Confocal Scanning Microscopy 16 hours after transfection. (original magnification 400x)

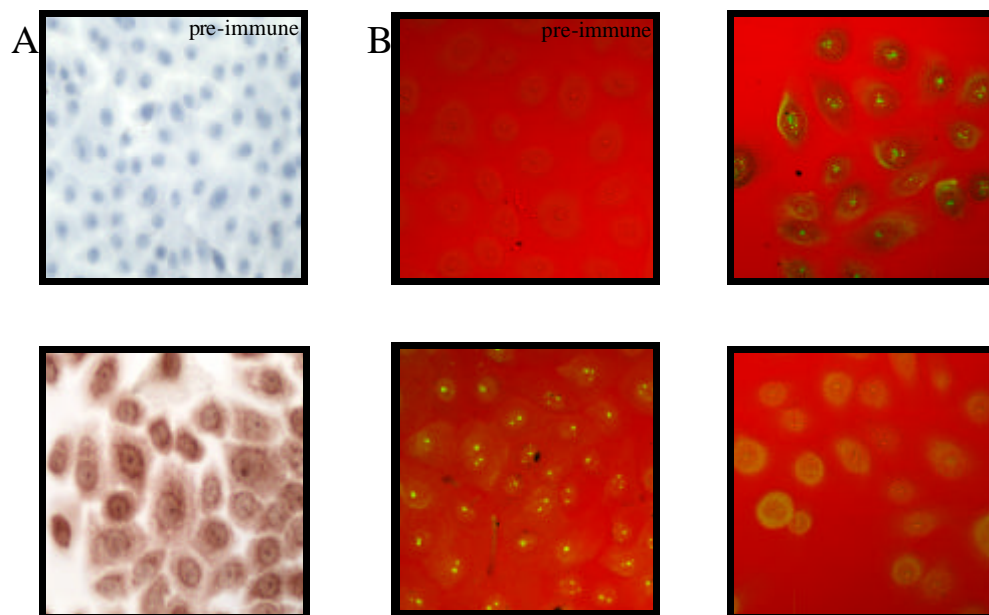


**Figure 13. Immunohistochemical Staining of *IEX-1* in Cultured Cells.<sup>1</sup> A Keratinocytes B HaCaT.** Cells were grown to 50% confluency, incubated with a peptide polyclonal antibody against *IEX-1*. Keratinocytes were incubated with a biotinylated secondary antibody, counterstained with hematoxylin and viewed by light microscopy (original magnification pre-immune: 200x, immune: 400x). HaCaT cells were stained with a FITC labeled secondary antibody and viewed by laser confocal microscopy (original magnification 400x).

<sup>1</sup> Special thanks to Dr. med. K. Feldmann for performing the immunostaining featured in this chapter.

### **3.5 *IEX-1* Overexpression - Influence on Cell Responses**

To gain further insight into the activities and possible functions of the *IEX-1* gene, two different HaCaT Cell lines were established. The genomic sequence of the *IEX-1* gene was subcloned into the pcDNA3.1 CMV expression vector. One cell line was established by transfection of HaCaT cells with this plasmid and subsequent negative selection, as described in Materials and Methods. Another cell line was established that contained the empty pcDNA3.1 CMV expression vector and served as control for all experiments.

In the following studies, the stably transfected *IEX-1* HaCaT cell line will be referred to as IEX-cell line, and the control cell line will be designated ZEO-cell line (referring to the Zeocin-resistance gene of the control plasmid).

#### **3.5.1 *IEX-1* Overexpression: mRNA levels in transfected HaCaT Cells**

To verify successful transfection and expression of the *IEX-1* expression plasmid, the ZEO and the IEX cell lines were grown to 90% confluency. Each culture was either lysed immediately or switched to DMEM medium without FBS for 48 hours before lysing and subsequent RNA extraction. Northern blotting for *IEX-1* mRNA and GAPDH mRNA was performed.

The expression of *IEX-1* mRNA in the IEX cell line was higher than in the ZEO control transfected cell line, for both cells grown in the absence or presence of serum (Figure 14).

#### **3.5.2 [<sup>3</sup>H]-Thymidine Incorporation Growth Assays: ZEO versus IEX cell lines**

During maintenance of the cell cultures it was observed that the IEX cell line routinely reached confluency faster than the ZEO cell line. Nonetheless ZEO and IEX cultures were passaged concurrently, such that for each experiment, ZEO and IEX cells at the same passage number were used. To demonstrate an increased growth rate in the IEX cell line, [<sup>3</sup>H]-thymidine incorporation growth assays were performed. For this assay, cell cultures were incubated in medium containing tritium-labeled thymidine for a defined time period. In actively cycling cells, radioactive thymidine is incorporated into the daughter strand DNA during S-phase. The amount of DNA

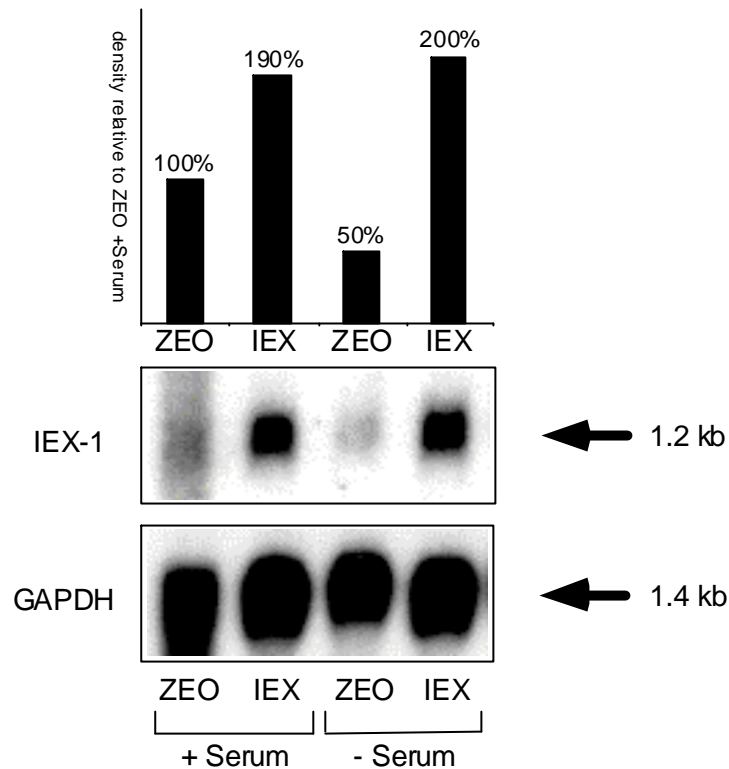


**Figure 14. HaCaT/IEX-1-zeo Cell line Overexpresses *IEX-1* mRNA.** HaCaT cell lines were established and contained either the empty pcDNA3.1/zeo(-) vector (ZEO) or the pcDNA3.1/zeo(-) vector subcloned with the full length *IEX-1* cDNA (IEX). Cultures were either grown in serum (+) or deprived of serum (-) for 48 hours.

replication and the level of proliferative activity for a given period can be quantified by measuring radioactivity incorporated into DNA of the cell culture.

24 well plates were used, three wells per time point. On day 0, both cell lines were plated at a density of  $1 \times 10^3$  cells/cm<sup>2</sup>. They were allowed to attach to the culture dish for one day. On Day 1 the initial growth assay was performed. In the experiment displayed in Figure 15 assays were performed daily until Day 6, and every other day thereafter.

Both the IEX and ZEO cell lines showed a sigmoid <sup>3</sup>H-thymidine incorporation curve, with a lower slope during the first few days, then a steep increase over the next several days, followed by a strong decrease after reaching peak activity. The IEX cell line reached the maximum slope of thymidine incorporation earlier and with a larger maximum level than the ZEO cell line. The marked decrease in radioactivity following the peak is explained by contact inhibition of cells, followed by a marked decrease in proliferative activity after reaching confluency.

During the first 3 days after plating, no difference in thymidine incorporation activity levels could be observed. Both cell lines exhibited only a moderate increase in [ $^3\text{H}$ ]-thymidine incorporation. At Day 5 however, IEX cells showed markedly higher proliferative activity than ZEO cells. By Days 9 and 11, the peak growth activity of the IEX cell line was observed, exceeding that of the ZEO cell line by 70%. ZEO only reached their maximum activity at day 11 (Figure 15).

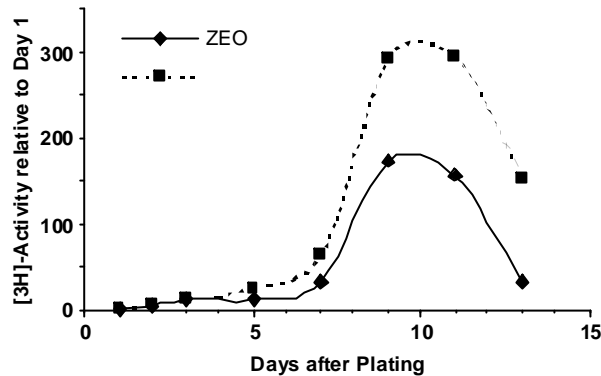


**Figure 15.** [ $^3\text{H}$ ]-Thymidine Incorporation Assay: IEX versus ZEO HaCaT. *IEX-1* overexpressing (IEX) and control HaCaT (ZEO) cultures were plated at  $1 \times 10^3$  cells/cm $^2$  and pulsed with [ $^3\text{H}$ ]-thymidine every other day. Cells were lysed and activity was counted in a scintillation counter. Upon reaching confluency, [ $^3\text{H}$ ]-thymidine activity decreased strongly (three independent experiments with different time courses were performed, a representative experiment is shown).

### 3.5.3 Induction of Apoptosis in *IEX-1* Overexpressing Cell Lines

The higher growth rate in the *IEX-1* transfected cell line could be due to a reduced rate of cell death in the growing cell culture. As a consequence, we investigated the rate of apoptosis in the IEX and the ZEO cell lines. The baseline apoptotic activity in unstressed IEX and ZEO cultures was examined, as well as their susceptibility to well-defined inducing agents of apoptosis.

Cells undergoing apoptosis show series of characteristic morphological and biochemical changes, such as membrane alterations, activation of specific proteases, known as caspases, and DNA fragmentation into specific ~180bp oligonucleosomes.

Amongst the proteolytic caspase enzyme cascade, Caspase 3 plays a key role as a downstream mediator of DNA degradation. The Caspase 3 Activity Assay, a fluorogenic enzyme assay, is a specific and sensitive assay to measure apoptotic activity of whole cell cultures.

In experiments where apoptosis induction was demonstrated by the Caspase 3 Activity Assay, the results were confirmed with the Cell Death Detection ELISA Assay. This sandwich-enzyme-immunoassay allows the specific determination of mono- and oligonucleosomes in the cytoplasmatic fraction of cell lysates. These fragments only occur in cells undergoing apoptosis, and therefore, are a specific parameter to determine the rate of apoptotic cells in culture.

#### ***3.5.3.1 Differences in Apoptotic Activity in Attached versus Detached Cells***

Within a few days of plating cells, an increased amount of detached or floating cells on the surface of the culture medium was observed in IEX cell cultures. Microscopically, the number of floating cells in the IEX cultures seemed to be greater compared to the ZEO cultures. To substantiate these microscopic findings, a method was sought to quantify the number of floating versus attached cells in each culture. Clotting of detached cells prevented conventional cell counting methods such as flow cytometry or counting chamber. Reproducible quantification was eventually obtained using a protein assay for floating versus attached cells in the culture.

To determine if the detached cells showed a higher apoptotic activity than attached cells, the Caspase 3 Activity Assay was carried out separately for the floating versus the attached cells. Cells were plated at a density of  $5 \times 10^4$  cells/cm<sup>2</sup> and grown for two days. To allow collection of sufficient amounts of floating cells, cultures were not refed for three days before the final assay was carried out. Floating cells were harvested by centrifugation, supernatant aspirated and the pellet lysed. Attached cells were lysed and the Caspase 3 Activity Assay was carried out as described in Materials and Methods for the floater sample and the attached sample separately.

At the time of harvest, the protein amount of the attached cells did not differ in the IEX and the ZEO cell line. However, the detached cell fraction contained 1.8 fold more protein in IEX versus ZEO cell cultures. Apoptotic activity was also slightly higher in the attached cells of the IEX culture compared to the ZEO culture. In IEX cells, Caspase 3 Activity in the detached fraction was 2.5 times higher than in the attached cells, compared to only a 1.4 fold difference in the ZEOs. (Table 3)

	Protein (mg)		Caspase 3 Activity ( $\times 10^4$ Fluor. Units)		<u>Caspase 3 Activity</u> Protein	
	Attached	Detached	Attached	Detached	Attached	Detached
ZEO	3.41	0.29	4.0	5.5	1.2	19.0
IEX	3.38	0.53	7.1	17.9	2.1	33.8

**Table 3. IEX-1 Overexpressing HaCaT Show More Detached Cells and Higher Caspase 3 Activity.** Cells were grown in +serum DMEM to 75% confluency. After three days without refeeding, detached, floating cells were harvested by centrifugation. Protein amount was determined and Caspase 3 Activity Assay was performed separately for attached or detached cells of the same culture.

### 3.5.3.2 Baseline Apoptotic Activity in Untreated Cells

A series of experiments was performed to detect apoptotic differences between IEX and ZEO cells in untreated conditions. In contrast to the experiments described in 3.5.4.2 this time cultures were refed every day until day of harvest to guarantee optimal growth conditions. Cultures were grown to 75% confluency and then assayed. Since only minor amounts of detached cells occurred, separate assaying for floating and attached cells was not carried out. Three different experiments, each time with cells from different passages, were performed. Three dishes per group were assayed in each experiment. As can be seen in Figure 16, the two cell cultures did not differ in their Caspase 3 activity in unstressed condition.

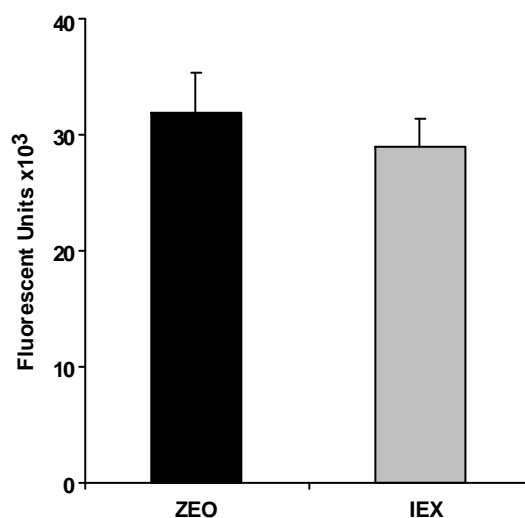


**Figure 16. Baseline Apoptotic Activity in Unstressed ZEO and IEX Cultures.** Baseline apoptotic activity in unstressed ZEO and IEX cell line was determined. Cultures were refed daily until reaching 75% confluency. Separate assays for floating and attached cells were not carried out. In three independent experiments, Caspase 3 activity was assayed and not found to be different in the IEX versus the ZEO cell line.



### 3.5.3.3 Induction of Apoptosis with UV-B Irradiation and Camptothecin

To investigate the influence of *IEX-1* overexpression in HaCaT cells on the susceptibility to inducers of apoptosis, a series of experiments examining UV-B irradiation or treatment with a DNA polymerase I inhibitor was performed.

Initially, the dose response for UV-B and camptothecin was determined and optimized for subsequent experiments. Timing experiments were also performed. At energies greater than 60 mJ/cm<sup>2</sup>, the extent of cell detachment several hours after treatment was excessive, such that necrotic cell death could not be excluded. At 40 mJ/cm<sup>2</sup> and eight hour incubation time, only few floating cells occurred. For the same reasons, a camptothecin concentration of 5 μM was chosen.

As already shown in the experimental series for untreated cells (see 3.5.4.2), no significant difference in apoptotic activity between IEX and ZEO cells in the untreated control groups could be noted. Furthermore no increase in apoptotic activity in untreated cells over the time course of the experiment could be observed (data not shown). Timing and dosing experiments were performed similarly for the Cell Death Detection ELISA. Again, no differences between *IEX-1* overexpressing cells and the control cells could be noted, concerning the number of cytoplasmatic oligonucleosomes in untreated condition. Also, there was no increase of cytoplasmatic nucleosomes over the period of treatment in either cell line (data not shown).

Compared to the control transfected cell line, radiation with 40 mJ/cm<sup>2</sup> UV-B was followed by a higher increase of Caspase 3 activity over time in the *IEX-1* overexpressing cells. Compared to the ZEO control, after three hours, Caspase 3 activity of the IEX cells was 1.6 (210% versus 120% of baseline activity) and after six hours, 2.1 fold (380% versus 180% of baseline activity) (Figure 17A).

These results were confirmed by nucleosome formation: Compared to the untreated control group, three hours after irradiation with 40 mJ/cm<sup>2</sup> UV-B, the nucleosome fraction in the cytoplasm was 1.4 fold higher in the *IEX-1* transfected cell line compared to the sham-transfected cell line (190% vs. 140% compared to untreated control). Six hours post irradiation, the nucleosome fraction in the IEX cells was about two fold higher than in the ZEOs (400% versus 190% compared to untreated control) (Figure 17B).

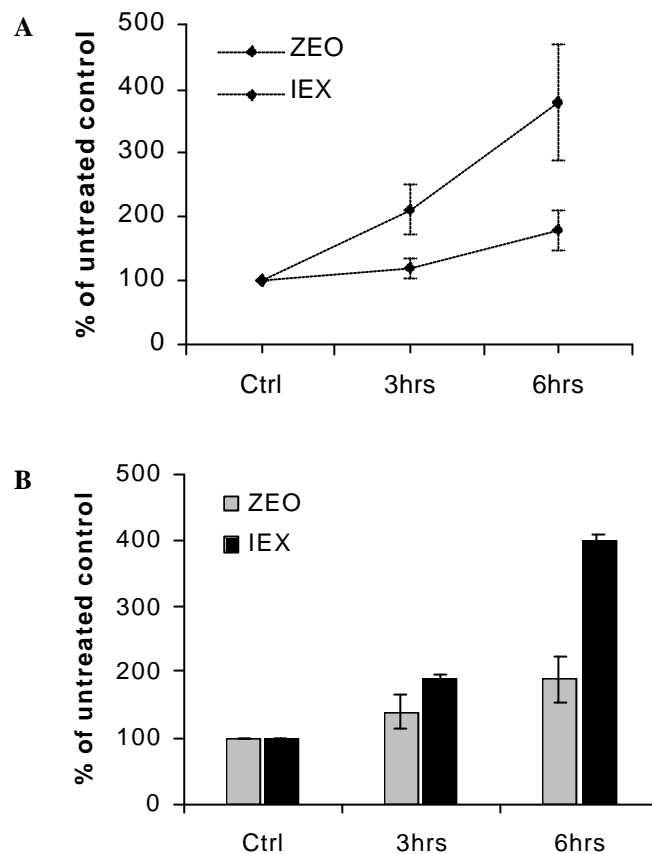


**Figure 17. Induction of Apoptosis by UV-B Irradiation.** Sham transfected cells (ZEO) and cells bearing the *IEX-1* expression vector (IEX) were irradiated with 40 mJ/cm<sup>2</sup> UV-B. (A) Apoptotic activity after various time periods was assessed by Caspase3 Activity Assay and confirmed by Life/Death Nucleosome ELISA (B). Line diagram in (A) expresses relative increase in enzyme activity, columns in (B) express relative amount of histones. Results of three independent experiments are shown, bars indicate standard error of the mean. Caspase activity as well as amount of cytoplasmic nucleosomes in untreated cells did not increase over time compared to the control at time 0 (data not shown).

Similar results were achieved by treatment with the apoptotic agent camptothecin. After three hours incubation with 5  $\mu$ M camptothecin, increase in Caspase 3 activity was twice as high in the *IEX-1* overexpressing cell line than in the sham cell line (210% versus 120% of baseline activity); after six hours of treatment, a 1.7 fold higher activity was noted in the IEX cells (260% versus 140% of baseline activity) (Figure 18A).

Confirmation by Cell Death ELISA revealed a 1.3 fold higher increase of oligonucleosomes in the IEX in relation to the ZEO cells (220% versus 170%) after three hours and 1.7 fold after six hours (380% versus 230%). (Figure 18B)

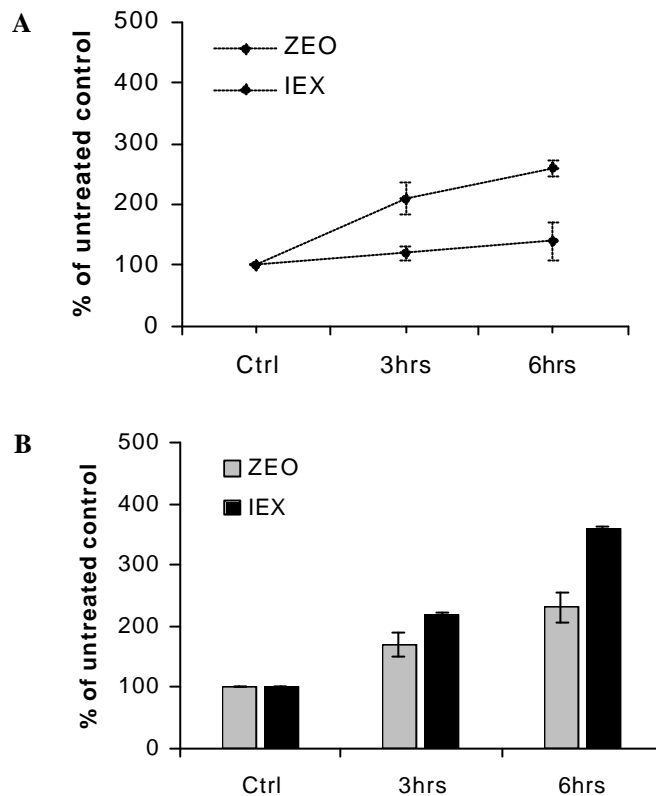


**Figure 18. Induction of Apoptosis by Incubation with Camptothecin.** (A) Caspase3 Activity Assay (B) Life/Death Nucleosome ELISA Sham transfected cells (ZEO) and cells bearing the *IEX-1* expression vector (IEX) were treated with 5  $\mu$ M camptothecin. Experimental setup as described for Figure 17.

As could be shown in the previously mentioned timing experiments, an increase of Caspase 3 activity following UV-irradiation as well as camptothecin incubation could already be observed after two hours, peaking around eight hours and starting to decrease between twelve and sixteen hours, (data not shown).

### 3.5.4 Serum Deprivation

Next, the effects of *IEX-1* overexpression on the rate of apoptosis in the serum deprived HaCaT cultures cells were examined.

For each time point one T60 tissue culture dish was plated at a density of  $2 \times 10^4$  cells/cm<sup>2</sup> with IEX and ZEO cells respectively. They were allowed to grow for two days in +Serum DMEM, before medium was exchanged to -Serum DMEM. At that time, dishes for +Serum control were harvested for later analysis: cells in the T60 were lysed and frozen at  $-70^\circ\text{C}$  for later Caspase 3 Activity Assay.

A +Serum DMEM control could not be assayed for each time point since dishes in +Serum conditions would have reached confluence at later time points, which would have effected the rate of apoptosis in the dishes. For this reason all time points were compared to the +Serum control, assayed at the day of medium change.

As noted before, baseline Caspase 3 activity under unstressed growth conditions in +Serum DMEM was about equal in IEXs and ZEOs. Compared to baseline, three days of serum withdrawal evoked a slight elevation in Caspase 3 activity, and after six days, a 100% activity increase was found in the IEX cell line.

Over the whole period of serum withdrawal, an increase in Caspase 3 activity in the ZEO cells could not be observed. These results could be repeated in several experiments with various time points and up to eight days of serum withdrawal. After eight days of serum deprivation, a slight increase of Caspase 3 activity but less marked than in the IEX cells, was also noted in the ZEO cultures. A representative experiment is shown in Figure 19.

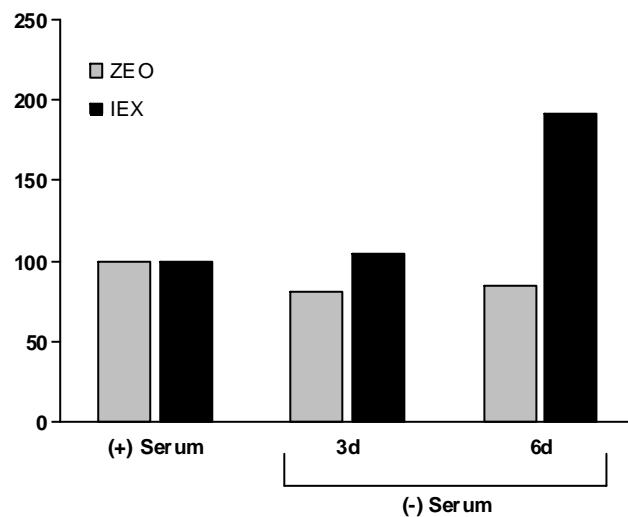


**Figure 19. Serum Deprivation of *IEX-1* Overexpressing HaCaT.** Cells were grown to 90% confluency in DMEM supplemented with 10% FBS and then switched to DMEM without FBS. Caspase 3 activity was assessed at designated time points after serum removal. Three independent experiments with varying time setups were performed, a representative experiment is shown. Caspase 3 activities are normalized over (+) serum control for each cell line (100%) (ZEO: Control cell line; IEX: *IEX-1* overexpressing cell line).

### 3.6 Localization of *IEX-1* in Skin Tissue<sup>1</sup>

To investigate the expression and distribution patterns of *IEX-1* in the epidermal layers of human skin, biopsy specimens (obtained from Rochester Methodist Hospital, Department of Pathology) were stained with a polyclonal peptide antibody directed against a portion of the *IEX-1* protein and incubated with a FITC labeled secondary antibody as described in the Materials and Methods section.

Staining was detected mainly in the epidermal layers of the skin. In the epidermis, the basal layer showed the strongest staining for *IEX-1*. Towards the upper layers, fewer cells were exhibiting less intense staining. The *stratum spinosum* showed only little staining, and in the *stratum corneum* no immunoreactivity was found.

The protein seems to be distributed diffusely in the cytoplasm, but towards the outer granular layer a perinuclear localization of the protein was observed (Figure 20).

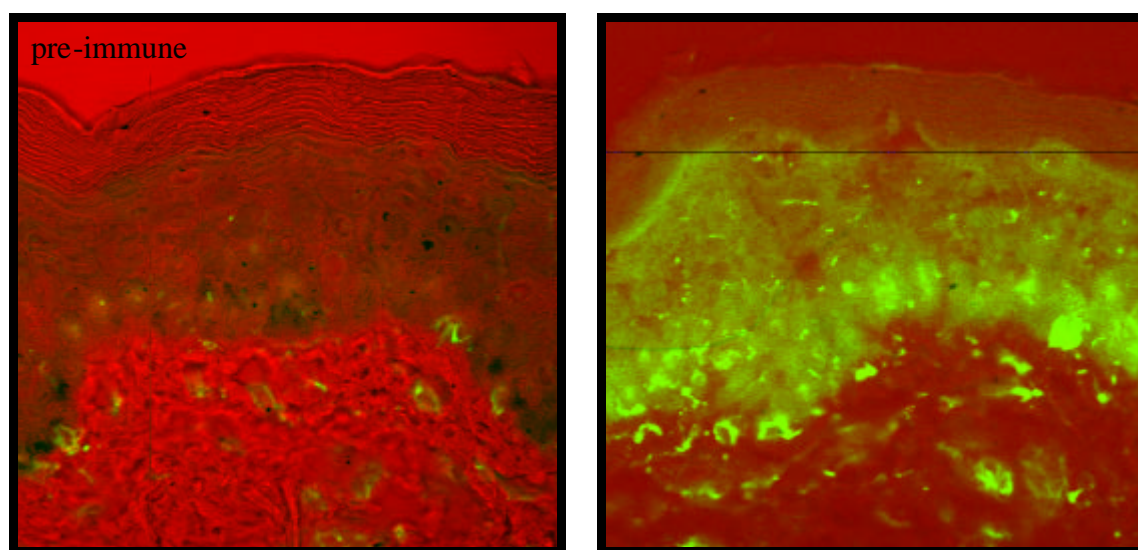


**Figure 20. Immunohistochemical Staining of Human Skin.** Skin samples were incubated with a peptide antibody directed to *IEX-1*, stained with a FITC labeled secondary antibody and viewed under a Laser Confocal Scanning Microscope. (original magnification: 200x)

<sup>1</sup> Special thanks to Dr. med. K. Feldmann for performing the staining and taking the pictures displayed in this chapter.

## 4. Discussion

### 4.1 Discussion of Methods

#### *In vitro studies using Keratinocytes and HaCaT Cells*

In the present studies, experiments were performed using primary human keratinocytes and the human keratinocyte derived, spontaneously immortalized HaCaT cell line. Keratinocytes are a widely used and well defined cell type for investigation of proliferation- and differentiation-regulating agents and conditions [22]. However, some limitations of the keratinocyte model must be kept in mind: interaction between dermis and epidermis, the *in vivo* responses to many systemic regulatory changes, the role of the cutaneous microvasculature, the neural responses and various other component networks of intact skin are not present in this culture system [75-77]. Keratinocytes can only be maintained in an undifferentiated, replicative state over a limited number of passages. Aging either reduces clonogenic potential [78], or differentiated phenotypes or spontaneous malignant transformation occur [79]. For this reason keratinocytes from more than one skin specimen have to be used over the course of experiments. Therefore there are donor-related variations in keratinocytes derived from different donors [78]. Experience shows that these differences are less marked with young age of the donor. For this reason, only skin samples of neonates were used in the present studies.

Because of the limited number of passages, stable transfection of normal keratinocytes is not possible. Additionally, primary keratinocytes are highly refractory to transfection, rendering transient gene expression studies difficult [80]. To circumvent these obstacles, frequently immortalized cell lines are used for gene expression studies. In contrast to primary keratinocytes, spontaneously immortalized keratinocyte cell lines are independent from donor variations and maintain their clonogenic potential, even after a high number of passages [81]. The spontaneously immortalized keratinocyte cell line HaCaT has been widely used as an *in vitro* substitute for normal human keratinocytes. Compared to primary keratinocytes, HaCaT cells show higher transfection efficiency and are less stringent in their growth requirements, which makes antibiotic selection and establishment of stably transfected cell lines possible [82].

In spite of cytogenetic alterations and mutation within the the *p53* gene as well as loss of various senescence genes [83], the HaCaT cell line exhibits non-tumorigenic growth [84] and has preserved the ability to express distinct differentiation markers, such as involucrin, filaggrin and keratins [76,81]. HaCaT cells are also sensitive to induction of apoptosis, similar to normal keratinocytes [85,86].

However, experimental results with HaCaT cell lines have to be viewed under the perspective that they do have genomic alterations for proteins that play a crucial role in cell cycle progression. Cell death, therefore, might express different reactive patterns than the wild type keratinocyte [86].

#### ***Northern Blot/Densitometric Analysis***

Quantitative comparison between different samples in Northern blotting is only valid when equal amounts of mRNA for each sample were loaded on the gel. In cell stress experiments, when cell death and detachment of cells occurs, variations between the samples can occur. For this reason results are typically equilibrated for the amount of so called house keeping genes, such as GAPDH, that are presumably expressed in equal amounts in each cell, independent from environmental conditions. In the present study, different samples in one experiment are compared by computer-densitometric equilibration for GAPDH. In time course experiments, equilibrated samples were related to untreated control. Relative extent of increase or decrease in mRNA expression therefore is dependent on basal expression in untreated control. For this reason, comparisons in quantity of expression changes are not possible between different experiments, since basal mRNA expression in untreated samples may vary for each experimental setup.

#### ***Induction of Apoptosis***

Various methods to induce apoptosis in cell cultures have been described. Incubation with ligands of death receptors such as FasL/CD95 or TNF- $\alpha$  [51,87],  $\gamma$ -radiation [88], UV-B radiation [89], DNA damaging agents [90], or deprivation of growth-factors [91] have been shown to induce apoptosis. These treatments act via different mechanisms to activate the cell death program, but eventually converge into the proteolytic cascade that leads to apoptosis [56,92].

In this study, human keratinocytes and HaCaT cells were stressed with different stimuli to induce apoptosis. Treatment with camptothecin results in DNA damage followed by nuclear death signals [93], deprivation of growth factors leads to sensitization of keratinocytes to apoptosis [94,95] and  $\gamma$ - radiation and UV-B radiation induce programmed cell death via multiple membrane-derived, cytosolic and nuclear signals [62,96]. In preliminary experiments the dose of each apoptosis inducing treatment was determined in order to achieve maximal *IEX-1* mRNA signal with minimal cell death via necrosis (or cell detachment).

By applying several different inducers of apoptosis to the keratinocyte model, multiple pathways to the suicide program are covered.

#### *Apoptosis Assays*

A multitude of assays exist to assess apoptotic activity in cell culture, ranging from pure microscopic analysis of cell morphologies to flow cytometric assessment of membrane and nuclear staining.

Microscopic assessment of apoptotic morphology and DNA fragmentation by Southern Blotting have been used to investigate apoptosis. However, they are not always accurate in differentiating necrotic from apoptotic cell death [97]. TUNEL assay with subsequent light microscopic analysis is a widely used method in apoptosis research, but exact standardization of the method is crucial and quantification remains a problem, if the number of apoptotic cells is very small [98]. Staining with annexin, a marker for apoptotic membrane changes, and counterstaining with propidium iodide, a marker for dead cells, with subsequent flow cytometric analysis (FACS) has been considered the method of choice for apoptosis measurement [99]. But application in adherent cell cultures remains a problem, since trypsinization of cultures for FACS effects the annexin staining [100,101].

For this present work, we were able to establish two apoptosis assays for adherent keratinocyte cultures. Neither test is dependent on subjective microscopic assessment. The two assays measure apoptotic activity at two different, crucial stages in the course of programmed cell death: the caspase 3 assay by biochemically measuring enzymatic activity of a key apoptotic enzyme, the nucleosome ELISA by immunologically showing abundance of a specific apoptotic product. Together these assays meet the demand that two independent methods should be applied to assess apoptosis [98].



In both assays, unequal cell number in the samples results in differences of signal activity. This problem was avoided in the Caspase 3 Activity Assay by equilibrating for same amounts of protein in all samples (method section 2.8.1).

Due to the experimental setup of the ELISA, an equilibration for cell number is not possible. Variations between the samples were kept as small as possible by plating equal numbers of cells at high density and by initiating the treatment during exponential growth, soon after the cells have attached to the culture dish.

## 4.2 Discussion of Results

Immediate-early genes are critical mediators of cell responses, resulting from alterations in environmental conditions or exposure to stress-inducing stimuli. Recently, a new member of the immediate-early gene family, *IEX-1*, with yet unknown function has been described. In this study, the role of *IEX-1* in regulating key functions of cell proliferation, differentiation and apoptosis of human keratinocytes was investigated.

*IEX-1* was initially found to be upregulated after  $\gamma$ -irradiation in the SCC-35 squamous carcinoma cell line [9]. The present study demonstrates that *IEX-1* is upregulated in a similar manner after  $\gamma$ -radiation in normal human keratinocytes (Figure 5). Interestingly, *IEX-1* mRNA reaches maximum levels earlier and returns to basal levels more promptly after radiation of human keratinocytes compared to SCC-35 cells. These differences in regulation of *IEX-1* expression and kinetics might be attributable to cell type-specific features, since carcinoma cell lines show variations in their response to mitogenic and stressful stimuli compared to primary cells [82]. Like the HaCaT cell line, the SCC-35 cell line is radiation resistant [102] and mutations in the tumor suppressor gene *p53* have been implicated in this resistance [103]. The *p53* gene is a nuclear phosphoprotein that has been demonstrated to play a key role in cellular damage responses, particularly in radiation-induced cell cycle arrest and apoptosis [104-106]. Wild type *p53* is a sequence specific DNA binding protein that regulates transcription of a variety of genes, such as *p21<sup>Waf1</sup>*, by binding to *p53* specific binding regions within their promoter element [107-109]. Similar to the *p21<sup>Waf1</sup>* gene [110], which is a well characterized *p53* target gene that is directly

involved in *p53* dependent cell cycle arrest [111], the promoter sequence of *IEX-1* contains a functional *p53* binding site [69]. It has been suggested that *IEX-1* is a *p53* target gene in *p53* dependent cell cycle arrest and apoptosis [112]. Mutation of *p53* in the SCC-35 cell line may be expected to result in changes in specific stress response regulatory pathways upstream of *IEX-1* and/or alter binding capacity of *p53* to the *IEX-1* promoter. In both cases *IEX-1* upregulation patterns might be changed in the carcinoma cell line compared to the primary keratinocytes. This may, in turn, provide the SCC-35 cell with the ability to become radiation resistant.

Similarly, this explanation might also be relevant to the observation of a prolonged *IEX-1* response after UV-B radiation of HaCaT cells compared to primary keratinocytes (Figures 6 and 9). Not only is *p53* involved in stress response after  $\gamma$ -radiation, but also seems to mediate stress response to UV-B induced cell damage: Studies examining UV-B induced tumors of the skin [113], upregulation in the epidermis after UV-B exposure *in vivo* [114] and mediation of UV-B induced apoptosis in keratinocytes *in vivo* [115] and *in vitro* [85] suggest an important role for *p53* in the UV-B stress response. A recent study postulates a repressor function of *p53* for *IEX-1* transcription. By systematic examination of the *IEX-1* promoter using gene reporter assays with *IEX-1* promoter truncations, the authors demonstrate a *p53* response element that represses *IEX-1* promoter activity [116]. The mutations in the *p53* gene in the HaCaT keratinocytes result in conformational changes in the *p53* protein [117,118]. Decreased affinity to the *p53* responsive element in the *IEX-1* promoter region due to altered protein structure might lead to decreased repression of transcription and therefore alter *IEX-1* upregulation pattern in HaCaT cells. Taken together these data indicate that *IEX-1* might be involved in cellular post-stress modifications and is at least partially controlled by the tumor suppressor *p53*. The role of *IEX-1* as a stress response gene is further supported by the fact that its expression is regulated by a number of transcription factors known to be involved in immediate cell cycle regulation. So is *SPI*, a preformed cytosolic transcription factor, a transcriptional activator of *IEX-1* and it seems that the ratio of *p53* and *SPI* is of importance for physiological levels of gene expression [116]. The *IEX-1* promoter sequence contains a *NFkB* binding site [69]. The *NFkB* family consists of transcriptional activators, such as *p65*, *p50*, *p52*, and *c-Rel*, that bind to DNA in a sequence specific manner [119]. In the cytosol *NFkB* is bound to *IkB*. Activation of

the pathway by extracellular signals, such as binding of transforming growth factor  $\beta$  (*TGF $\beta$* ) to its receptor leads to phosphorylation and degradation of *I $\kappa$ B*. *NF $\kappa$ B* is translocated to the nucleus and activates transcription of immediate early genes [120]. Recently it has been shown that overexpression of a dominant negative inhibitor of *NF $\kappa$ B* ablated *TGF $\beta$*  mediated induction of *IEX-1* [121]. The fact that the regulating elements in the *IEX-1* promoter sequence are highly conserved among different mammalian species [66,122] supports the hypothesis that the *IEX-1* promoter evolved to mediate transcriptional response under the influence of a variety of distinct types of growth related stimuli [122].

Marked differences in *IEX-1* upregulation dynamics after stress of keratinocytes with  $\gamma$ - or UV-B irradiation were observed (Figures 5 and 6) and can be explained by the physical differences and physiological consequences of treatment with either  $\gamma$ - or UV-rays. It is difficult to define an equivalent energy dose of UV-B irradiation and  $\gamma$ -irradiation to directly compare the differences in cell damage and stress response on a target cell. Gamma- or UV-B irradiation exert their effects in the cell via distinct mechanisms: Gamma-radiation with 10 Gy damages DNA to a greater extent than UV-B, but does not affect targets typically involved in the response to UV-B radiation at 40 mJ/cm<sup>2</sup>, such as the cell-membrane, membrane bound receptors and cytosolic kinases [89,123].

Gamma-radiation mediated DNA damage might directly lead to activation of preformed transcription factors [124], mediating upregulation of *IEX-1* and thereby causing a rapid and transient induction. UV-B radiation results in the recruitment of various pathways [89,125,126] that might first have to be activated to upregulate *IEX-1*. Various pathways might result in the upregulation of *IEX-1* at different stages, evoking a delayed and more persistent *IEX-1* response after UV-B, as compared to  $\gamma$ -irradiation (Figure 21).

UV-B radiation induces multiple cellular events that can lead to transcriptional activation of cell stress response genes. An important effect of UV radiation is ligand-independent dimerization and activation of membrane bound receptors, leading to activation of specific downstream pathways [62]. The death receptor FAS/CD95 can be activated independently from its ligand, mediating apoptosis in HaCaT cells after

UV-radiation [127]. Similarly, the EGF receptor is phosphorylated in keratinocytes after UV-radiation [128], and it has been shown that  $\text{H}_2\text{O}_2$  plays a major role in mediating phosphorylation of the autocatalytic EGFR kinase domain [26,129].

Ultraviolet radiation leads to extensive formation of reactive oxygen species, such as hydrogen peroxide ( $\text{H}_2\text{O}_2$ ), superoxide radical ( $\cdot\text{O}_2$ ) and hydroxyl radical ( $\cdot\text{OH}$ ) [123]. It has been proposed that  $\text{H}_2\text{O}_2$  serves as an intracellular second messenger [130,131].

In keratinocytes *IEX-1* is upregulated in a time and dose dependent manner by UV-B radiation hydrogen peroxide ( $\text{H}_2\text{O}_2$ ) and treatment with epidermal growth factor (EGF), the natural ligand of EGFR (Figures 6-8). Taken together, these findings indicate that UV-B induced upregulation of *IEX-1* mRNA may be mediated by EGFR dependent pathways. This hypothesis is further supported by the finding that blocking EGFR-signaling with the highly specific EGFR-tyrosine kinase inhibitor PD153035 significantly decreases *IEX-1* promoter activity (Figures 11 and 21). The observed downregulation of *IEX-1* mRNA at later time points in the course of the experiments in spite of persisting EGF or  $\text{H}_2\text{O}_2$  treatment can be explained by desensitization, internalization or downregulation of EGFR, and degradation of  $\text{H}_2\text{O}_2$  respectively (Figures 7 and 8).

To show a direct connection between formation of hydrogen peroxide and EGFR-mediated *IEX-1* upregulation, further experiments with UV-B radiation of cell cultures after blocking of EGFR, or pretreatment with radical scavengers are needed.

The fact that withdrawal of serum results in an even greater decrease in *IEX-1* promoter-activity than blockade of EGFR with PD153035 suggests that EGF might not be the only regulating mitogen inducing *IEX-1*, since fetal bovine serum contains a variety of undefined mitogenic substances that can interfere with growth related gene expression [132]. One known mitogen known to effect *IEX-1* expression is  $1,25(\text{OH})_2$ -Vitamin- $\text{D}_3$ . The steroid hormone vitamin D has been shown to promote cell differentiation in keratinocytes [133] and alter expression of known growth controlling genes [134]. After binding to a cytosolic receptor, the hormone-receptor complex is translocated to the nucleus where it exerts transcriptional modulation at specific Vitamin D response elements (VDRE) in the promoter region of growth regulating genes [135,136]. The *IEX-1* protein has been shown to be translocated from the nucleus to the perinuclear region after keratinocyte treatment with  $1,25(\text{OH})_2$ -

Vitamin-D<sub>3</sub> [70]. Also Vitamin D inhibits *IEX-1* on a transcriptional level [70], and an active vitamin-D response element (VDRE) in the *IEX-1* promoter region has been identified [122]. These data implicate that *IEX-1* not only is responding to immediate cell stress but also is involved in long lasting growth and differentiation control mechanisms.

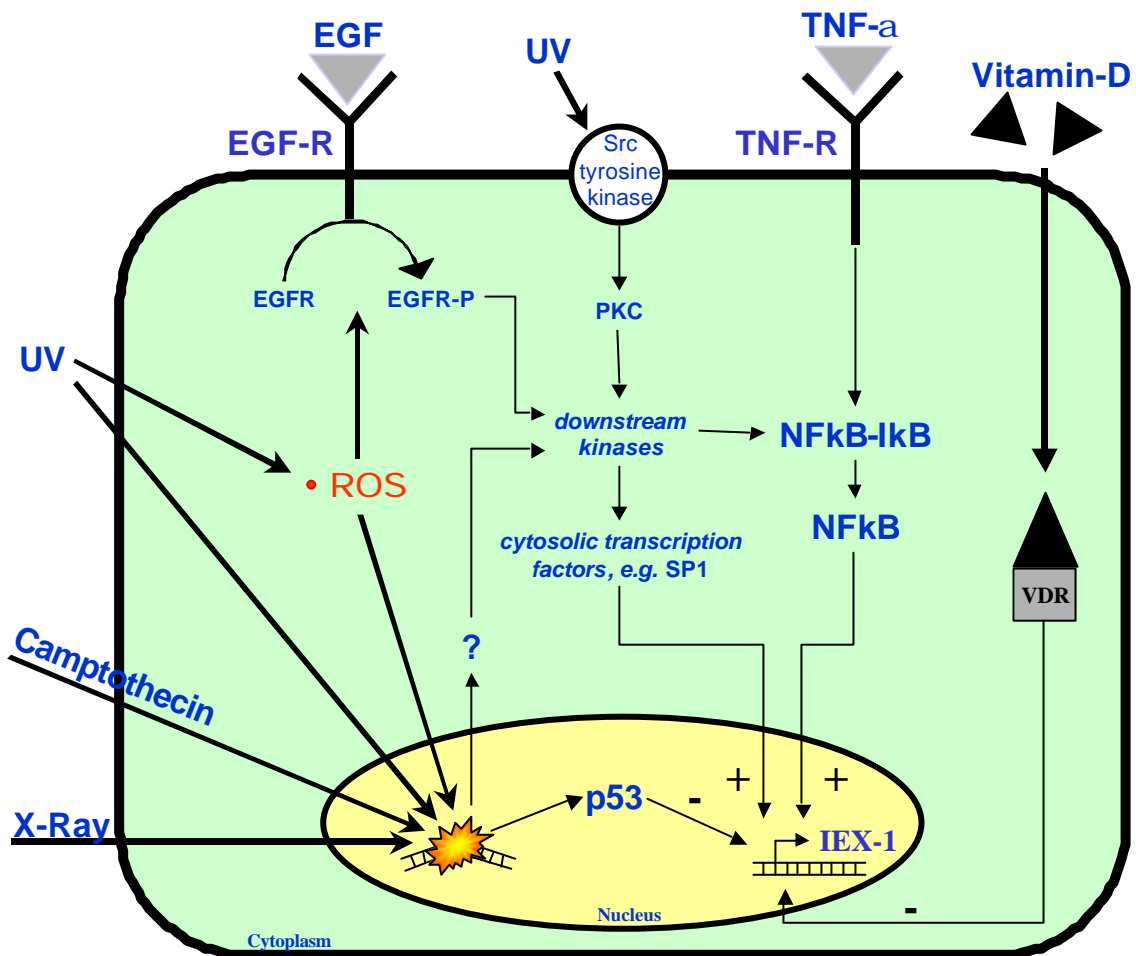


**Figure 21. Overview of Potential Pathways Regulating *IEX-1* Expression.** Stress-inducing stimuli lead to DNA damage. Intranuclear proteins translocate or are induced and lead to activation of cytoplasmic kinases that, in turn, activate transcription factors, such as *SP1* or *NFκB*, that induce transcription of *IEX-1*. *p53* activation in turn leads to repression of *IEX-1* transcription. UV-B also induces formation of reactive oxygen species (ROS) that damage DNA and activate EGFR tyrosine kinase. Recruitment of downstream pathways leads to activation of transcription factors that induce *IEX-1*. In addition, UV-B irradiation activates membrane bound kinases that lead to initiation of PKC-dependent pathways which also regulate transcription. *TNFα* pathway activation leads to dissociation of *IκB* and *NFκB*. *NFκB* is translocated to the nucleus and activates *IEX-1* transcription. Binding of 1,25(OH)<sub>2</sub>-Vitamin D<sub>3</sub> to its cytosolic receptor (VDR) leads to nuclear translocation of the complex and modification of *IEX-1* transcription.

*IEX-1* overexpression increases the growth rate in non-stressed, replicating HaCaT cell cultures (Figure 15). It was not clear whether this could be attributed to decreased cell death or to enhanced proliferation. The observation that *IEX-1* overexpressing cell cultures demonstrate greater numbers of detached, floating cells with higher apoptotic activity compared to control cell cultures suggested enhanced proliferation rather than decreased cell death (Table 3). Interestingly, in non-stressed, replicating cell cultures, no difference in Caspase 3 activity between *IEX-1* overexpressing or control-transfected HaCaT cells was observed (Figure 16). This shows that *IEX-1* overexpression alone does not alter the rate of apoptosis in the absence of stress. However, cell stress with apoptosis-inducing treatments, such as UV-B, camptothecin or withdrawal of serum lead to markedly higher Caspase 3 activity and nucleosome formation in the *IEX-1* over-expressing HaCaT cell line, compared to the control cell line (Figures 17 and 18). Furthermore, the observation that detached cells of the *IEX-1* cell culture exhibit higher Caspase 3 activity than sham-transfected cell cultures, supports these findings, since cell-cell interaction and communication with the extracellular matrix are important for cell integrity, and loss of these interactions can induce apoptosis [137-139].

In summary, over-expression of *IEX-1* in HaCaTs promotes growth and does not affect basal levels of apoptosis, but additional cellular stress stimuli lead to activation of an intracellular cell death program that might be crucially dependent on *IEX-1*.

In accordance with these results recently Arlt *et al.* showed that in HeLa cells ectopic expression of *IEX-1* does not prevent cell death, but instead triggers apoptosis induced by FASL, TNF $\alpha$  or etoposide. Transfection with *IEX-1*-antisense hammerhead ribozyme decreased apoptotic response to death ligands and etoposide [140]. In addition, Grobe *et al.* demonstrated that 293 cells, in which the *IEX-1* gene had been functionally disrupted, were significantly less sensitive to the above mentioned cell death promoting treatments [141]. Moreover, it has been shown that *IEX-1* overexpressing HeLa cells display accelerated cell cycle progression [140], whereas functional disruption of *IEX-1* slowed progression from G1 to S-phase [141].

In contrast to the pro-apoptotic *IEX-1*, its long form *IEX-1L* has been reported to be an apoptosis-inhibitor [67]. It was suggested that *IEX-1L* was a non-spliced, anti-apoptotic variant of the original *IEX-1*. Meanwhile the existence of *IEX-1L* has been

```

(151) //...cccgcagcggcccctgccgggcgccagcgcctctcgcgggcaccgaaagcgcagccgc
      -
(211) agggg tctctaccctcgagtg[gtgagtatcgccgaagtgggcattcggggggtgcgctgc
      c
(271) cctggagtcactggggaacgacccgactccagaggcctcgacctgacctgtctcctgttt
      -
(331) tgctccccttag]gtccggcgccagctgccagtcgaggaaccgaaccagccaaaaggct
      •
(391) tctctttctgctgctcaccatcgtcttctgccagatcctgatggctgaaggggtgtgcc ...//
      •

```

**Table 4. *IEX-1* Gene: Region of Intron Site.** Intron bold and in brackets, arrows indicate differences between the long form *IEX-1L* and wild type (wt) *IEX-1*. Deletion of a guanine base at position 344 (●) results in lack of an acceptor site for splicing. This causes transcription of the intron sequence. The deletion of a guanine at position 303 (●) explains why the expressed intron in *IEX-1L* is only 111bp compared to the 112bp in the wt-sequence. The insertion of a cytosine base in position 215 prevents nonsense transcription.

questioned, and is thought to be an artificial, mutated PCR product, not expressed *in vivo* (Table 4). The anti-apoptotic effects of *IEX-1L* are likely due to dominant-negative inhibition of endogenous *IEX-1* [68].

The differences between the *IEX-1* and *IEX-1L* protein sequences might also explain the different subcellular localization. *IEX-1L* was reported to be predominantly found in perinuclear regions and in the endoplasmatic reticulum [67], whereas the present study reveals intranuclear localization of *IEX-1* in HaCaT cells, by GFP-tagging, as well as immunostaining (Figures 12 and 13). Translation of the intron sequence might lead to conformational changes in the protein, preventing its nuclear translocation. Extranuclear localization and nuclear-cytoplasmatic translocation of GFP-tagged wild-type *IEX-1* has been reported [67,70]. The *IEX-1* protein sequence contains putative glycosylation and phosphorylation sites [9]. Glycosylation status and/or phosphorylation with subsequent conformational changes might be responsible for the subcellular distribution of the protein. The conformational changes of the protein might prevent immunostaining of the extranuclear *IEX-1* protein. Similar observations were made for the *p53* protein, when exclusively intranuclear or extranuclear *p53* was found, depending on the antibody used for immunostaining [142]. Immunohistochemical staining has also been reported to depend on the phosphorylation status of the *p53* protein [118]. Conformational and structural changes of proteins may result in functional alterations, for nuclear exclusion of *p53* results in inactivation of *p53* function [143,144]. Similarly, *IEX-1* could exert functions in different subcellular localizations, depending on cell type, differentiation status or environmental conditions.

*In vitro*, the protein seems to accumulate in distinct nuclear regions (Figures 12 and 13), suggesting that the protein is exerting its function at specific intranuclear sites. The protein might be binding to certain DNA regions and play a regulatory role in gene transcription. The putative histone binding region [9] might enable the *IEX-1* protein to bind to histone-DNA complexes. In the nucleus double helix DNA is wound twice around DNA-binding nuclear protein-polymers, called histones to protect and stabilize chromosomes [145]. Gene transcription requires separation of DNA from histones [146], and access to DNA is regulated by a diverse array of post-translational modifications of histones. Acetylation of histone amino-termini leads to transcriptional activation, whereas de-acetylation and methylation of histones results in transcriptional silencing [147]. Transition between these states is generated by enzyme families called histone acetyl-transferase (HAT), histone de-acetylase (HDAC) and histone methyl-transferase (HMTase). These enzymes can be recruited by chromatin-modifying complexes, consisting of DNA sequence specific transcription factors and proteins of the transcription factor family *E2F* and the pocket protein family *pRB*, that seem to modulate histone modification [147,148]. A number of immediate early response genes have been shown to exert their functions at least partially by modifying histone modulation. So is *p53* mediated upregulation of the cell cycle regulatory protein *p21<sup>Waf1</sup>* dependent on recruitment of the *p300* acetyl-transferase [149], and the immediate early gene *c-myc* has been shown to build complexes with proteins that possess HAT-activity [150], and possibly is involved in activation of deacetylated, silenced genes in G0 cell cycle phase upon transition into G1 phase [151].

*IEX-1* might be functioning in a similar way: Hypothetically, *IEX-1* could be activated under certain conditions, bind to histones, recruit other proteins to form a histone modifying complex and thereby promote the transcription of cell cycle regulatory genes involved in cell growth, survival and differentiation.

In the epidermis, *IEX-1* is predominantly expressed in basal cell layers. In upper layers, *IEX-1* protein abundance was decreased, and in the stratum corneum no *IEX-1* expression was observed (Figure 20). Upon migration from basal layers to the upper layers in the epidermis, keratinocytes enter the process of terminal differentiation, characterized by changes in morphology and expression of specific differentiation markers [22,23].



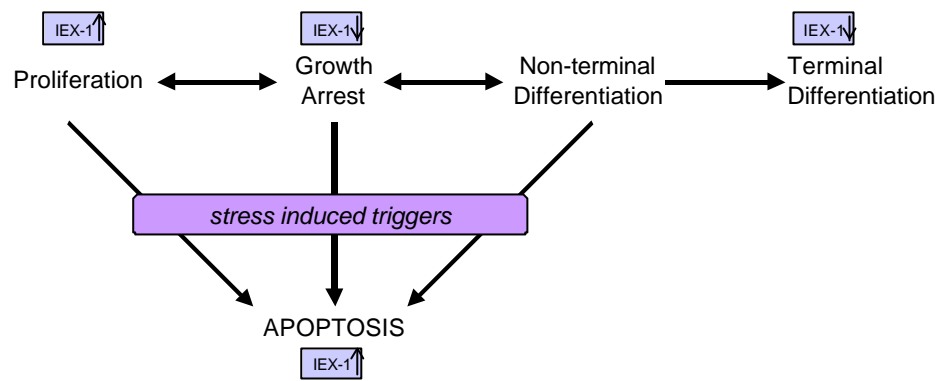


**Figure 22.** Stages in Cell Life and Correlation with *IEX-1* Expression.

This suggests that *IEX-1* expression in keratinocytes might be dependent on the differentiation status of the cell. This hypothesis is also supported by the previous observation that *IEX-1* mRNA expression was downregulated in primary keratinocyte cultures after reaching confluence, after Vitamin D treatment and after growth factor withdrawal [70]. Either of these conditions or treatments induce growth arrest and have been suggested to induce differentiation in human keratinocytes [72,133,152]. Similarly, *IEX-1* was reported to be significantly downregulated in freshly isolated monocytes upon differentiation to macrophages by exposure to differentiation inducing stimuli [11].

Recent unpublished Northern blotting experiments show delayed expression of the keratinocyte differentiation markers *K1*, *K10* and *Involucrin* in *IEX-1* overexpressing HaCaT as compared to sham-transfected HaCaT following serum deprivation. These experiments imply that *IEX-1* is not only downregulated during cell differentiation, but downregulation of *IEX-1* might be required for initiation of differentiation. These findings are in accordance with the proliferation-promoting function of *IEX-1*: Upon differentiation, keratinocytes and HaCaT cells in culture lose clonogenic potential [81,153,154]. *In vivo*, differentiation of keratinocytes in the epidermis is accompanied by loss of mitotic activity [155]. Additionally, it has been shown that growth arrest of keratinocytes and HaCaT is followed by decreased susceptibility to apoptosis [86]. The proliferation-promoting function of *IEX-1* in differentiated cells is not required, and therefore, its expression is decreased upon differentiation or growth arrest *in vitro* and in differentiated epidermal layers *in vivo*.

In this context, the observed high apoptotic activity in *IEX-1* overexpressing HaCaT cells during withdrawal of serum (Figure 19) might not necessarily be a direct response to the cell stress, but rather represent a response to an internal conflict

between contradicting signals. Similar observations have been made for the proto-oncogene *c-myc*: Overexpression of *c-myc* drives cell cycle progression and promotes proliferation [156]. Following growth factor withdrawal, *c-myc* expression was downregulated, and cells exited the cell cycle, whereas *c-myc* overexpressing cells underwent apoptosis [157]. Deprivation of serum results in intracellular signaling changes that induce growth arrest and initiate differentiation [72]. This stays in conflict with constitutive overexpression of growth promoting genes like *IEX-1* or *c-myc*, resulting in an impaired balance of growth-arresting and proliferation-enhancing signaling pathways. It has been shown that, in the case of conflicting information about further progression through the cell cycle the cell suicide program is activated [5,158] (Figure 23).

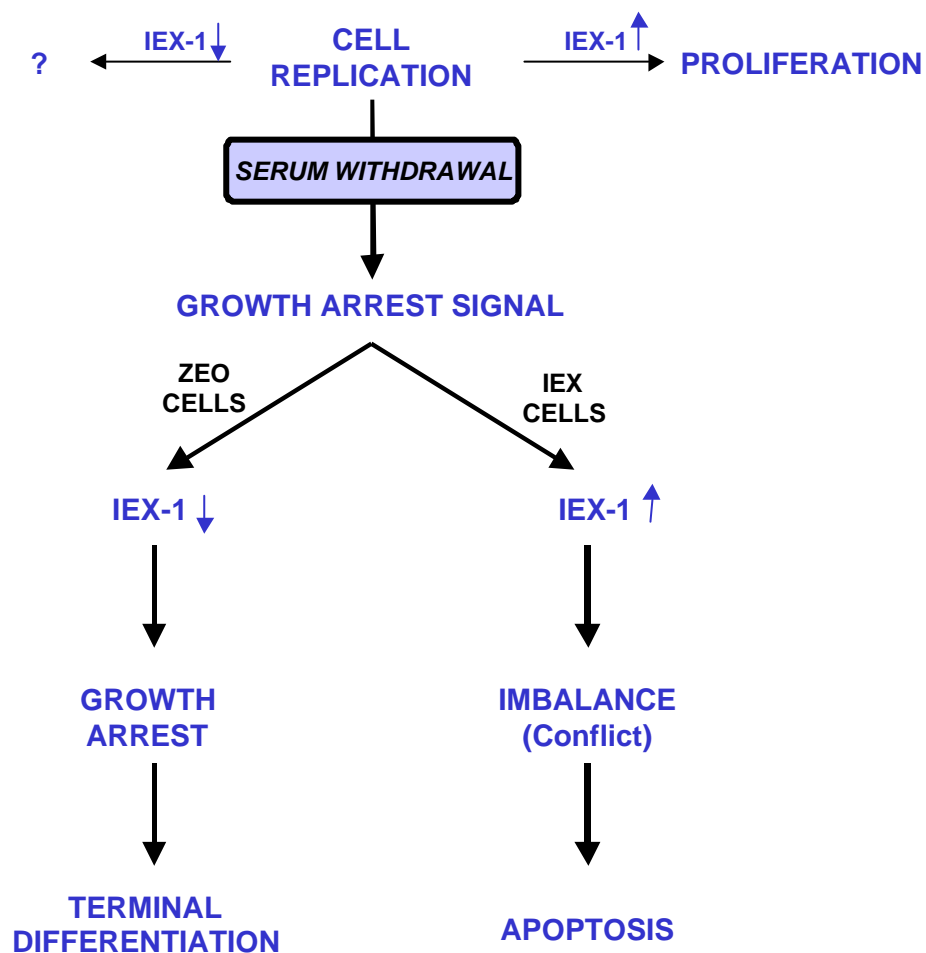


**Figure 23.** Conflict Model for *IEX-1* Overexpressing HaCaT

It seems paradoxical that a proliferation enhancing gene is significantly upregulated as a response to damaging cell stress, since DNA damage results in a transient cell cycle arrest to allow for damage repair or, in case of extensive damage, programmed cell death [8,91]. A similar observation has been made for *c-jun*, a transcription factor that drives proliferation and G1- to S-phase progression by repression of *p53* controlled upregulation of the cyclin-dependent kinase (CDK) inhibitor *p21<sup>Waf1</sup>* [159]. Surprisingly *c-jun* is upregulated and activated as a result to treatment with various DNA damaging agents [160,161]. In a recent study Shaulian *et al.* proposed an explanation for this phenomenon: *C-jun* deficient mouse fibroblasts exhibited prolonged cell cycle arrest and resistance to apoptosis following UV irradiation. *C-jun* overexpressing fibroblasts, in contrast, did not growth arrest, but underwent apoptosis as a response to UV irradiation. These effects were exerted through inhibition of *p53* association with the *p21<sup>Waf</sup>* promoter. The authors argue that *c-jun* might be crucial for cell-cycle re-entry following growth arrest after UV-irradiation [162]. *IEX-1* could be involved in similar cell cycle regulatory mechanisms. Under physiological conditions *IEX-1* could be promoting proliferation by either repressing transcription of cell cycle regulatory genes like *p21<sup>Waf</sup>* or by enhancing expression of CDK-like proteins that promote transgression of the cell cycle. In case of damaging cell stress an attenuation of the *IEX-1* signal in form of transcriptional upregulation might be necessary to overcome growth arrest signals. Transgression through cell cycle checkpoints, without growth arrest and damage repair, driven by constitutive *IEX-1* expression might lead to activation of cell suicide programs following DNA damaging insults and explain the observed high apoptotic activity in the IEX cell line after Camptothecin or UV-B treatment. Further studies investigating *IEX-1* expression after inducing growth arrest at various points in the cell cycle and investigation of interaction with other cell cycle proteins will reveal more insight into *IEX-1* cell cycle control.

In this way *IEX-1* could be having a dual role in cell cycle decisioning: On the one hand proliferation enhancement, on the other hand apoptotic-facilitation. In the absence of stress the pro-apoptotic effects of *IEX-1* might be suppressed by anti-apoptotic signals. The significant upregulation of *IEX-1* after cell damage might overcome the anti-apoptotic suppression and lead to caspase activation with subsequent initiation of the cell death program. In this case the proliferation enhancing function of *IEX-1* is possibly suppressed. If *IEX-1* upregulation does not

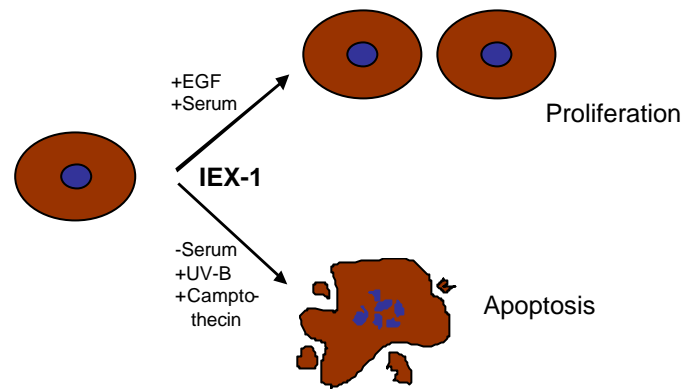


**Figure 24. Dual Role of *IEX-1***

result in cell death or cell cycle progression, *IEX-1* expression is rapidly downregulated, to allow cell damage repair.

Similar findings have been reported for the cell growth regulatory gene *c-myc*: In cell culture, *c-myc* activation is followed by increased cell growth preceding DNA synthesis and accelerated proliferation [163]. Alternatively, *c-myc* is interfering with CD95/FAS and TNF-death pathways, promoting cell death [55,164]. Consequently a modified dual function has recently been proposed for *c-myc*: Via one pathway the gene promotes proliferation and primes the cell for apoptosis, while it triggers apoptosis via a second, distinct pathway, that is suppressed under normal conditions by survival factors [55]. Like *c-myc*, *IEX-1* might serve a role as coordinating element between cell proliferation and apoptosis, recruiting distinct pathways according to varying environmental conditions.

### 4.3 Conclusions

The complexity of gene expression in cellular responses to stress, damage and mitogenic stimuli is only beginning to be understood. With new applications in molecular biology, important tools to investigate normal gene expression, pathologic gene responses and therapeutic intervention in diseases, characterized by disturbed cell proliferation will be available.

The immediate early response gene *IEX-1* is involved in cellular stress response and proliferation. Like other known immediate early genes, such as *c-myc*, *c-jun* or *p21<sup>Waf1</sup>* that are involved in the cellular stress response, *IEX-1* might also control

progression through the cell cycle and play a role in mediating DNA damage repair, growth arrest or apoptosis.

*IEX-1* may be directly involved in the pathway of apoptosis but, more likely, indirectly controls pro- or anti-apoptotic signals by gene regulation on a transcriptional level. By dual signaling activities, *IEX-1* may serve as a default regulator within the cell, to promote its proliferation when cellular conditions are favorable but also, to facilitate elimination of the cell by enhancing pro-apoptotic or inhibiting anti-apoptotic pathways when stress is encountered. The rapid increase in *IEX-1* expression could be responsible for the default switch that converts proliferation to programmed death within the cell.

These attempts to characterize the role of *IEX-1* in keratinocyte proliferation, differentiation and apoptosis, could give some insight into the function of *IEX-1*. The exact functions and pathways in which *IEX-1* plays a regulatory role remain unclear and further investigations will define the importance of *IEX-1* for cell integrity.

#### **4.4 Future Perspectives in *IEX-1* Research**

Future research to reveal more knowledge on the function of *IEX-1* should focus on three related main fields: i) The question of how *IEX-1* gene expression is regulated ii) Detailed analysis of protein structure and iii) Functional analysis of the protein.

*IEX-1* gene regulation and the question in which pathways *IEX-1* is involved could be addressed by more extensive promoter studies. The promoter sequence could be analyzed for known regulatory sequences and more detailed promoter-gene-reporter experiments with truncated promoter elements could be performed.

The structure of the protein could be analyzed to reveal specific properties of the function and importance of the glycosylation and phosphorylation sites. Studies of intracellular, especially subcellular localization or intracellular trafficking will give insight into the function.

The most promising field is predicted to be functional analysis of the *IEX-1* gene. Gene over-expression studies of the *IEX-1* in primary keratinocytes could be performed using viral expression vectors.

Gene suppression studies could also give valuable information about possible functions of *IEX-1*. In this context the *IEX-1L* protein could be used as a dominant negative to suppress wild type *IEX-1*-protein function by competitive inhibition. Another possibility is overexpression of *IEX-1* anti-sense mRNA or blocking gene transcription by binding peptide nucleic acids (PNA) to parts of the coding region of *IEX-1*.

Finally, transgenic animal models could give new insight into *IEX-1* function and its relevance *in vivo*. In our laboratories a transgenic murine model is currently being established. In this model *IEX-1* overexpression is directed exclusively to the epidermis by subcloning the *IEX-1* sequence into a vector bearing the involucrin promoter, to study the impacts of *IEX-1* overexpression on keratinocytes *in vivo*.

## 5. Summary

In the present study *IEX-1* a novel, stress induced and differentiation regulated immediate early gene has been further characterized. Gene-regulation and function were investigated in the keratinocyte and HaCaT model.

Gene regulation after cell stress or mitogenic treatment were investigated with Northern blotting and promoter studies. In gene expression studies in HaCaT cells effects of *IEX-1* on proliferation, differentiation and programmed cell death were examined. In addition, subcellular localization of *IEX-1* protein *in vitro* was investigated using immunohistochemical and molecular-biological methods. Tissue distribution of *IEX-1* protein in the epidermis was defined.

It was attempted to define possible activation pathways of *IEX-1* and its involvement in proliferation, differentiation and programmed cell death. The results of the present study can be summarized as follows:

Treatment of primary keratinocytes and HaCaT cells with stress or mitogenic stimuli is followed by a rapid and transient up-regulation of *IEX-1* mRNA, that possibly is mediated by an EGFR-controlled pathway.

Over-expression of *IEX-1* enhances proliferation in HaCaT cells without changing death rate in the culture.

*IEX-1* over-expression does not enhance apoptosis of HaCaT cells in unstressed, replicating cell cultures, but renders HaCaT cells susceptible to apoptosis inducing treatments.

*In vitro* and *in vivo* *IEX-1* expression is dependent on an undifferentiated state of the cell.

## 6. References

1. Leffell D (2000 Jan) The scientific basis of skin cancer. *J Am Acad Dermatol* 42: 18-22
2. Yuspa S (1998 May) The pathogenesis of squamous cell cancer: lessons learned from studies of skin carcinogenesis. *J Dermatol Sci* 17: 1-7
3. Weisburger J (2001 Sep 1) Antimutagenesis and anticarcinogenesis, from the past to the future. *Mutat Res* 480-481: 23-35
4. Wyllie AH (1997) Apoptosis and carcinogenesis. *Eur J Cell Biol* 73: 189-197
5. Evan G, Littlewood T (1998) A matter of life and cell death. *Science* 281: 1317-1322
6. Jehn BM, Osborne BA (1997) Gene regulation associated with apoptosis. *Crit Rev Eukaryot Gene Expr* 7: 179-193
7. Zhou B, Elledge S (2000 Nov 23) The DNA damage response: putting checkpoints in perspective. *Nature* 408: 433-439
8. Coultas L, Strasser A (2000 Dec) The molecular control of DNA damage-induced cell death. *Apoptosis* 5: 491-507
9. Kondratyev AD, Chung KN, Jung MO (1996) Identification and characterization of a radiation-inducible glycosylated human early-response gene. *Cancer Res* 56: 1498-1502
10. Kumar R, Kobayashi T, Warner GM, Wu Y, Salisbury JL, Lingle W, Pittelkow MR (1998) A novel immediate early response gene, IEX-1, is induced by ultraviolet radiation in human keratinocytes. *Biochem Biophys Res Com* 253: 336-341
11. Pietzsch A, Buchler C, Aslanidis C, Schmitz G (1997) Identification and characterization of a novel monocyte/macrophage differentiation-dependent gene that is responsive to lipopolysaccharide, ceramide, and lysophosphatidylcholine. *Biochem Biophys Res Com* 235: 4-9
12. Watt F (1989) Terminal differentiation of epidermal keratinocytes. *Curr Opin Cell Biol* 1: 1107-1115
13. Montagna W, Kligmann AM, Carlisle KS. *Atlas of normal human skin*, Springer-Verlag New York, Heidelberg, Berlin, 1992.
14. Watt FM (1998) Epidermal stem cells: markers, patterning and the control of stem cell fate. *Philosoph Transact of the Royal Soc London - Series B: Biological Sciences* 353: 831-837
15. Turksen K, Troy T (1998) Epidermal cell lineage. *Biochem Cell Biol* 76: 889-898
16. Fuchs E, Byrne C (1994) The epidermis: rising to the surface. *Curr Opin Genet Dev* 4: 725-736
17. McCall CA, Cohen JJ (1991) Programmed cell death in terminally differentiating keratinocytes: role of endogenous endonuclease. *J Invest Dermatol* 97: 111-114
18. Haake AR, Polakowska RR (1993) Cell death by apoptosis in epidermal biology. *J Invest Dermatol* 101: 107-112
19. Polakowska RR, Piacentini M, Bartlett R, Goldsmith LA, Haake AR (1994) Apoptosis in human skin development: morphogenesis, periderm, and stem cells. *Dev Dyn* 199: 176-188



20. Gandarillas A, Davies D, Blanchard J (2000 Jul 6) Normal and c-Myc-promoted human keratinocyte differentiation both occur via a novel cell cycle involving cellular growth and endoreplication. *Oncogene* 19: 3278-3289
21. Jetten AM, Harvat BL (1997) Epidermal differentiation and squamous metaplasia: from stem cell to cell death. *J Dermatol* 24: 711-725
22. Eckert RL, Crish JF, Robinson NA (1997) The epidermal keratinocyte as a model for the study of gene regulation and cell differentiation. *Physiol Rev* 77: 397-424
23. Mischke D (1998) The complexity of gene families involved in epithelial differentiation. Keratin genes and the epidermal differentiation complex. *Sub-Cell Biochem* 31: 71-104
24. Huang S, Ingber DE (1999) The structural and mechanical complexity of cell-growth control. *Nature Cell Biol* 1: E131-138
25. Presland R, Kuechle M, Lewis S, Fleckman P, Dale B (2001 Nov 1) Regulated expression of human filaggrin in keratinocytes results in cytoskeletal disruption, loss of cell-cell adhesion, and cell cycle arrest. *Exp Cell Res* 270: 199-213
26. Hackel PO, Zwick E, Prenzel N, Ullrich A (1999) Epidermal growth factor receptors: critical mediators of multiple receptor pathways. *Cur Opin Cell Biol* 11: 184-189
27. Gandarillas A (2000) Epidermal differentiation, apoptosis, and senescence: common pathways? *Exp Gerontol* 35: 53-62
28. Carpenter G, Cohen S (1990) Epidermal growth factor. *J Biol Chem* 265: 7709-7712
29. Nanney L, Magid M, Stoscheck C, King LJ (1984) Comparison of epidermal growth factor binding and receptor distribution in normal human epidermis and epidermal appendages. *J Invest Dermatol* 83: 385-393
30. King LJ, Gates R, Stoscheck C, Nanney L (1990) Epidermal growth factor/transforming growth factor alpha receptors and psoriasis. *J Invest Dermatol* 95: 10S-12S
31. Oyama N, Sekimata M, Nihei Y, Iwatsuki K, Homma Y, Kaneko F (1998) Different growth properties in response to epidermal growth factor and interleukin-6 of primary keratinocytes derived from normal and psoriatic lesional skin. *J Dermatol Sci* 16: 120-128
32. Mendelsohn J, Baselga J (2000) The EGF receptor family as targets for cancer therapy. *Oncogene* 19: 6550-6565
33. Shimizu T, Izumi H, Oga A, Furumoto H, Murakami T, Ofuji R, Muto M, Sasaki K (2001) Epidermal growth factor receptor overexpression and genetic aberrations in metastatic squamous-cell carcinoma of the skin. *Dermatology* 202: 203-206
34. Gulliford T, Ouyang X, Epstein R (1999) Intensification of growth factor receptor signalling by phorbol treatment of ligand-primed cells implies a dimer-stabilizing effect of protein kinase C-dependent juxtamembrane domain phosphorylation. *Cell Signal* 11: 245-252
35. Pittelkow M, Cook P, Shipley GD, R., Coffey RJ (1993) Autonomous growth of human keratinocytes requires epidermal growth factor receptor occupancy. *Cell Growth Differ*. 4: 513-521
36. Margolis B, Skolnik E (1994 Dec) Activation of Ras by receptor tyrosine kinases. *J Am Soc Nephro* 5: 1288-1299

37. Opresko L, Chang C, Will B, Burke P, Gill G, Wiley H (1995 Mar 3) Endocytosis and lysosomal targeting of epidermal growth factor receptors are mediated by distinct sequences independent of the tyrosine kinase domain. *J Biol Chem* 270: 4325-4333
38. Burke P, Wiley H (1999 Sep) Human mammary epithelial cells rapidly exchange empty EGFR between surface and intracellular pools. *J Cell Physiol* 180: 448-460
39. Chen N, Ma W, She Q, Wu E, Liu G, Bode A, Dong Z (2001 Dec 14) Transactivation of the Epidermal Growth Factor Receptor Is Involved in 12-O-Tetradecanoylphorbol-13-acetate-induced Signal Transduction. *J Biol Chem* 276: 46722-46728
40. Bos M, Mendelsohn J, Kim Y, Albanell J, Fry D, Baselga J (1997) PD153035, a tyrosine kinase inhibitor, prevents epidermal growth factor receptor activation and inhibits growth of cancer cells in a receptor number-dependent manner. *Clin Cancer Res* 3: 2099-2106
41. Kunkel M, Hook K, Howard C, Przybranowski S, Roberts B, Elliott W, Leopold W (1996) Inhibition of the epidermal growth factor receptor tyrosine kinase by PD153035 in human A431 tumors in athymic nude mice. *Invest New Drugs* 13: 295-302
42. Modjtahedi H, Affleck K, Stubberfield C, Dean C (1998) EGFR blockade by tyrosine kinase inhibitor or monoclonal antibody inhibits growth, directs terminal differentiation and induces apoptosis in the human squamous cell carcinoma HN5. *Int J Oncol* 13: 335-342
43. Peter ME, Heufelder AE, Hengartner MO (1997) Advances in apoptosis research. *Proc Natl Acad Sci U S A* 94: 12736-12737
44. Jacobson MD, Weil M, Raff MC (1997) Programmed cell death in animal development. *Cell* 88: 347-354
45. Kerr JF, Wyllie AH, Currie AR (1972) Apoptosis: a basic biological phenomenon with wide-ranging implications in tissue kinetics. *Br J Cancer* 26: 239-257
46. Saraste A, Pulkki K (2000) Morphologic and biochemical hallmarks of apoptosis. *Cardiovasc Res* 45: 528-537
47. Leppa S, Bohmann D (1999) Diverse functions of JNK signaling and c-Jun in stress response and apoptosis. *Oncogene* 18: 6158-6162
48. Casaccia-Bonnel P (2000) Cell death in the oligodendrocyte lineage: a molecular perspective of life/death decisions in development and disease. *Glia* 29: 124-135
49. Eisel D, Fertig G, Fischer B, Manzow S, Schmelig K. Apoptosis and Cell Proliferation. Mannheim, Boehringer Mannheim GmbH, Biochemica, 1998.
50. Green D, Amarante-Mendes G (1998) The point of no return: mitochondria, caspases, and the commitment to cell death. *Results Probl Cell Differ* 24: 45-61
51. Ashkenazi A, Dixit VM (1998) Death receptors: signaling and modulation. *Science* 281: 1305-1308
52. Tan S, Sagara Y, Liu Y, Maher P, Schubert D (1998) The regulation of reactive oxygen species production during programmed cell death. *J Cell Biol* 141: 1423-1432
53. Li G (1999) The role of mismatch repair in DNA damage-induced apoptosis. *Oncol Res* 11: 393-400

54. Maclean K, Yang H, Cleveland J (2001 Apr 2-27) Serum suppresses myeloid progenitor apoptosis by regulating iron homeostasis. *J Cell Biochem* 82: 171-186
55. Prendergast GC (1999) Mechanisms of apoptosis by c-Myc. *Oncogene* 18: 2967-1987
56. Thornberry NA, Lazebnik Y (1998) Caspases: enemies within. *Science* 281: 1312-1316
57. Earnshaw W, Martins L, Kaufmann S (1999) Mammalian caspases: structure, activation, substrates, and functions during apoptosis. *Annu Rev Biochem* 68: 383-424
58. Gandarillas A, Goldsmith LA, Gschmeissner S, Leigh IM, Watt FM (1999) Evidence that apoptosis and terminal differentiation of epidermal keratinocytes are distinct processes. *Exp Dermatol* 8: 71-79
59. Teraki Y, Shiohara T (1999) Apoptosis and the skin. *Europ J Dermatol* 9: 413-25
60. Danno K, Horio T (1987) Sunburn cell: factors involved in its formation. *Photochem Photobiol* 45: 683-690
61. Murphy G, Young A, Wulf H, Kulms D, Schwarz T (2001) The molecular determinants of sunburn cell formation. *Exp Dermatol* 10: 155-160
62. Schwarz T (1998) UV light affects cell membrane and cytoplasmic targets. *J Photochem Photobiol. B - Biology* 44: 91-96
63. Homo sapiens radiation-inducible immediate early response gene IEX1(IEX1) mRNA, complete cds. *GeneBank* *ACCESSION* AF083421.
64. Pietzsch A, Buchler C, Schmitz G (1998) Genomic organization, promoter cloning, and chromosomal localization of the Dif-2 gene. *Biochem Biophys Res Com* 245: 651-657
65. Charles CH, Yoon JK, Simske JS, Lau LF (1993) Genomic structure, cDNA sequence, and expression of gly96, a growth factor-inducible immediate-early gene encoding a short-lived glycosylated protein. *Oncogene* 8: 797-801
66. Schafer H, Trauzold A, Siegel EG, Folsch UR, Schmidt WE (1996) PRG1: a novel early-response gene transcriptionally induced by pituitary adenylate cyclase activating polypeptide in a pancreatic carcinoma cell line. *Cancer Res* 56: 2641-2648
67. Wu MX, Ao Z, Prasad KV, Wu R, Schlossman SF (1998) IEX-1L, an apoptosis inhibitor involved in NF-kappaB-mediated cell survival. *Science* 281: 998-1001
68. Schafer H, Arlt A, Trauzold A, Hunermann-Jansen A, Schmidt WE (1999) The putative apoptosis inhibitor IEX-1L is a mutant nonspliced variant of p22(PRG1/IEX-1) and is not expressed in vivo. *Biochem Biophys Res Com* 262: 139-145
69. Schafer H, Diebel J, Arlt A, Trauzold A, Schmidt WE (1998) The promoter of human p22/PACAP response gene 1 (PRG1) contains functional binding sites for the p53 tumor suppressor and for NFkappaB. *FEBS Lett* 436: 139-143
70. Kobayashi T, Pittelkow MR, Warner GM, Squillace KA, Kumar R (1998) Regulation of a novel immediate early response gene, IEX-1, in keratinocytes by 1alpha,25-dihydroxyvitamin D3. *Biochem Biophys Res Com* 251: 868-873
71. Feldmann K, Pittelkow M, Roche P, Kumar R, Grande J (2001) Expression of an immediate early gene, IEX-1, in human tissues. *Histochem Cell Biol* 115: 489-497

72. Poumay Y, Pittelkow MR (1995) Cell density and culture factors regulate keratinocyte commitment to differentiation and expression of suprabasal K1/K10 keratins. *Journal of Investigative Dermatology* 104: 271-276
73. Kumar R, Schaefer J, Grande JP, Roche PC (1994) Immunolocalization of calcitriol receptor, 24-hydroxylase cytochrome p-450, and calbindin D28k in human kidney. *Am J Physiol* 266: F477-485
74. Diffey BL, Whillock MJ, McKinlay AF (1984) A preliminary study on photoaddition and erythema due to UVB radiation. *Phys Med Biol* 29: 419-425
75. Watt F (1991) Cell culture models of differentiation. *FASEB J* 5: 287-294
76. Schoop V, Mirancea N, Fusenig N (1999) Epidermal organization and differentiation of HaCaT keratinocytes in organotypic coculture with human dermal fibroblasts. *J Invest Derm* 112: 343-353
77. Huttunen M, Hyttinen M, Nilsson G, Butterfield J, Horsmanheimo M, Harvima I (2001) Inhibition of keratinocyte growth in cell culture and whole skin culture by mast cell mediators. *Exp Dermatol* 10: 184-192
78. Jones G. Establishment and Maintenance of Normal Human Keratinocyte Cultures. In: *Methods in Molecular Medicine: Human Cell Culture Protocols*. Linge C (ed.) Totowa, NJ, Humana Press Inc., 1996.
79. Sanford K, Evans V (1982) A quest for the mechanism of "spontaneous" malignant transformation in culture with associated advances in culture technology. *J Natl Cancer Inst* 68: 895-913
80. Staedel C, Remy J, Hua Z, Broker T, Chow L, Behr J (1994) High-efficiency transfection of primary human keratinocytes with positively charged lipopolyamine:DNA complexes. *J Invest Dermatol* 102: 768-772
81. Boukamp P, Petrussevska RT, Breitkreutz D, Hornung J, Markham A, Fusenig NE (1988) Normal keratinization in a spontaneously immortalized aneuploid human keratinocyte cell line. *J Cell Biol* 106: 761-771
82. Fusenig N, Boukamp P. Carcinogenesis studies in human cells: Reliable in vitro models. In: Fusenig N, Graf H (eds.) *Cell Culture in Pharmaceutical Research*. Berlin, Springer-Verlag Berlin Inc., 1994.
83. Fusenig N, Boukamp P (1998) Multiple stages and genetic alterations in immortalization, malignant transformation, and tumor progression of human skin keratinocytes. *Mol Carcinog* 23: 144-158
84. Boukamp P, Popp S, Altmeyer S, Hulsen A, Fasching C, Cremer T, Fusenig N (1997) Sustained nontumorigenic phenotype correlates with a largely stable chromosome content during long-term culture of the human keratinocyte line HaCaT. *Gen Chromosom Cancer* 19: 201-214
85. Henseleit U, Zhang J, Wanner R, Haase I, Kolde G, Rosenbach T (1997) Role of p53 in UVB-induced apoptosis in human HaCaT keratinocytes. *J Invest Dermatol* 109: 722-727
86. Chaturvedi V, Qin JZ, Denning MF, Choubey D, Diaz MO, Nickoloff BJ (1999) Apoptosis in proliferating, senescent, and immortalized keratinocytes. *J Biolog Chem* 274: 23358-23367
87. Nagata S (1997) Apoptosis by death factor. *Cell* 88: 355-365
88. Verheij M, Bartelink H (2000) Radiation-induced apoptosis. *Cell Tissue Res* 301: 133-142
89. Bender K, Blattner C, Knebel A, Iordanov M, Herrlich P, Rahmsdorf HJ (1997) UV-induced signal transduction. *J Photochem Photobiol. B - Biology* 37: 1-17

90. Chen F, Vallyathan V, Castranova V, Shi X (2001) Cell apoptosis induced by carcinogenic metals. *Mol Cell Biochem* 222: 183-188
91. Taylor W, Stark G (2001) Regulation of the G2/M transition by p53. *Oncogene* 20: 1803-1815
92. Green DR (1998) Apoptotic pathways: the roads to ruin. *Cell* 94: 695-698
93. Huang T, Wuerzberger-Davis S, Seufzer B, Shumway S, Kurama T, Boothman D, Miyamoto S (2000) NF-kappaB activation by camptothecin. A linkage between nuclear DNA damage and cytoplasmic signaling events. *J Biol Chem* 275: 9501-9509
94. Rodeck U, Jost M, Kari C, Shih D, Lavker R, Ewert D, Jensen P (1997) EGF-R dependent regulation of keratinocyte survival. *J Cell Sci* 110: 113-121
95. Stoll SW, Benedict M, Mitra R, Hiniker A, Elder JT, Nunez G (1998) EGF receptor signaling inhibits keratinocyte apoptosis: evidence for mediation by Bcl-XL. *Oncogene* 16: 1493-1499
96. Szumiel I (1994) Ionizing radiation-induced cell death. *Int J Radiat Biol* 66: 329-341
97. Stadelmann C, Lassmann H (2000) Detection of apoptosis in tissue sections. *Cell Tissue Res* 301: 19-31
98. Saraste A (1999) Morphologic criteria and detection of apoptosis. *Herz* 24: 189-195
99. Vermesc I, Haanen C, Reutelingsperger C (2000) Flow cytometry of apoptotic cell death. *J Immunol Methods* 243: 167-190
100. Sgonc R, Gruber J (1998) Apoptosis detection: an overview. *Exp Gerontol* 33: 525-533
101. van Engeland M, Ramaekers FC, Schutte B, Reutelingsperger CP (1996) A novel assay to measure loss of plasma membrane asymmetry during apoptosis of adherent cells in culture. *Cytometry* 24: 131-139
102. Weichselbaum RR, Dahlberg W, Beckett M, Karrison T, Miller D, Clark J, Ervin TJ (1986) Radiation-resistant and repair-proficient human tumor cells may be associated with radiotherapy failure in head- and neck-cancer patients. *Proc Natl Acad Sci U S A* 83: 2684-2688
103. Jung M, Notario V, Dritschilo A (1992) Mutations in the p53 gene in radiation-sensitive and -resistant human squamous carcinoma cells. *Cancer Res* 52: 6390-6393
104. Lu X, Lane D (1993) Differential induction of transcriptionally active p53 following UV or ionizing radiation: defects in chromosome instability syndromes? *Cell* 75: 765-778
105. Lowe S, Schmitt E, Smith S, Osborne B, Jacks T (1993) p53 is required for radiation-induced apoptosis in mouse thymocytes. *Nature* 362: 847-849
106. Schwartz D, N. A, Peled A, Goldfinger N, Rotter V (1997) Role of wild type p53 in the G2 phase: regulation of the gamma-irradiation-induced delay and DNA repair. *Oncogene* 15: 2597-2607
107. Owen-Schaub L, Zhang W, Cusack J, Angelo L, Santee S, Fujiwara T, Roth J, Deisseroth A, Zhang W, Kruzel E, et al. (1995) Wild-type human p53 and a temperature-sensitive mutant induce Fas/APO-1 expression. *Mol Cell Biol* 15: 3032-3040
108. Buckbinder L, Talbott R, Velasco-Miguel S, Takenaka I, Faha B, Seizinger B, Kley N (1995) Induction of the growth inhibitor IGF-binding protein 3 by p53. *Nature* 377: 646-649

109. Polyak K, Xia Y, Zweier J, Kinzler K, Vogelstein B (1997) A model for p53-induced apoptosis. *Nature* 389: 300-305
110. El-Deiry WS, Tokino T, Velculescu VE, Levy DB, Parsons R, Trent JM, Lin D, Mercer WE, Kinzler KW, Vogelstein B (1993) WAF1, a potential mediator of p53 tumor suppression. *Cell* 75: 817-825
111. El-Deiry WS, Harper JW, O'Connor PM, Velculescu VE, Canman CE, Jackman J, Pietenpol JA, Burrell M, Hill DE, Wang Y (1994) WAF1/CIP1 is induced in p53-mediated G1 arrest and apoptosis. *Cancer Res* 54: 1169-1174
112. Schafer H, Trauzold A, Sebens T, Deppert W, Folsch UR, Schmidt WE (1998) The proliferation-associated early response gene p22/PRG1 is a novel p53 target gene. *Oncogene* 16: 2479-2487
113. McNutt N, Saenz-Santamaria C, Volkenandt M, Shea C, Albino A (1994) Abnormalities of p53 protein expression in cutaneous disorders. *Arch Dermatol* 130: 225-232
114. Campbell C, Quinn A, Angus B, Farr P, Rees J (1993) Wavelength specific patterns of p53 induction in human skin following exposure to UV radiation. *Cancer Res* 53: 2697-2699
115. Ziegler A, Jonason AS, Leffell DJ, Simon JA, Sharma HW, Kimmelman J, Remington L, Jacks T, Brash DE (1994) Sunburn and p53 in the onset of skin cancer. *Nature* 372: 773-776
116. Im HJ, Pittelkow MR, Kumar R (2002) Divergent Regulation of the Growth-promoting Gene IEX-1 by the p53 Tumor Suppressor and Sp1. *J Biol Chem* 277: 14612-14621
117. Lehman T, Modali R, Boukamp P, Stanek J, Bennett W, Welsh J, Metcalf R, Stampfer M, Fusenig N, Rogan E, et al. (1993) p53 mutations in human immortalized epithelial cell lines. *Carcinogenesis* 14: 833-839
118. Paramio J, Segrelles C, Lain S, Gomez-Casero E, Lane D, Lane E, Jorcano J (2000) p53 is phosphorylated at the carboxyl terminus and promotes the differentiation of human HaCaT keratinocytes. *Mol Carcinog* 29: 251-262
119. Baichwal VR, Baeuerle PA (1997) Activate NF-kappa B or die? *Curr Biol* 7: R94-R96
120. Barkett M, Gilmore TD (1999) Control of apoptosis by Rel/NF-kappaB transcription factors. *Oncogene* 18: 6910-6924
121. Segev DL, Ha TU, Tran TT, Kenneally M, Harkins P, Jung M, MacLaughlin DT, Donahoe PK, Maheswaran S (2000) Müllerian Inhibiting Substance Inhibits Breast Cancer Cell Growth through an NFkB-mediated Pathway. *J Biol Chem* 275: 28371-28379
122. Im HJ, Craig TA, Pittelkow MR, Kumar R (2002) Characterization of a novel hexameric repeat DNA sequence in the promoter of the immediate early gene, IEX-1, that mediates 1,25-dihydroxyvitamin D3-associated IEX-1 gene response. *Oncogene* 21: 3706-3714
123. Griffiths HR, Mistry P, Herbert KE, Lunec J (1998) Molecular and cellular effects of ultraviolet light-induced genotoxicity. *Crit Rev Clin Lab Sci* 35: 189-237
124. Bouvard V, Zaitchouk T, Vacher M, Duthu A, Canivet M, Choisy-Rossi C, Nieruchalski M ME (2000) Tissue and cell-specific expression of the p53-target genes: bax, fas, mdm2 and waf1/p21, before and following ionising irradiation in mice. *Oncogene* 19: 649-660

125. Merienne K, Jacquot S, Zeniou M, Pannetier S, Sassone-Corsi P, Hanauer A (2000) Activation of RSK by UV-light: phosphorylation dynamics and involvement of the MAPK pathway. *Oncogene* 19: 4221-4229
126. Kulms D, Schwarz T (2002) Mechanisms of UV-induced signal transduction. *J Dermatol* 29: 189-196
127. Aragane Y, Kulms D, Metze D, Wilkes G, Poppelmann B, Luger TA, Schwarz T (1998) Ultraviolet light induces apoptosis via direct activation of CD95 (Fas/APO-1) independently of its ligand CD95L. *J Cell Biol* 140: 171-182
128. Wan Y, Wang Z, Voorhees J, Fisher G (2001) EGF receptor crosstalks with cytokine receptors leading to the activation of c-Jun kinase in response to UV irradiation in human keratinocytes. *Cell Signal* 13: 139-144
129. Peus D, Vasa RA, Meves A, Pott M, Beyerle A, Squillace K, Pittelkow MR (1998) H<sub>2</sub>O<sub>2</sub> is an important mediator of UVB-induced EGF-receptor phosphorylation in cultured keratinocytes. *J Invest Dermatol* 110: 966-971
130. Simon A, Rai U, Fanburg B, Cochran B (1998) Activation of the JAK-STAT pathway by reactive oxygen species. *Am J Physiol* 275: C1640-1652
131. Lee A, Fenster B, Ito H, Takeda K, Bae N, Hirai T, Yu Z, Ferrans V, Howard B, Finkel T (1999) Ras proteins induce senescence by altering the intracellular levels of reactive oxygen species. *J Biol Chem* 274: 7936-7940
132. Lebkowski J, Schain L, Okarma T (1995) Serum-free culture of hematopoietic stem cells: a review. *Stem Cells* 13: 607-612
133. Johansen C, Ryborg A, Kragballe K. (2000) 1 $\alpha$ ,25-dihydroxyvitamin D<sub>3</sub> induced differentiation of cultured human keratinocytes is accompanied by a PKC-independent regulation of AP-1 DNA binding activity. *J Invest Dermatol* 114: 1174-1179
134. Wu Y, Haugen JD, Zinsmeister AR, Kumar R (1997) 1  $\alpha$ ,25-Dihydroxyvitamin D<sub>3</sub> increases transforming growth factor and transforming growth factor receptor type I and II synthesis in human bone cells. *Biochem Biophys Res Com* 239: 734-739
135. Haussler MR, Mangelsdorf DJ, Komm BS, Terpening CM, Yamaoka K, Allegretto EA, Baker AR, Shine J, McDonnell DP, Hughes M, et al. (1988) Molecular biology of the vitamin D hormone. *Rec Prog Horm Res* 44: 263-305
136. Norman AW, Nemere I, Zhou LX, Bishop JE, Lowe KE, Maiyar AC, Collins ED, Taoka T, Sergeev I, Farach-Carson MC (1992) 1,25(OH)<sub>2</sub>-vitamin D<sub>3</sub>, a steroid hormone that produces biologic effects via both genomic and nongenomic pathways. *J Ster Biochem Mol Biol* 41: 231-240
137. Meredith JJ, Fazeli B, Schwartz M (1993) The extracellular matrix as a cell survival factor. *Mol Biol Cell* 4: 953-961
138. Frisch S, Francis H (1994) Disruption of epithelial cell-matrix interactions induces apoptosis. *J Cell Biol* 124: 619-626
139. Frisch S, Vuori K, Ruoslahti E, Chan-Hui P (1996) Control of adhesion-dependent cell survival by focal adhesion kinase. *J Cell Biol* 134: 793-799
140. Arlt A, Grobe O, Sieke A, Kruse M, Folsch U, Schmidt W, Schafer H (2001) Expression of the NF-kappa B target gene IEX-1 (p22/PRG1) does not prevent cell death but instead triggers apoptosis in Hela cells. *Oncogene* 20: 69-76
141. Grobe O, Arlt A, Ungefroren H, Krupp G, Folsch U, Schmidt W, Schafer H (2001) Functional disruption of IEX-1 expression by concatemeric hammerhead ribozymes alters growth properties of 293 cells. *FEBS Lett* 494: 196-200

142. Zhao M, Laissue JA, Zimmermann A. (1994) Immunohistochemical analysis of p53 protein overexpression in liver cell dysplasia and in hepatocellular carcinoma. *Virchows Arch* 424: 613-621
143. Moll U, Riou G, Levine A (1992) Two distinct mechanisms alter p53 in breast cancer: mutation and nuclear exclusion. *Proc Natl Acad Sci U S A* 89: 7262-7266
144. Schlamp C, Poulsen G, Nork T, Nickells R (1997) Nuclear exclusion of wild-type p53 in immortalized human retinoblastoma cells. *J Natl Cancer Inst* 89: 1530-1536
145. Arents G, Moudrianakis EN (1993) Topography of the histone octamer surface: repeating structural motifs utilized in the docking of nucleosomal DNA. *Proc Natl Acad Sci U S A* 90: 10489-10493
146. Woodcock C, Dimitrov S (2001) Higher-order structure of chromatin and chromosomes. *Curr Opin Genet Dev* 11: 130-135
147. Jenuwein T, Allis CD (2001) Translating the histone code. *Science* 293: 1074-1080
148. La Thangue NB (2002) Chromatin Control - a Place for E2F and Myc to meet. *Science* 296: 1034-1035
149. Espinosa JM, Emerson BM (2001) Transcriptional regulation by p53 through intrinsic DNA/chromatin binding and site-directed cofactor recruitment. *Mol Cell* 8: 57-69
150. Luscher B (2001) Function and regulation of the transcription factors of the Myc/Max/Mad network. *Gene* 277: 1-14
151. Ogawa H, Ishigoro K, Gaubatz S, Livingston DM, Nakatani Y (2002) A complex with chromatin modifiers that occupies E2F- and Myc-responsive genes in G0 cells. *Science* 296: 1132-1136
152. Hashimoto K (2000) Regulation of keratinocyte function by growth factors. *J Dermatol Sci* 24 Suppl 1: S46-50
153. Zhu S, Oh H, Shim M, Sterneck E, Johnson P, Smart R (1999) C/EBPbeta modulates the early events of keratinocyte differentiation involving growth arrest and keratin 1 and keratin 10 expression. *Mol Cell Biol* 19: 7181-7190
154. Jensen U, Petersen M, Lund T, Jensen T, Bolund L (2000) Transgene expression in human epidermal keratinocytes: cell cycle arrest of productively transfected cells. *Exp Dermatol* 9: 298-310
155. Fuchs E (1990) Epidermal differentiation: the bare essentials. *J Cell Biol* 111: 2807-14
156. Henriksson M, Lüscher B (1996) Proteins of the Myc network: essential regulators of cell growth and differentiation. *Adv Cancer Res* 68: 109-182
157. Evan GI, Wyllie AH, Gilbert CS, Littlewood TD, Land H, Brooks M, Waters CM, Penn LZ, Hancock DC (1992) Induction of apoptosis in fibroblasts by c-myc protein. *Cell* 69: 119-128
158. Lee R, Rosson D (2001) 12-O-tetradecanoylphorbol-13-acetate induces apoptosis in renal epithelial cells through a growth signal conflict which is prevented by activated ras. *Arch Biochem Biophys* 385: 378-386
159. Schreiber M, Kolbus A, Piu F, Szabowski A, Möhle-Steinlein U, Tian J, Karin M, Angel P, Wagner EF (1999) Control of cell cycle progression by c-Jun is p53 dependent. *Genes Dev* 13: 607-619
160. Angel P, Karin M (1991) The role of Jun, Fos and the AP-1 complex in cell-proliferation and transformation. *Biochim Biophys Acta* 1072: 129-157



161. Karin M (1998) Mitogen-activated protein kinase cascades as regulators of stress response. *Ann N Y Acad Sci* 851: 139-146
162. Shaulian E, Schreiber M, Piu F, Beeche M, Wagner EF, Karin M (2000) The mammalian UV response: c-Jun induction is required for exit from p53-imposed growth arrest. *Cell* 103: 897-907
163. Schmidt EV (1999) The role of c-myc in cellular growth control. *Oncogene* 18: 2988-2996
164. Hoffman B, Liebermann DA (1998) The proto-oncogene c-myc and apoptosis. *Oncogene* 17: 3351-3357

## Figures and Tables

Figure 1. Cellular Stress Responses.....	2
Figure 2. Structure of Epidermis .....	3
Figure 3. Stages in Apoptosis. ....	6
Figure 4. Protein Structure of <i>IEX-1</i> .....	8
Figure 5. <i>IEX-1</i> mRNA Expression after $\gamma$ -Radiation of Human Keratinocytes. ....	32
Figure 6. <i>IEX-1</i> Expression after UV-B Irradiation of Human Keratinocytes. ....	32
Figure 7. <i>IEX-1</i> Expression after H <sub>2</sub> O <sub>2</sub> Exposure.....	33
Figure 8. <i>IEX-1</i> Upregulation after EGF-Stimulation of Human Keratinocytes .....	33
Figure 9. <i>IEX-1</i> Upregulation after UV-B Radiation of HaCaT Cells. ....	35
Figure 10. <i>IEX-1</i> mRNA Upregulation by Camptothecin Treatment of HaCaTs. ....	36
Figure 11. <i>IEX-1</i> Promoter Activity after Blockade of EGFR or Serum-deprivation.....	37
Figure 12. Localization of GFP-tagged <i>IEX-1</i> .....	39
Figure 13. Immunohistochemical Staining of <i>IEX-1</i> in Cultured Cells.....	39
Figure 14. HaCaT/ <i>IEX-1</i> -zeo Cell line Overexpresses <i>IEX-1</i> mRNA.....	41
Figure 15. [3H]-Thymidine Incorporation Assay: <i>IEX</i> versus <i>ZEO</i> HaCaT.....	42
Figure 16. Baseline Apoptotic Activity in Unstressed <i>ZEO</i> and <i>IEX</i> Cultures.....	44
Figure 17. Induction of Apoptosis by UV-B Irradiation .....	46
Figure 18. Induction of Apoptosis by Incubation with Camptothecin .....	47
Figure 19. Serum Deprivation of <i>IEX-1</i> Overexpressing HaCaT.....	48
Figure 20. Immunohistochemical Staining of Human Skin .....	49
Figure 21. Overview of Potential Pathways Regulating <i>IEX-1</i> Expression. ....	57
Figure 22. Stages in Cell Life and Correlation with <i>IEX-1</i> Expression. ....	61
Figure 23. Conflict Model for <i>IEX-1</i> Overexpressing HaCaT .....	62
Figure 24. Dual Role of <i>IEX-1</i> .....	64
Table 1. Features of Necrosis and Apoptosis .....	5
Table 2. Overview of <i>IEX-1</i> Features. ....	9
Table 3. <i>IEX</i> Show More Detached Cells and Higher Caspase 3 Activity. ....	44
Table 4. <i>IEX-1</i> Gene: Region of Intron Site. ....	59

## Acknowledgements

Primarily and foremost I want to thank my teacher and mentor Professor Mark Robert Pittelkow, M.D. for the very warm welcome in his laboratory, his steady guidance, constant advice and the many intense discussions in an extremely personal atmosphere.

Equally grateful am I towards Professor Dr. med. Dr. h.c. Gerd Plewig who willingly accepted my thesis and offered much mental support throughout my stays abroad. His diligent and detailed correction of the manuscript and his valuable suggestions were of great importance in the final phase of the work.

All my efforts and work would never have been successful without the excellent technical help and the patient teaching of Karen Squillace. She contributed immensely in making my stays in Rochester an unforgettable experience.

With Professor Rajiv Kumar, M.D. I had many inspiring discussions. He helped pursue the *IEX-1* project by giving new perspectives and by allowing me to work in his laboratory.

In Aleksandar Seculic, M.D. PhD. I found not only a valuable source for information but I also learned from his personal attitudes in research as well as in life.

Especially do I want to thank Dr. med. Kathrin Feldmann. With her work on the immunological staining of *IEX-1* and parts of the northern blotting, she contributed to the chapters on cellular localization of *IEX-1* and *IEX-1* stress response.

Marly, Nel and Gina are kindly acknowledged for their technical support, Karsten Krautmacher for showing me the first steps in the laboratory and Dr.med.Thomas Comfere for his mental support and scientific advice.

Thanks to Dr. med. Dominik Peus for offering me his contacts to the Mayo Clinic and introducing me to the laboratory.

## Lebenslauf

### Persönliche Informationen

Geburtstag 24. 1. 1974  
Geburtsort München  
Nationalität deutsch

### Berufliche Tätigkeit

1/2002 – Klinik für Chirurgie, Kantonsspital St.Gallen/Schweiz

### Schulbildung

1984 – 1993 Albert Einstein Gymnasium München  
1990 Barker College Hornsby, Sydney – Australien

### Medizinische Ausbildung

1998 – 2001 Ludwig Maximilians Universität München  
1998 – 2000 Mayo Medical School/USA (Student Research Fellowship)  
1997 – 1998 Freie Universität zu Berlin  
1994 – 1997 Leopold Franzens Universität Innsbruck

### Medizinische Prüfungen

2001 3. Staatsexamen  
2000 United States Medical Licensing Examination Step II  
2000 2. Staatsexamen  
1998 United States Medical Licensing Examination Step I  
1998 1. Staatsexamen  
1996 1. Rigorosum (österreichisches Physikum)

### Praktisches Jahr

6/2001 – 9/2001 Innere Medizin: Mount Sinai Medical Center, New York  
4/2001 – 5/2001 Allgemeine Urologie: Krankenhaus München Bogenhausen  
2/2001 – 4/2001 Onkologische Urologie und Rekonstruktive Chirurgie: Norris  
Cancer Center, Los Angeles  
10/2000 – 2/2001 Allgemeine Chirurgie: Hospital de Clinicas, Buenos Aires

### Famulaturen

10/1999 Mayo Clinic Rochester: Urologie  
4/1999 Mayo Clinic Rochester: Nephrologie, Transplantationsdienst  
3/1999 Mayo Clinic Rochester: Dermatologie  
9/1997 Praxis Dr. Vogel, München: Urologie  
8/1997 Cedars Sinai Medical Center, Los Angeles: Anästhesie

### Zivildienst/Ehrenamt

1993 – 1994 Zivildienst als Rettungssanitäter, BRK München  
1990 - Ehrenamtliche Tätigkeit im Rettungsdienst, BRK München